1-1-2021

Development of Exosomal Protein Detection Assays for Cancer Diagnostics Using Nanomaterials in Conjunction with Optical Spectroscopy and Imaging

Vojtech Vinduska

DEVELOPMENT OF EXOSOMAL PROTEIN DETECTION ASSAYS FOR CANCER DIAGNOSTICS USING NANOMATERIALS IN CONJUCTION WITH OPTICAL SPECTROSCOPY AND IMAGING

By

Vojtěch Vinduška

A Dissertation

Submitted in Partial Fulfillment of the

Requirements for the Degree of

Doctor of Philosophy

Major: Chemistry

The University of Memphis

August 2021

DEDICATION

This dissertation is wholeheartedly dedicated to the two most important women in my life. To my mother, Iva Švarcová, who supported me through all my study hardships and difficulties during my academic life. Her determination, wisdom, and brilliance have always been my motivation not to give up and to continue my education. Further, then to my girlfriend, Karolina Štetinová, who never stopped believing in me, followed me on the pilgrimage of my life, and without whom I would not have even written the first line.

AKNOWLEDGEMENT

First and foremost, I would like to express my sincere gratitude to my advisor Dr. Xiaohua Huang for the continuous guidance and support on my doctoral journey. Her immense patience and admirable inventiveness have made this all possible, and I am very grateful that I had the opportunity to grow professionally and personally under her mentorship.

I would like to thank my committee members, especially, Dr. Yongmei Wang and Dr. Paul S. Simone, who have been here for me for the past five years on every stage of my research. They managed and guided me, and they have seen my potential in moments when I have not seen it. I am also very grateful to Dr. Hoang Thang and Dr. Tomoko Fujiwara who dedicated their precious time to be a part of my committee and provided me with invaluable inputs on my projects.

I would also like to thank my former and current colleagues: Dr. Elyahb A. Kwizera, Dr. Ryan T. O'Connor, Raymond E. Wilson, Zechariah J. Avello, Kristopher D. Amrhein, Alberto Rodriguez, Mitchell L. Taylor for their warm help and cooperation in our collaborative projects and creating a memorable collective that I could be a part of.

Lastly, I would like to express my perpetual appreciation to the Department of Chemistry for material and financial support and for providing me with an opportunity to obtain a doctorate in chemistry.

PREFACE

This dissertation is written based on three journal articles. Chapter 2 is partially based on an article that was published in the Journal of *Theranostics* with emphasis on 3D printing towards exosome detection: “E. A. Kwizera, R. O’Connor, V. Vinduška, M. Williams, Y. Wang, X. Huang. Detection and Molecular Profiling of Exosomes Using Surface-Enhanced Raman Scattering Small Gold Nanorod and Miniaturized Device. Theranostics 2018; 8(10):2722-2738.”

Chapter 3 is based upon a manuscript that has been submitted to the Journal of *Nanomaterials*: “V. Vinduška, C. E. Gallops, R. O’Connor, Y. Wang, X. Huang. Exosomal Surface Protein Detection with Quantum Dots and Immunomagnetic Capture for Cancer Detection.” In this chapter, all tables, figures, schematics, and references have been reformatted and renumbered to fit into one document. The references and style used withing this chapter reflect the standards of Journal of Nanomaterials.

Chapter 4 is based on the paper “Purification-free Single Exosomes Protein Profiling with Fluorescence and Darkfield Imaging for Early Cancer Detection” which is currently in preparation by the authors.

ABSTRACT

Vojtěch Vinduška. The University of Memphis. August 2021. Development of Exosomal Protein Detection Assays for Cancer Diagnostics using Nanomaterials in Conjunction with Optical Spectroscopy and Imaging. Major Professor: Prof. Xiaohua Huang

Cases of cancer are on the rise, and cancer continues to be the major cause of death in the world. It has been known for years that the survival rate and possible recovery depend on early diagnosis and personalized treatment. However, tumors are in most cases almost undetectable until cancer has already invaded the surrounding tissue and begins to metastasize to distant organs at which point the treatment is significantly less effective or completely ineffective. And even if the tumor is detected, its analysis requires a tissue biopsy, which in many instances is a risky invasive procedure that does not allow regular monitoring of the effectiveness of treatment. Therefore, any strategy for early cancer identification will be based on the correct identification of cancer detection markers found in body fluids in various forms such as proteins, RNAs, and DNA. Emerging evidence points to extracellular vesicles, more precisely their subgroup - exosomes, as an abundant source in proteins and nucleic acids that reflects the state of the parental cell. In this dissertation, we summarize the exosomal biogenesis and composition, influence of exosomes on cancer development and progression with emphasis on breast cancer, and major analytical methods applied to exosomal protein detection. Further, we report our take on exosomal protein detection as a form of novel bulk detection and single vesicle profiling techniques, which are designed for liquid biopsy in a clinical environment. Our approaches are based on optical spectroscopy and imaging such as surface enhanced Raman scattering (SERS), fluorescence, and dark-field light scattering imaging, and are designed to operate with small amounts (8-50 μL) of already diluted samples. We demonstrated the potential of 3D printing and its applicability to create a miniaturized

device that made it possible to customize detection conditions for nanosized exosomes and microvolume samples. Additionally, we developed a simple, fast, and inexpensive bulk method for detection of exosomal surface proteins using quantum dots in conjunction with fluorescent spectroscopy and we demonstrated its clinical potential on detection of HER2 cancer marker in plasma samples from a breast cancer patient. Lastly, we report single vesicle technology (SVT) based on dual fluorescent and dark-field imaging to achieve protein profiles at a single exosome level. Our SVT can overcome many obstacles that bulk technologies cannot and can bring long-sought-after early cancer detection into the clinical setting.

TABLE OF CONTENT

LIST OF FIGURES

LIST OF SYMBOLS AND ABBREVIATIONS

~	Approximately
=	Equal to
>	Greater than
<	Less than
Ø	Diameter
℃	Degrees Celsius
μM	Micromolar
μg	Microgram
μL	Microliter
λ	Wavelength
3-D	3-dimension
Ag	Silver
ANOVA	Analysis of variance
Au	Gold
AuNRs	Gold nanorods
AuNPs	Gold nanoparticles
BC	Breast cancer
BRCA	Breast cancer gene
cfDNA	Cell-free DNA
CTC	Circulating tumor cells
Cy5	Cyanine 5
Da	Dalton
DLS	Dynamic light scattering
DiO	3,3’-Dioctadecyloxacarbocyanine perchlorate
DMEM	Dulbecco’s Modified Eagle Medium
DMEM/F-12	Dulbecco's Modified Eagle Medium: Nutrient Mixture F-12
DNA	Deoxyribonucleic acid

DPBS	Dulbecco's phosphate-buffered saline
ELISA	Enzyme linked immunosorbent assay
Emλ	Emission wavelength
EpCAM	Epithelial cell adhesion molecule
EV	Extracellular vesicles
Exλ	Excitation wavelength
Exo-Anx II	Exosomal protein Annexin II
FBS	Fetal bovine serum
FDM	Fused deposition modeling
FL	Fluorescence
FN	Fibronectin
GLUT-1	Glucose transport 1
GPC-1	Glypican 1
h	Height
H2SO4	Sulfuric acid
HER2	Human epidermal growth factor receptor 2
HRP	Horseradish peroxidase
HSP	Heat shock protein
HS-PEG-Ab	Antibody-linked polyethylene glycol thiols
HS-PEG-NHS	Thiol- polyethylene glycol- N-hydroxysuccinimide esters
ICAM1	Intercellular adhesion molecule 1
ICP	Ion concentration polarization
IgG	Immunoglobulin xvii
ILV	Intraluminal vesicles
IR	Infrared
l	Length
lncRNA	Long noncoding ribonucleic acid
M	Molarity; moles per liter

MB	Magnetic beads
mg	Milligram
min	Minute
mL	Milliliter
mM	Millimoles per liter
MHC	Major histocompatibility complex
mPEG	Monomethoxypolyethylene glycol
miRNA	Micro ribonucleic acid
mRNA	Messenger ribonucleic acid
MuTEG	(11-Mercaptoundecyl)tetra(ethylene glycol)
MVB	Multivesicular body
MW	Molecular weight
nm	Nanometer
NPs	Nanoparticles
NIR	Near-infrared
NR	Nanorod
NSP	Nanosphere
NTA	Nanoparticle tracking analysis
PBS	Phosphate buffer solution
PBST	Phosphate buffer solution-tween
PDMS	Polydimethylsiloxane
PEG	Polyethylene glycol
PMT	Photomultiplier
QDot	Quantum dot
RNA	Ribonucleic acid
ROC	Receiver operation characteristic
RT	Room temperature
SEDIA	Single Exosome Dual Analysis

SERS	Surface-Enhanced Raman Scattering
SLA	Stereolithography
SNHG	Small nucleolar RNA host gene
STL	STereoLithography file format
SVT	Single vesicle technology
TGF-β	Transforming growth factor beta
TMB	3,3,5,5-tetramethylbenzidine solution
TNBC	Triple-negative breast cancer
TNF	Tumor necrosis factor
tRNA	Transfer ribonucleic acid
TRPS	Tunable resistive pulse sensing
UV	Ultraviolet
w	width

Chapter 1. INTRODUCTION

1. Morphology and Composition of Exosomes

1.1 Morphology of Exosomes

Exosomes are nanosized membrane-bound vesicles of endocytic origin released by all types of eukaryotic cells into extracellular space. They are considered as a subgroup of extracellular vesicles (EVs) together with microvesicles, microparticles, prostatosomes, apoptotic blebs, and many other small, defined, cell-secreted vesicles.[4,5] The morphology and size of exosomes are commonly reported as round or cup-shaped vesicles with a diameter in the range from 40 to 200 nm,[6–8] even though, the definition based on size and morphology is greatly challenged by the experimental difficulties associated with accurate purification and enrichment of these particles. Current methodologies for the isolation of exosomes cannot unambiguously discriminate exosomes from other cell-secreted vesicles like small microvesicles. In addition, there is still some uncertainty about protein exosomal markers, since exosomes are enriched with different proteins based on the cell of origin or even purification method. For this reason, we can expect the definition of the term exosome will continue to shape and evolve with ongoing efforts to better track its endocytic origin.[9]

1.2 Composition of Exosomes

The composition of the exosome reflects, to some extent, the molecular composition of the originating cell. Their content is made of proteins, lipids, and nucleic acids well encapsulated within the lipid bilayer of cellular origin (Figure 1.1).[10,11] Exosomes contain both cytosolic and membrane proteins. Among those cytosolic proteins belongs tubulin, actin, ESCRT protein complex, as well as proteins with enzymatic function like pyruvate kinase, glucose-6-phosphate

isomerase, lactate dehydrogenase.[12] Further, in exosomes, we can also find many heat shock proteins like HSP70 and HSP90, and proteins involved in the translation and transcription of genetic material.[13] Membrane proteins then include but are not limited to tetraspanins (CD9, CD63, CD81, and CD82), integrins, epithelial cell adhesion molecules (EpCAM), members of the human epidermal receptor (HER), and major histocompatibility complexes (MHC I and II).[14,15]

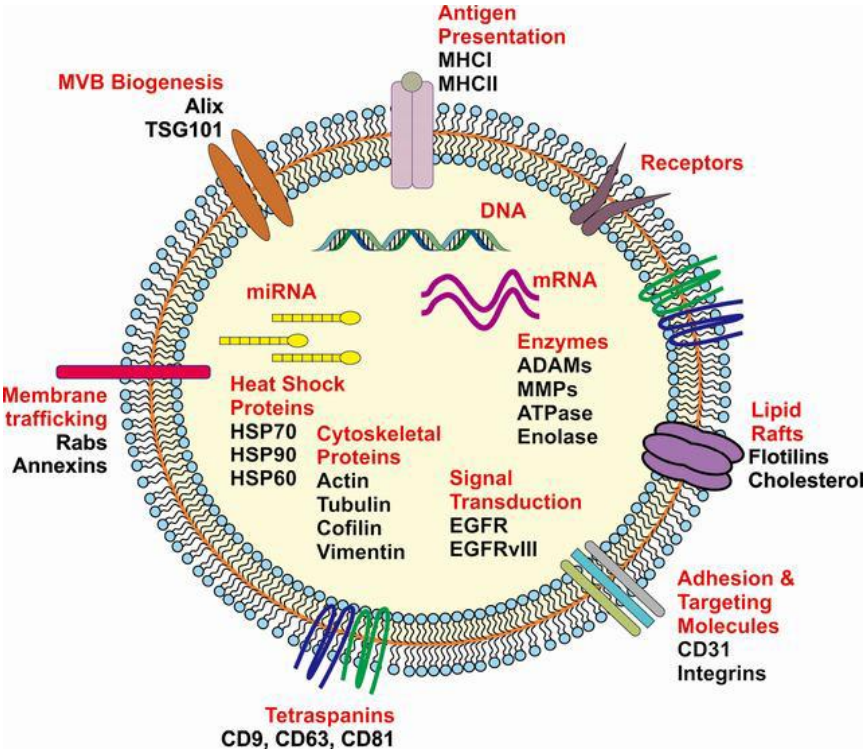

Figure 1.1. The molecular components of exosomes—they are known as a phospholipid bilayer (coloured blue) enclosed vesicle which contain various proteins on their surface membrane. Internally, their cargo can be comprised of nucleic acids and numerous proteins.[1] Reprinted with permission from Whitehead, C.A.; Luwor, R.B. (2012) Copyright 2012, Nancy International LTD Subsidiary AME Publishing Company.

Exosomes are composed of a number of lipids. They contain many membrane lipids like cholesterol, sphingomyelin, hexosylceramides, phosphatidylserine, and saturated fatty acids as well as cytosolic lipids including leukotrienes and prostaglandins.[9,16,17] In addition to proteins and lipids, exosomes also contain a variety of nucleic acids. Numerous studies have reported the

presence of RNAs – messenger RNAs (mRNAs), transfer RNAs (tRNAs), microRNAs (miRNAs), viral RNAs, as well as long noncoding RNAs (lncRNAs). Balaj *et al.* and Kahler *et al.* also reported findings of single-stranded DNA and double-stranded DNA, respectively, inside of exosomes.[18,19]

2. Exosome Biogenesis, Extracellular Transfer, and Function

2.1 Biogenesis

Biogenesis of exosomes and their consecutive release into extracellular space is one of the possible outcomes of a complex multistep process that starts with an early endosome. Endosomes are primarily set of intracellular sorting organelles in eukaryotic cells. The early endosome goes through maturation, a process that is characterized by acidification and changes in protein content. The maturation of early endosomes into late exosomes can be distinguished by changes in shape and intracellular location. The shape of the early endosome is tubular, and they are in close proximity to the cellular membrane. On the other hand, late endosomes are round and near the nucleus. The maturation of endosomes can be also observed in the formation of intraluminal vesicles (ILVs) by budding of an endosomal membrane.[20,21] During this process, a portion of cytosol together with proteins, nucleic acids, and other macromolecules gets incorporated into newly formed ILVs. The subgroup of late endosomes that progressed through the formation of ILVs is known as multivesicular bodies (MVBs).

The fate of MVBs may vary and may have one of two possible outcomes depending on molecular regulatory mechanisms that are not fully understood. One hypothesis suggests that the fate of MVBs is dependent on the cholesterol content of those organelles. The MVBs with high cholesterol content may fuse with a cellular membrane, resulting in the secretion of ILVs into the extracellular region. ILVs that enter extracellular regions are then known as exosomes. If the

cholesterol content is low a fusion with a lysosome takes a place and MVBs get degraded along with their cargo. Another theory describes ISGylation of MVB proteins inhibiting exosome release, and thus promoting the fusion with lysosomes. In this hypothesis, MVBs fusion with a cellular membrane is facilitated by Rab GTPases, SNARE proteins, many others.[22–24] The fusion of MVBs with a cellular membrane is induced by two categories of SNARE proteins, one being on the surface of MVBs and the other resides in the plasma membrane. The affinity of SNARE proteins for each other causes their binding and initiates vesicle fusion.[25]

2.2 Extracellular Transfer

Secretion of exosomes into an extracellular region filled with bodily fluids allows them to act locally or at distant sites. Their presence in blood, urine, saliva, breast milk, amniotic fluid, cerebrospinal fluid, and other fluids as well as their release by most of the eukaryotic cells was well summarized by Chahar et al.[26] The molecular composition of the environment and exosomes plays a vital role in their fate. After entering the extracellular region, exosomes can be dissolved, their content gets released into extracellular space, and the released molecules can travel on their own. An example of such molecules would be TNF, interleukin-β1, and growth factors. The second outcome for exosomes is to stay intact, travel as a vesicle, and interact with cells directly via docking at the cellular membrane, fusing with the cellular membrane, or being internalized through a process known as endocytosis (Figure 1.2). It is important to mention that uptake of exosomes does not appear as a random event and recent reports suggest a mechanistic basis of entry selection to recipient cell by invoking tetraspanin markers.[17,27,28]

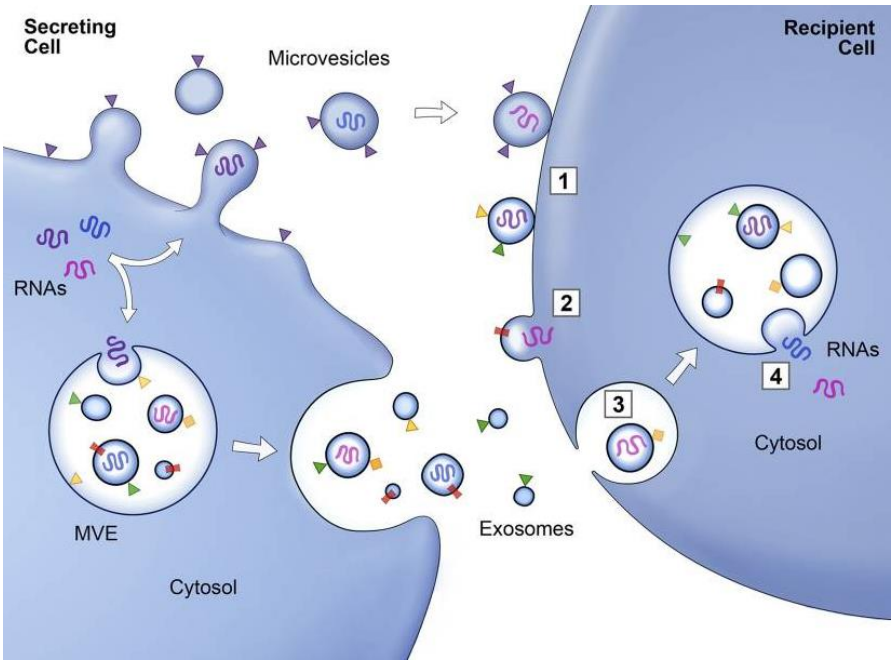

Figure 1.2. Schematic of protein and RNA transfer by EVs**.** Membrane-associated (triangles) and transmembrane proteins (rectangles) and RNAs (curved symbols) are selectively incorporated into the ILV of MVEs or into MVs budding from the plasma membrane. MVEs fuse with the plasma membrane to release exosomes into the extracellular milieu. MVs and exosomes may dock at the plasma membrane of a target cell (1). Bound vesicles may either fuse directly with the plasma membrane (2) or be endocytosed (3). Endocytosed vesicles may then fuse with the delimiting membrane of an endocytic compartment (4). Both pathways result in the delivery of proteins and RNA into the membrane or cytosol of the target cell.[2] Reprinted with permission from Raposo, G.; Stoorvogel, W. (2013) Copyright 2013, Rockefeller University Press.

2.3 Function

Despite a limited understanding of the exact effect that exosomes have on the recipient cell, there are many proposed functions of exosomes. In 1987, exosomes were first identified as cellular waste disposal vesicles by Johnstone et al.[29] This idea was further confirmed by many when exosomes were characterized as an alternative way for cellular waste elimination and a mean for homeostasis upkeep.[30] Nowadays, exosomes are best known as cell-to-cell communicators and cargo transporters. As mentioned in section 1.1.2 exosomes can be carriers for signaling molecules, proteins, lipids, and nucleic acids including but not limited to miRNA, mRNA, and other small

RNAs. The membrane of the exosome provides protection for these macromolecules outside the cell. As an example, the exosomal lumen can protect RNAs from RNases while in the extracellular region. Intercellular transport of functional RNA via exosomes was reported by Valadi et al.[31] They found that RNAs delivered through the exosomes can still be translated into functional proteins.

Exosomes are directly involved in both, regulation of immune responses and aiding in antigen presentation by immune cells. An exosome facilitated transport of antigen between dendric cells using major histocompatibility complex (MHC) and subsequent activation of T-lymphocytes is one of many examples where exosomes play a key role in up and downregulation of the immune system.[32] In addition, exosomes can also reprogram recipient cells either as a consequence of fusion or through horizontal transfer. As the two membranes are fusing together the exosome surface proteins like integrins, annexins, galectin, and intercellular adhesion molecule 1 (ICAM1) can be incorporated into a cellular membrane and causing recipient cells to acquire new characteristics.[33] The reprogramming of the recipient cell can also be induced by the horizontal transfer of nucleic acids. These transferred nucleic acids can cause phenotype changes in the recipient cells resulting in silencing of protein expression and thus causing inhibition or stimulation of various signaling pathways.[34]

3. Role of Exosomes in Cancer

Cancer is a group of diseases characterized by the unregulated proliferation of abnormal cells. The gradual growth of abnormal cells leads to the destruction of normal tissue and organs in the surrounding area, and in addition, cells of the primary tumor can spread to more distant areas in the body via a process known as metastasis. So, it is no surprise that cancer is considered one of the most serious types of diseases. Even though there are many types of cancer, only a few of

them are common. Ten of these types then account for more than three-quarters of all cancer cases, with breast, prostate, and lung cancer being the top three. From a gender perspective, breast cancer is a leading source of cancer in women. Just in the United States 281,550 (female) and 2,620 (male) new cases are expected in 2021.[35] Despite a significantly higher percentage of cases being women, breast cancer certainly cannot be ignored even in the male population.

Breast cancer usually begins with a genetic mutation of a single cell in the milk-producing ducts. Unlike a normal cell, the mutated cell has a growth advantage, and its proliferation is uncontrolled. The exact cause of the mutation in not entirely clear, but the responsible factors that play a significant role in oncogenesis are, but are not excluded to, genetic predisposition, alcohol consumption, excess of stress, hormonal disbalance, and diet. The genetic mutation frequently occurs on BRCA1 and BRCA2 genes. BRCA1 is located at the 17th chromosome and is involved in cancer development in up to 85% of cases. While BRCA2 can be found on the 13th chromosome and is detected in up to 84% of breast cancer cases. Both of those genes can be found in the male and female genome, but despite their presence, they can break out or remain hidden. Thus, breast cancer does not have to break out in each generation of a family tree unless triggered by other factors.[36,37]

The hormonal imbalance is considered as one of the significant factors that can initiate cellular mutation. Among the causes of hormonal imbalance in women belong menarche, late menopause, first pregnancy after 30 years of age, short lactation, and extensive use of estrogen supplements.[38,39] For example, during pregnancy hormone secretion is increased to supply both mother and fetus. This hormonal state creates an abundant environment not only for a new life but also for tumor growth.[40] Another important factor involved in oncogenesis is dietary related. This factor includes, but is not limited to consumption of alcohol, an unbalanced and fat-based diet in

childhood and puberty, and obesity. For instance, intake of erucic, palmitic, margaric, linoleic acids is reported to be linked with an increased risk of breast cancer.[41] Lastly, the correlation between the excess amount of stress and oncogenesis is still a controversial topic. According to a review on psychological stress and breast cancer incidence, 26 articles out of 52 identified and linked stressful events and breast cancer.[42] The authors of the remaining articles did not find strong enough evidence or could not be classified. It is important to mention that occurrence of breast cancer increases with age, and every decade probability doubles until menopause. The highest risk group are women around the age of 50, while women in their twenties are an exception. However, breast cancer in young women is usually more serious and is associated with more aggressive forms of the disease.[43]

With growing interest in cancer research and new findings in the field of exosomes, it is becoming more obvious how exosomes play crucial roles in cancer development (Figure 1.3). As described in section 1.2.3 Function, exosomes play a role in cell-to-cell communication, horizontal transfer of genetic material, induction or inhibition of protein translation, disposal of cellular waste, and regulation of immune responses. Since exosomes are secreted by all types of cells including cancer cells then the same exosome's mechanisms are used against our immune system in disease.

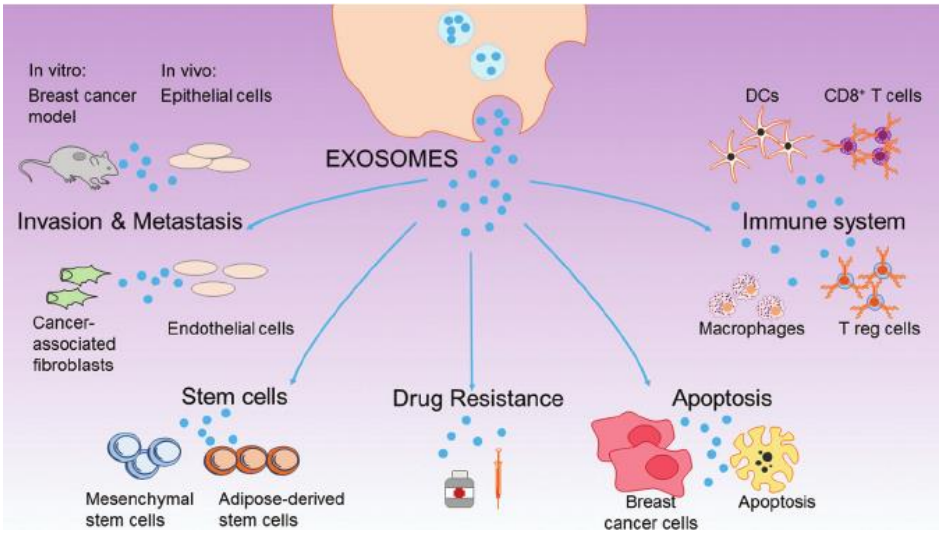

Figure 1.3. The role of exosomes in breast cancer. Exosomes are released from breast cancer and stromal/cancer associated fibroblast cells into the extracellular milieu and tumor microenvironment.[3] Reprinted with permission from Lowry, M.C.; Gallagher, W.M. (2015) Copyright 2015, Oxford University Press.

3.1 Invasion and Metastasis

The role of exosomes in breast cancer metastasis and invasion of normal tissue can be seen in all metastatic processes. Reports show their involvement from initial steps of local invasion of surrounding tissue by primary tumor cells to remodeling of the extracellular matrix for upcoming tumorigenesis, acquisition of migration capacity, and distant spread to the most common metastasis sites for BC (bone, brain, liver, or lung).[44] Exosomal role in metastasis was first reported in triple-negative breast cancer (TNBC) cell line Hs578T.[45] In this study, authors found the exosomal transfer of aggressive phenotypical traits into secondary breast cancer cells including SKBR3, MDA-MB-231, and HCC1954. These newly acquired traits caused an increase in proliferation, migration, and invasion. Further, angiogenesis in human endothelial cells was also increased when exosomes from TNBC were introduced into a normal cell. Other studies then show findings such as an enrichment of the enzyme responsible for degradation of extracellular matrix

in exosomes derived from TNBC, presence of a migration promoting protein Caveolin-1 in MDA-MB-231 derived exosomes or specific exosomal miRNA signatures found in HER2 positive breast cancer patients.[46]

3.2 Immune System

Despite all the efforts of the immune system to prevent cancer development, the tumor cells developed various mechanisms to surpass host defenses and they appear to be ahead in this regard. One such mechanism is tumor-derived exosomes. It has been reported that exosomes have both positive and negative effects on the immune response.[47] There are many ways how tumor-derived exosomes influence the host immune system and promote tumorigenesis. One of such ways is suppression of T cell activity, upregulation of regulatory T cell activity, apoptosis of T cells, and suppression of natural killer cells.[48,49] Rong et al. reported a potent immunosuppression activity, negatively modulating T-cell proliferation through TGF-β when they used exosomes isolated from two breast cancer cell lines MDA-MB-231 and BT-474.[50] Moreover, a work done by Jang et al. showed inhibition of macrophages activity after they transport miRNA miR-16 derived from murine breast cancer cell through the use of tumor-derived exosomes into tumor-associated macrophages.[51] Further, it has been demonstrated that exosomes derived from MBA-MB-231 can induce platelet aggregation, a crucial step for circulating tumor cells (CTC) to avoid immune system surveillance.[52]

3.3 Apoptosis

A deliberate cellular death also known as apoptosis is a key mechanism in control over the healthy cellular balance between cell division and cell death. Avoidance of apoptosis is one of the pivotal efforts of tumor cells, and thus it should not be surprising that exosomes take a part in the

prevention of such a process. For example, it has been reported that exosomes derived from 4T1 breast cancer cells suppressed apoptosis in CD133+ stem cell-like tumor cells.[53] In this case, exosomes not only prevented apoptosis of CD133+ cells but also induced their proliferation. Additionally, the work of Dong et al. also shows inhibition of apoptosis by long non-coding RNA-small nucleolar RNA host gene 14 (lncRNA-SNHG14).[54] They were interested in the regulatory functions of lncRNA-SNHG14 within exosomes during the formation of chemoresistance in breast cancer. They report lncRNA-SNH14 to target apoptosis regulator Bcl-2/apoptosis regulator BAX signaling pathway and thus promoting the uncontrolled proliferation of tumor cells.

3.4 Drug Resistance

The success of cancer treatment does not only rely on the strength of the medicine, but also on the therapeutic's ability to target the affected area and overcome the cellular mechanisms ensuring cellular resilience and self-preservation. Exosomes were first described as a waste eliminating vesicles serving to remove all unwanted materials from the cytosol into extracellular space. Unfortunately, the same mechanism complicates the work of the newly developed therapeutics, which, despite their potentially high efficiency might be disposed from the cell before their effect occurs.[55,56] In addition, tumor-derived exosomes induce drug resistance in BC by causing changes in the tumor immune microenvironment, boosting DNA damage repair, triggering a bypass in signaling or pro-survival pathways, and transferring functional cargo to upregulate Erα expression and hormone-independent signaling.[57,58] Interestingly, a decoy mechanism was also observed in HER2 targeting therapeutics. HER2 overexpression in BC patients is mostly associated with a poor prognosis.[59] Novel HER2 targeting therapeutics show an effective initial response, however, their potency significantly diminishes in the first year of treatment.[60] After administration of these therapeutics, tumor cells initiate a release of HER2 overexpressed

exosomes to directly interact with the targeted drug. By doing so exosomes significantly reduce the interaction of therapeutics with tumor cells and reduce their effectiveness.

4. Current Diagnostic Applications of Exosomes with Emphasis on Proteomics

4.1 Exosomes in Liquid Biopsy

Over the year's exosomes have proven to be ideal detection biomarkers for the detection, analysis, and monitoring of the disease. Their presence in all body fluids makes it relatively easy to obtain a sample without the need for invasive surgery and thus promote periodic medical examination. For example, due to their general presence, their isolation is much more convenient than the isolation of circulating tumor cells (CTC).[61] Exosomes are also highly resistant vesicles that allow both short-term storage in 4ºC, as well as long-term storage in -80ºC or cryo freezing.[62] In terms of short-term storage, due to their biological stability, they can reduce the costs required for their processing and transport. Another advantage of using the exosome as detection biomarkers is their macromolecular content, both on the surface of the exosome and inside. Exosomes, for example, contain genetic material such as DNA, mRNA, miRNA, lncRNA, etc. that provides much more representative information than ordinary cell-free DNA (cfDNA) samples.[19] For instance the National Comprehensive Cancer Network recommends the usage of exosome RNA-based prostate cancer test, which has already aided over 50 000 patients in their decision-making process.[63] Furthermore, exosomes contain a wide collection of surface proteins with few being considered as exosomes specific including CD81, Alix, or TS101,[64] thanks to which they can be selectively isolated, and their analysis can then help determine the stage and course of the disease. In addition, exosomes appear as superior biomarkers in diagnostic accuracy compared to other serum-based biomarkers such as carcinoembryonic antigen.[65]

4.2 Quantitative Characterization of Exosomes

Nanoparticle Tracking Analysis (NTA) is one of the most commonly used methods for quantitative characterization of the exosome. This technique works based on video analysis of particles in a liquid. The particles are illuminated by a laser and the scattered light is then recorded using a CCD or CMOS camera.[66,67] The video sequences are then analyzed based on the Brownian motion of the recorded particles. The results of NTA provide both concentrations of particles per milliliter and particle sizes in the range between 10 and 1000 nm. An additional option for this instrument can be the fluorescent mode, used to analyze only selected particles prelabeled with fluorophores.

Dynamic light scattering (DLS) is another possible method of exosome analysis. DLS works on a similar basis as NTA. This method will provide a size distribution based on the intensity of the scattered light after radiation from the laser source. The particle size is then calculated based on the transformation between the fluctuation rates and the diffusivities of the particles.[68] The larger the particle, the higher the intensity of the scattered light. DLS, unlike NTA, does not determine particle concentration in the sample.

A lesser-known method used to quantify the exosome is Tunable resistive pulse sensing (TRPS). With the use of this method, it is possible to measure both the size distribution of exosomes and their concentration.[69] The measurement with TRPS is based on voltage difference generated by the analyzed particles suspended in electrolytes. The voltage pulse is generated every time the particle passes through the nanopore. The measured values are then fitted to a standard concentration set, and thus size distribution and concentration of the exosome can be calculated. Compared to NTA, TRPS offers greater sensitivity and accuracy due to the tunable size selection

of used nanopores.[70] However, this method, unlike the NTA and DLS, requires more effort in terms of maintenance to prevent clogging of particles inside of nanopores.

4.3 Proteomics

As previously reported, the protein composition of the exosome is fundamentally affected by the cell of origin. Therefore, reliable detection of specific tumor-derived proteins on the surface as well as inside of these vesicles is a pivotal idea for the detection and diagnosis of cancer using the exosome. From more than 75 current studies, more than 2,300 proteins have been identified to be linked with exosomes.[71] It is therefore quite obvious that the detection of protein markers from exosomal samples has very promising preconditions to help with the early detection of breast cancer.[71] Western Blot, ELISA, mass spectrometry, and flow cytometry are among the most conventional detection techniques in protein analysis.[72] However, these techniques usually represent a barrier between the potential of exome detection and clinical application, mostly because they are time-consuming, require considerable experience, and in many cases require complex pre-processing of the sample.[73] Therefore, recent advances in improving and simplifying these methods, together with the development of new analytical technologies for exosome detection, are expected to finally enable the transition between science research and clinical application.

4.4 Western Blotting

Western blotting, also known as immunoblotting, is a commonly used and widely recognized technique to determine the presence and integrity of proteins in exosomes.[74–84] This technique consists of three steps: gel electrophoresis, membrane blotting, and probing with antibodies.[85] Since proteins are separated based on physical properties such as molecular weight and charge, the specificity of this technique is very high and can provide useful information on the size of different proteins. However, this analysis is very time-consuming and requires the analyte to be lysed prior to electrophoresis.[86,87] In the case of exosomes, this means that exosomes cannot be analyzed as whole vesicles. The group of Maji et al. analyzed the functions of the exosomal protein Annexin II (exo-Anx II) using atomic force microscopy and Western Blotting. Exo-Anx II is one of the most abundant proteins in exosomes.[88] The author aimed to reveal the exact function of exo-Anx II in the development and metastasis of breast cancer. Their study was performed both in vitro on specific metastatic breast cancer cells MCF10CA1 and MDA-MB-231 and in vivo on animal models. Their results revealed almost five times higher expression of this protein in exosomes derived from these aggressive types of breast cancer cells in comparison with normal and premetastatic cells. Furthermore, the in vivo study revealed the role of exo-Anx II in the transformation of the microenvironment in favor of metastasis. Accordingly, based on their findings they stated that the function of exo-Anx II is to promote angiogenesis and metastasis.

4.5 ELISA

The enzyme-linked immunosorbent assay (ELISA) is one of the gold standards in the field of proteomics. Its advantage are cost-effectiveness, good reproducibility, high sensitivity, and quantification of data, but the whole process is considerably time and labor intensive and requires a relatively large amount of sample and reagents.[89] Furthermore, in order to attain appropriate

sensitivity, most ELISAs rely on enzyme-mediated signal amplification which may not always be linear and may affect the results.[90] Nevertheless, ELISA has long been the predominant method for detecting analytes in biological samples, both in scientific research and in the clinical setting, and also has an inherent application in exome protein analysis.[91–97] In example, Moon et al. used this technique to document the increased expression of fibronectin (FN) on circulating extracellular vesicles in a breast cancer patient to determine whether this protein had the potential to become one of the key markers in early detection.[98] They targeted blood samples from healthy donors, from a patient with breast cancer, from a patient after a successful surgery, from a patient with benign tumors, and a patient with non-cancer diseases. Based on their results, they found significantly higher FN values in the group with breast cancer compared to all other groups. They further report the independence between elevated FN and breast cancer subtype and identified FN as a potential marker for early detection.

4.6 Mass Spectrometry

The current mass spectrometry-based analytical methods offer high accuracy, sensitivity, and resolution for proteomic studies of extremely heterogenous sample.[99,100] On the other hand, their use is time-consuming, requires significant expertise, comes with limitations and disadvantages associated with the coupling methods, and doesn't not allow analysis of exosomes as whole vesicles.[72,101] Prior to mass spectroscopy analysis exosomes needs to be fractionated into peptide fractions which is usually done by one of these common approaches: 1) Sodium dodecyl-sulfate polyacrylamide gel electrophoresis (SDS-PAGE), 2) two-dimensional liquid chromatography, or 3) isoelectric-focusing based fractionation.[72] Nevertheless, MS-based proteomic profiling enables the identification and quantification of exosomes derived proteins on a large scale, and thus greatly facilitates the creation of data libraries.[102–106] For instance, Risha et

al. studied a difference in protein composition between metastatic breast cancer MDA-MB-231 derived exosomes and normal epithelial cell MCF10A derived exosomes.[107] Based on these differences, they wanted to identify new potential protein markers that could be used for early detection of breast cancer. For exosome analysis, they used nano-liquid chromatography coupled with tandem mass spectrometry. Using this approach, they were able to identify 726 unique exosomal proteins in MDA-MB-231 derived exosomes out of a total of 1,107 exosomal proteins identified in both cell lines. Moreover, 87 proteins were characterized as associated with cancer and 16 proteins were then classified as important for metastasis. They also identified four surface protein markers, Glypican 1 (GPC-1), glucose transport 1 (GLUT-1), metallopreinase and disintegrin, as potentially unique to breast cancer.

4.7 Flow Cytometry

Although flow cytometers are very expensive instruments that are not built to analyze particles below ~ 300-500 nm,[72,108,109] at least not in their conventional form, they are still the method of choice in protein exosome analysis for many researchers.[110–118] Flow cytometry provides very accurate quantitative data and can facilitate subpopulation analysis, which makes it the most suited for diagnostic and clinical research in comparison to the above-mentioned methods.[119] However, exosome analysis is notoriously difficult because, compared to cell analysis, the size of the extracellular vesicles causes: 1) less fluorescence emitted from each vesicle due to fewer number of antigen present on its surface 2) limitation in post stain washing which is necessary to minimize background signal.[120] In many cases, researchers are thus confronted with a high optical background that masks the presence of small vesicles and false-positive signal caused by immunoglobulin aggregates.[72] New adaptations for flow cytometry consist, for example, in the application of micrometer-sized latex beads designed for multivesicular binding or

construction of highly sensitive flow cytometry instruments which can distinguish nanoparticles <100 nm. The use of highly sensitive flow cytometers thus allows EVs detection to be performed at a single molecular level, as has already been demonstrated on exosomes by Kibria et al.[121] With their rapid analytical approach for a micro flow cytometer, they were able to measure the expression of two targeted proteins, CD44 and CD47, on the surface of an exosome derived from either the cell medium or the blood plasma of a healthy individuals and breast cancer patients. The CD44 protein marker is associated with tumorigenesis and progression and CD47 is known to affect the recognition of the host's defense mechanism, especially macrophage and natural killer cell. Using this technique, they were able to differentiate healthy populations from cancer patients based on CD47 marker expression. However, their current method has not been able to detect the difference between the two groups for the protein marker CD44. As they say, even though more improvements are needed in flow cytometry methods, it has great potential in research of exosomes and early detection of disease.

4.8 Miscellaneous Techniques

Over the past decade, many has also reported other techniques that include novel or unique approaches towards detecting of proteomic content of exosomes. Due to the lack of previously discussed conventional techniques, researchers have expanded their focus on combining the principle of advanced physical detection methods with immune-based EV capture and immune-labeling probes. Exosome detection has also shifted from standard application to so-called lab-on-chip format, thus combining the qualities of conventional methods with small volume sample requirements and minimal sample processing. These new emerging approaches are based on: surface plasmon resonance (SPR),[122–127] fluorescence techniques,[77,128–134] Interferometric

imaging,[135] Electrochemical sensing,[136–141] colorimetric,[142] Micro-Nuclear Magnetic Resonance (μNMR),[143,144] surface enhanced Raman scattering (SERS).[145–147]

5. Overview of Chapter Contents

In chapter two, we demonstrate how 3D printing can aid in modifying analytical assays used in the field of extracellular vesicles. An ongoing effort to reduce the amount of sample required in liquid biopsies asks for new tools that are designed to operate with nanoparticles such as exosomes on microvolume levels. In this chapter, we discuss the procedure that was used to design, print, and assemble a 3D printed miniature device which played a crucial role in the SERS-based detection assay of surface proteins on exosomes. We also focus on challenges and limitations that have emerged when we used different templet designs and ideas to build our microarray devices which would be comparable or better in performance to conventional microvolume platforms such as 96-well microplate.

In chapter three, we describe our fluorescence-based protein detection assay which uses semiconductor quantum dots probes to target cancer markers on the exosomes. The study aimed to create a simple, reliable, and inexpensive assay using conventional fluorescent spectroscopy coupled with a novel strategy for photostable fluorescence labeling. In addition, we explain how we eliminated the lengthy process of exosome purification by using magnetic beads coupled to anti-CD81 Ab and thus created suitable conditions for a possible clinical application. In approximately 4 hours, using a three-step procedure, we were able to distinguish exosomes derived from three breast cancer cell lines MDA-MB-231, SKBR3, and MCF7, and one normal epithelial breast cell line MCF12A. We further successfully applied this method to blood plasma studies where we demonstrated its potential by discriminating healthy donors from stage three HER2-positive breast cancer patients based on HER2 cancer marker expression.

In chapter four, we report a Single Vesicle Technology (SVT) which allows protein expression profiling of individual exosomes. Due to its high sensitivity and specificity of our assay can identify even a very rare exosome population mixed with exosomes of various origins. Therefore, the technology opens space for early-stage cancer detection since cancer-derived exosomes are naturally mixed in a very complex body fluid environment and are masked by the predominant population of exosomes released by normal cells. Similarly, as in chapter three, exosomes are first captured based on CD81 exosomal marker expression and subsequently, their phospholipid bilayer and proteins of interest are labeled with two consecutive approaches. Here we discuss three different approaches we tested to achieve our final double imaging strategy combining fluoresce imaging to determine the exact position of each captured exosome and darkfield imagining detecting targeted protein expression.

Chapter 2. 3D PRINTING FOR EXOSOME DETECTION

1. Introduction

Satisfactory conditions for the clinical use of analytical methods require ease of use, undemanding sample preparation, low reagent consumption, and, above all, low sample volumes within the range of human patients' accessibility. Standard analytical methods and procedures are generally not suitable for achieving these conditions.[148,149] Many of these methods and procedures used in the bioanalytical field are designed to analyze tissues and cells in which the number of tested macromolecules is significantly higher than in the exosome.[150] Therefore, it is not a surprise that with the increasing growth in evidence of the clinical importance and potential of the exosome as valid biomarkers for the host's medical condition, many new methods and procedures have been developed that are specifically scaled down to suit clinical conditions. 3D printing has become a key method for creating novel sample arrays and microchips that can precisely operate with micro volumes of already diluted samples.

The original micro fabrications of these microfluidic platforms have been accomplished using techniques such as photolithography, micromachining, and injection molding. [131,148,151–160] Despite their high resolution and accuracy, these techniques are costly, complex in processing, and difficult to reproduce. The application of 3D printing in bioprinting and microfluidic has opened the door to the creation of new tools that can be used either on their own or applied as modifications to already used analytical methods. Nowadays, 3D printing is significantly cheaper, widely available not only in laboratory and industrial conditions, and the wide range of software provides a simple navigation to design own image, even for free.

Fused deposition modeling (FDM) and stereolithography (SLA) methods are most often used for the common application of 3D printing. FDM is a simple and affordable method of 3D

printing. With this method, printing filament is heated and directed through the nozzle to print the first layer on the printing bed.[161] The printing bed is then lowered and ready for the next layer to be deposited. The whole 3D image is printed from the bottom to top, layer by layer. The advantage of this method is in the simplicity of the instrument and the possibility of using a large variety of different types of filaments, but usually at the cost of lower quality and lower resolution of the final product. The SLA printing approach uses a liquid filament bath in which the printing bad is submerged in an upside-down position.[162] With the help of an ultraviolet laser and X and Y, scanning mirrors the liquid filament is hardened on the surface of the printing bed. After hardening of each layer, a recoater blade events out the newly deposited layer to make sure that the new layer is evenly spread. By repeating these steps, the 3D object is built from the bottom up. The final print than must be cleaned in a chemical bath and can additionally require post-cured in an ultraviolet oven.

Multiple recent "proof of principle" laboratory studies have demonstrated various methods for isolation, amplification, and characterization of the exosomes in a microfluidic setting based on several physical parameters such as mechanical, electromechanical, electrochemical, electrostatic potential, optical, non-optical, and others.[163] In example, Kheyrabadi et. al reported the construction of a specific microfluidic platform with an integrated electrochemical sensor to quantify cancer-derived exosomes.[164] With the help of SLA 3D printing, they were able to create a device that would allow a combination of a fabricated aptasensor and a microfluidic vortexer and thus increase the collision rate between exosomes and sensing surface and reduce the required sample volume to 10 uL. Meanwhile, Cheung et al. fabricated 3D printed concentration on-chip device for liquid biopsy, which allows locally enhance exosome concentration using ion concentration polarization (ICP)-based electrokinetic concentrator.[165] They reported that with the

help of their concentrator device the limit of detection for their fluorescence analysis increased by two orders of magnitude when tested on exosomes derived from the MDA-MB-231 breast cancer cell line. Further, Zhao et al. created 3D printed mold using SLA print.[166] This mold was then used to create a PDMS microfluidic cell for exosome engineering applications. To demonstrate the applicability of their platform, they inserted a melanoma tumor peptide on the surface of exosomes. These engineered exosomes were then used in immune response studies through antigen presentation and T cell activation.

In this chapter we will focus on the techniques that were used to create and assemble portable microfluidic device employed in capture and detection of exosomes in a study done by Kwizera, et al.[146] Our goal was to create a reusable multi-well platform for sample placement, which would be freely attachable on a gold-coated substrate with dimensions 75 x 25 x 1 mm. The aim of this platform was to achieve the largest possible throughput of individual samples that could be detected at the same time on one device, and thus be comparably effective as other high throughput platforms such as 96-well ELISA plate (127.7 x 85.4 mm). To fulfil these requirements, individual wells had to be less than be 2 mm in diameter to fit such high density of wells on ~6-fold smaller area of our gold-coated substrate, but still with sufficient spacing between them to avoid cross contamination across the samples. Additionally, our goal was to significantly reduce amount of sample and reagents required for reliable and reproducible operation within the needs of our portable Raman spectroscope. This would not only address unnecessary waste that is often typical of commercial platforms (96-well plate) but it also would also make it more suited for a clinical application.

2. Materials and Methods

2.1 Au Thin Film Deposition on Microscopy Glass Slides

A standard microscopy glass slide (75 × 25 × 1 mm) was coated with a 10 nm thick Au film by the magnetron sputtering technique using an ORIONAJA system from a 99.99% pure Au target. The deposition of the Au layer was performed on a 4 nm titanium layer previously deposited from a 99.99% pure titanium target on the glass slide. The slide-target distance was kept at 15 cm during the process. The film thickness was controlled by an INFICON SQM-160 quartz crystal monitor/controller equipment. The rotating substrate-holder was kept at 80 rpm. The films were grown in an atmosphere of argon at 3.0 mTorr and a gas flow of 15 sccm, with the DC power supply set to 100 W and the pressure before inserting the argon was 4.0×10^{-8} Torr. The whole process took 4 h.

2.2 Fabrication of Array Template

The 3D design was drawn using TinkerCAD (tinkercad.com). Plastic (polylactic acid) array templates with specified well size and inter-well distance were fabricated using a MakerBot Replicator PC 3D printer. The template was attached to a rubber array via a layer of glue composed of 60% silicone and 40% mineral spirit. This rubber array was made from a 1.6 mm thick rubber sheet with the same dimensions as the template via puncture. The assembled plastic and rubber arrays were used as a template array to make an antibody array on the Au-coated glass slides.

3. Results and Discussion

3.1 Designing of 3D-Printed Template

To design and draw a plastic template for the future microarray device we used the online software TinkerCAD. TinkerCAD is a free software designed for 3D modeling in a web browser. With this software, the final layout can be exported in the standard STereoLithography (STL) format, which is recognized by the vast majority of 3D printers. The major advantages of TinkerCAD are that it is relatively easy to use, and it has a simple interface for 3D modeling. For the template, we chose a cuboid with dimensions of 75 x 25 x 4.5 mm (l, w, h), which corresponds to the size of a standard microscope glass slide. The cuboidal template and lateral interface for the selection of individual geometric shapes are shown in Figure 2.1.A. An important parameter was the height of the template 4.5 mm, not only because of the desired volume for a sample application (15 µL) but also because previous experience showed that there is a longitudinal bending of the template and loss of adhesion of the array from the attached slide in thinner versions. The next step was to create an array of perforations that would serve as wells for an individual sample application. Since this microarray device was to be operated by a researcher, the size of the individual wells could not be less than 2 mm. The distance between the individual wells also could not be less than 2 mm to avoid leakage and cross-contamination between the individual samples. A series of cylinders were used as a building block to create these perforations. These cylinders were drawn in the “Hole” filling mode, which means that such objects are perceived as hollow objects when printed (Figure 2.1.B). To meet all the criteria, the final design contained 85 wells (17x5) with an individual volume of 56.55 µL. This makes our micro-array device 5.8 times more “sample per area” efficient than ELISA plate. Both designs were completed by embedding the set of cylinders in a cuboidal template (Figure 2.1.C) and “grouped” into one final layout (Figure

2.1.D). The final pattern was exported as STL file and printed on a MakerBot Replicator PC 3D printer using Polylactic Acid (PLA) thermoplastic filament.

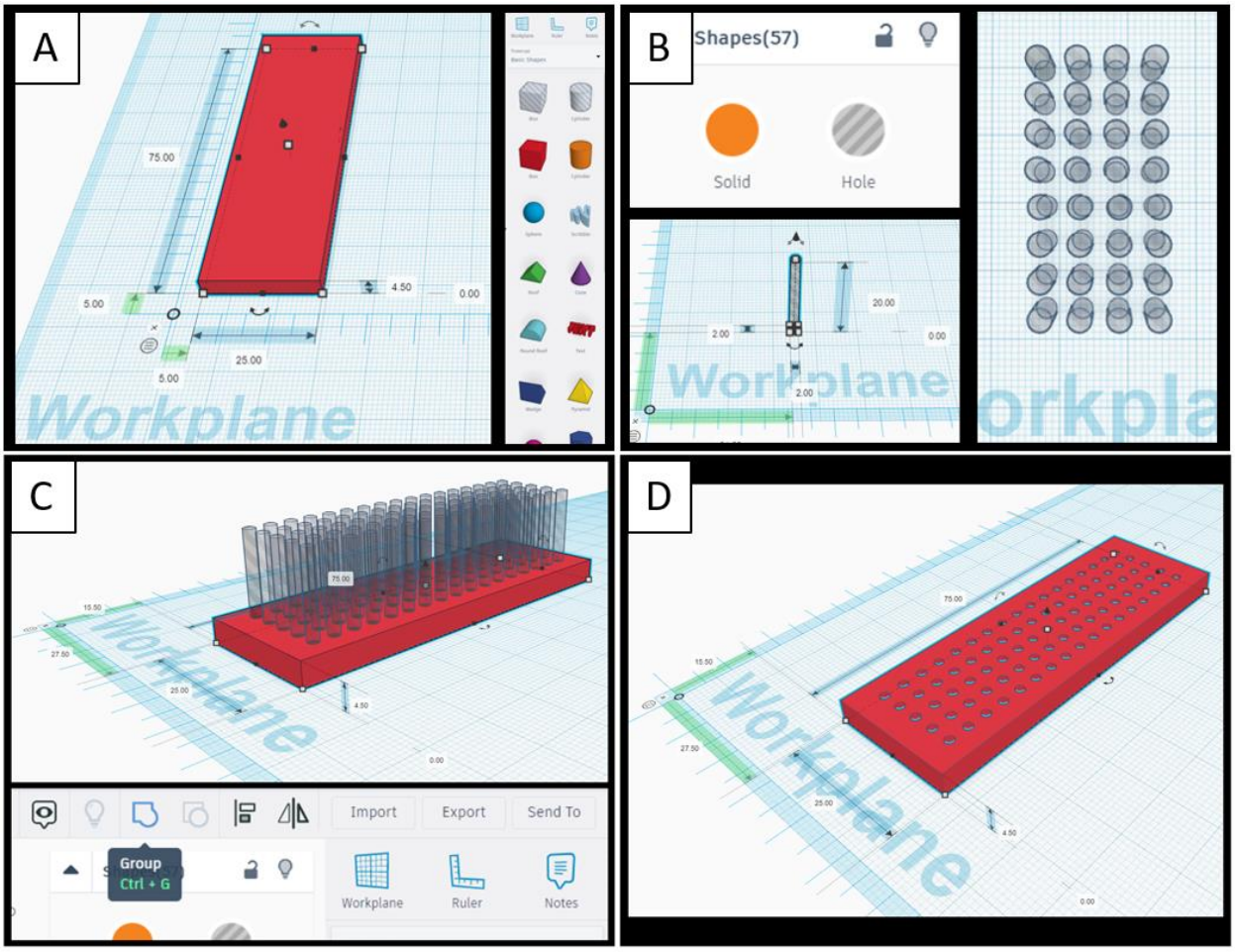

Figure 2.1. Process of designing a micro-array template in TinkerCAD. (A) Primary shape selection of the microarray template with dimension 75 x 25 x 4.5 mm (l, w, h). (B) Cylinders with "Hole" filling used as a shape for individual wells. (C) A grouped set of 85 cylinders together with a cuboidal template. (D) A finalized design ready for 3D printing.

3.2 Assembly of Micro-Array Device

In addition to the largest possible number, specific volume, and diameter of wells, other criteria for our design of micro-array template were an impermeable seal between individual wells and the possibility to detach the template from the Au surface and reuse it again. Since the seal between the microarray template (Figure 2.2 A&B) and the Au slide could not be permanent, we

had to choose a waterproof adhesive material. The rubber seal offers sufficient sealing if adequate pressure is applied to the link between the template and the Au slide, and at the same time, it offers a smoother surface than, for example, a silicone coating. The exact pattern of each perforation was traced on a rubber sheet (1.6 mm thick) and the holes were cut out using a mechanical hole puncher (Figure 2.2.C).

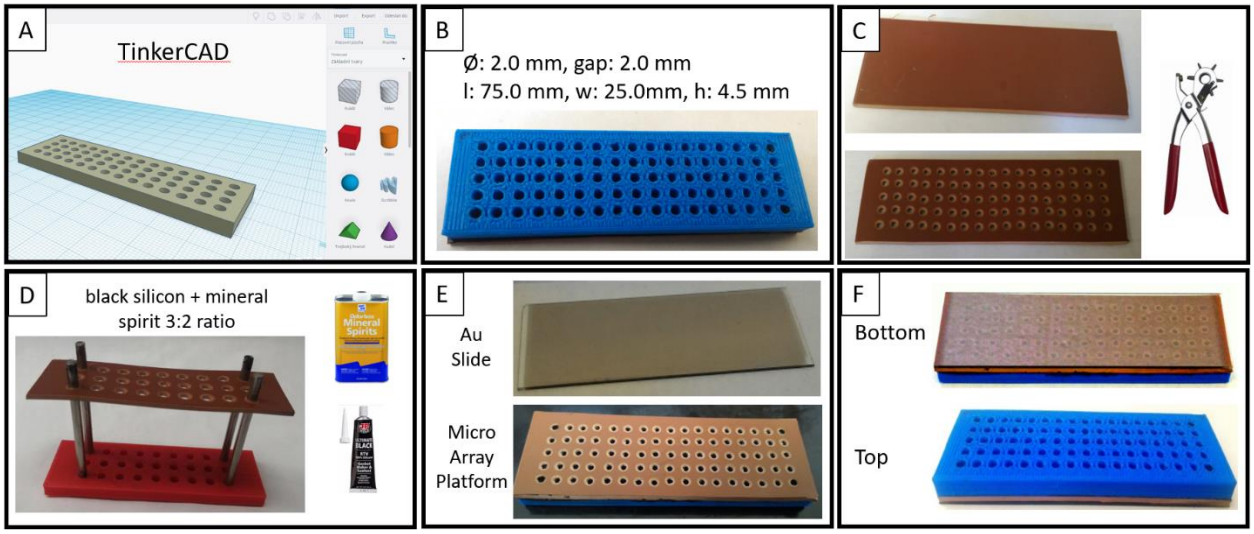

Figure 2.2. Assembly of micro-array device. (A) The final design of the template in TinkerCAD. (B) 3D printed template made of thermoplastic polymer. (C) A gasket rubber sheet cut out according to the template layout using a mechanical hole puncher. (D) Bonding the template and the rubber cutout using black silicone and mineral spirits. (E) Two-piece set of a micro-array device composed of: i) Au slide ii) micro-array template. (F) Combined micro-array device.

To seal the 3D printed template to rubber cutout, we used black silicon diluted with mineral spirits (3:2 ratio) for better spreadability (Figure 2.2.D). The mixture of black silicone and mineral spirits was applied to the rubber surface in a ~0.5 mm layer and the coated rubber cutout was pressed onto the plastic template. The combined layers were allowed to dry for one day. The dried product was cleaned with a scalpel knife and sandpaper and washed with water and ethanol. Using binder clips the micro-array template was ready to be pressed on an Au slide and ready to be used as a Micro-Array Device for Raman-based exosome detection (Figure 2.2.F).

3.3 3D Printing Ideas, Schematics, and Templates

Initial design on how to adhere the plastic micro-array template to a gold-coated microscope slide involved a thick silicone coating (Figure 2.3.A). However, the silicone layer was laborious to apply evenly without clogging the perforations and dried imperfections were very difficult to clean without damaging the silicone surface. In addition, the silicone surface took a long time to dry and was not smooth enough to prevent leakage between the individual wells. For this reason, using a gasket rubber has been a much more effective and effort-making solution. In Figure 2.3.B, we show the different distributions of the perforations, where we tested whether a well diameter lesser than 2 mm allows the researcher to apply the samples. A smaller diameter of the wells would increase the number of individual samples that could be tested simultaneously with this device, but the narrow shape of the wells prevented liquid to reach the bottom due to capillary action. Figure 2.3.C&D shows a proposed design for a thinner micro-array template that would solve the problem with capillary action. However, the reduced thickness increased the flexibility of the plastic material and did not allow the pressure to be evenly distributed on the plastic template when attached to the Au slide. The template would thus require a permanent adhesive which would make the template nonreusable again. The bending was addressed in Figure 2.3.E by additional support from thicker walls around the template.

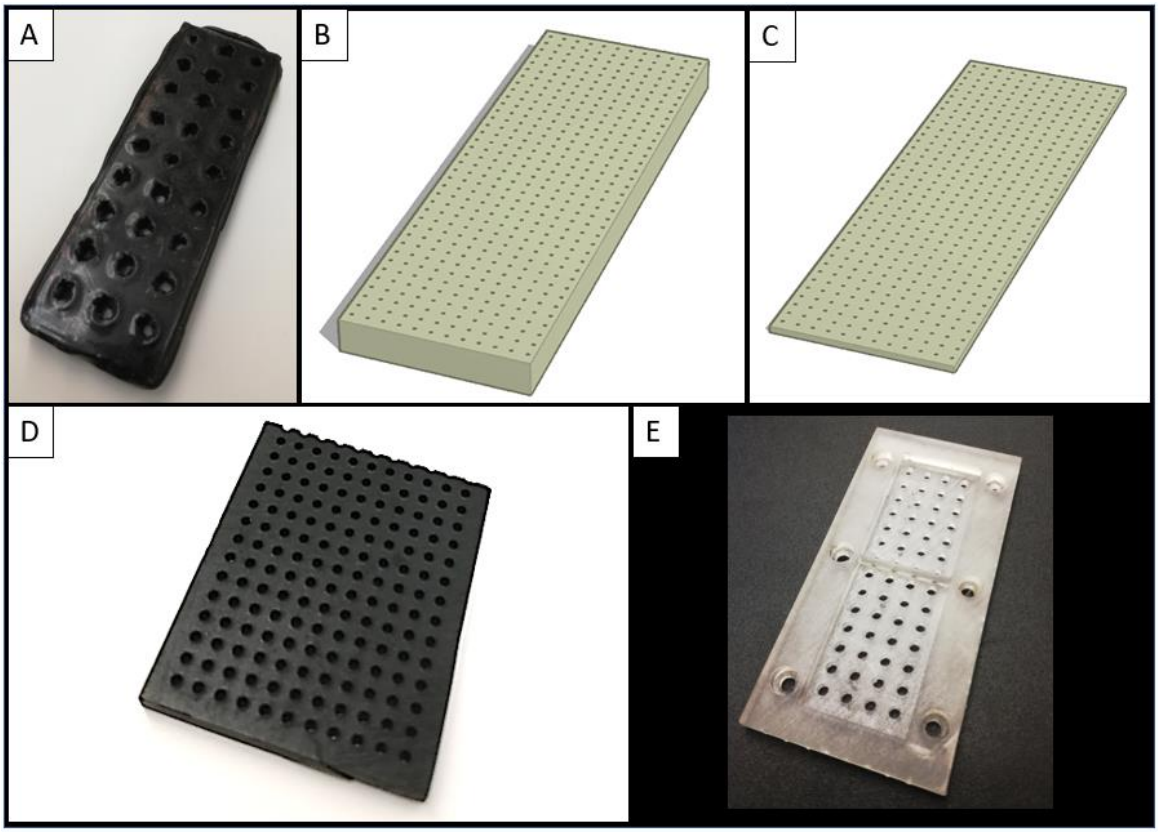

Figure 2.3. 3D printing schematics and templates. (A) Initial design using a thick silicon layer to provide a seal between the template and gold-coated slide (27 wells, well Ø = 5 mm). (B) A template designed for high throughput performance (444 wells, well Ø = 0.5 mm) (C-D) Thinner version of design Fig.3B. The height was reduced from 4.5 to 1 mm to mitigated unwanted capillary interactions. A templet was printed at a higher resolution with SLA 3D printer. (E) The idea of an SLA printed template. The thin surface is supported with a thicker side and inner frame to prevent bending. The template is no longer attached to a gold-coated slide with paper clamps, but with wing screws instead.

4. Conclusion

3D printing proves to be an effective, affordable, and replicable method in making and development of miniature devices and microfluidics systems for the detection of biological samples such as exosomes. In this chapter, we demonstrated how we designed and manufactured a micro-array template for a Raman spectroscopy application using a freely accessible web design software and an FDM 3D printer. Thanks to 3D printing, we were able to quickly modify and redesign our layout based on our specific requirements and needs without significant limitations.

Our final design allowed the detection of 85 samples simultaneously on one gold slide, which is 5.8 times more efficient in terms of sample per area than 96-well microplate used in ELISA. Demonstrative use and application of our miniaturized device in the detection of protein markers on the surface of the exosome is described in Kwizera EA, O'Connor R, Vinduska V, Williams M, Butch ER, Snyder SE, Chen X, Huang X. Molecular Detection and Analysis of Exosomes Using Surface-Enhanced Raman Scattering Gold Nanorods and a Miniaturized Device. Theranostics 2018; 8(10):2722-2738. doi:10.7150/thno.21358.

Chapter 3. EXOSOMAL SURFACE PROTEIN DETECTION WITH QUANTUM DOTS AND IMMUNOMAGNETIC CAPTURE FOR CANCER DETECTION

1. Introduction

Cancer is a heterogeneous disease that is manifested by mutations of certain groups of cells in the human body, resulting in uncontrolled growth and damage of surrounding organs. Breast cancer is the most common type of cancer and second cause of death in women, but it also poses an undeniable threat to health in men. Just in the United States 281,550 (female) and 2,620 (male) new cases are expected in 2021.[35] Two factors that affect tumorigenesis and tumor advancements are genetics/epigenetics changes in the cancer cells and the rearrangement of the components of the tumor microenvironment (TME).[167] Based on Stephen Paget's "seed and soil" theory, metastases of cancer involve both cancer cell dissemination – "seed" and a special affinity for the growth-enhancing environment of specific organs – "soil".[168] The composition of TME is rather complex consisting of blood and lymph vessels, fibroblasts, endothelial cells, immune cells, cytokines, extracellular vesicles, and extracellular matrix.[169–171] In TME, cellular and extracellular components contribute to almost all carcinogenesis processes. For instance, extracellular vesicles (EVs) from breast and ovarian cancer cells can induce the conversion of healthy mesenchymal cells to myofibroblasts, which are abundantly represented in the tumor stroma and induce the formation of the tumor microenvironment. EVs induce the expression of tumor growth-promoting cytokines (SDF-1 and TGF-β) and their receptors in mesenchymal cells, and thus, activate signaling pathways associated with tumor differentiation, progression, and metastasis.[172]

Exosomes (EXOs), a subgroup of EVs, are nanosized membrane-bound vesicles of cellular origin that are present in a variety of body fluids including blood, saliva, urine, and cerebrospinal fluid.[173–175] Their continuous secretion via exocytosis is mediated by the fusion of multivesicular

bodies with the cell membrane. EXOs represent an important mode of intracellular communication.[176,177] More interestingly, the molecular composition of EXOs consists of a variety of macromolecules including proteins, lipids, nucleic acids, and coding and non-coding RNA that are reflective of a cell of their origin.[11,178] Research has shown that EXOs can reflect both the nature of the parent cells as well as their pathophysiological state through, for example, surface protein composition or exosome cargo content.[179–181] For instance, the cancer protein marker human epidermal growth factor 2 (HER2) is known to be overexpressed in primary cases of cancer.[182–184] Elevated levels of HER2 positive EXOs have been reported in serum samples from breast cancer patients in comparison to healthy donors.[185] These changes can then contribute to the body's immune responses, resistance to apoptosis, induction of proliferation, and formation of metastatic deposits enabling oncogenesis and cancer development.[186–188] Thus, molecular detection of EXOs in body fluids is very promising for disease detection without invasive sampling.[61,77,148,189–200]

Surface proteins are the contact point for cell-to-cell communication. Oncogenic receptors often reside within regions of the plasma membrane. This allows for their detection with external optical labeling for facile cancer detection. For signal readout, quantum dots (QDs) are extremely attractive for exosome labeling and optical detection because they are small (2-10 nm) and they have strong fluorescence properties and superior photostability.[136,184,201–211] For example, Bai et al. used QDs to label and detect EXOs of different surface markers after trapping magnetic bead (MB)-isolated EXOs in a microfluidic micropillar chip.[205] Kim et al. developed a colorimetric-based lateral-flow assay to improve exosome detection using QD embedded in silica-encapsulated nanoparticles.[209] QDs have also been used to improve nanoparticle tracking analysis (NTA) by characterizing surface immunophenotypes besides exosome size distribution and concentration.[210,211]

In this study, we demonstrate a simple yet effective method for EXOs detection using QDs in conjunction with immunomagnetic exosome isolation with MB targeting CD81 exosome markers. Tetraspanin CD81 has been proven a reliable marker for exosome identification.[212] CD81 expression is low on platelet cells, a major contributor of normal EXOs in plasma.[213] Thus, using CD81 capture ligands dramatically decreases the contamination of normal EXOs, enhancing the sensitivity of detecting tumor-derived EXOs. Although CD81 is not ubiquitously expressed on every exosome, CD81 expressions are common in different cancer EXOs.[77,146,214] We use MB conjugated with CD81 antibody for exosome capture to eliminate the need for long sample purification. For detection, we use highly fluorescent and universal QD 655 linked with secondary antibody to recognize primary antibodies that bind to targeted surface protein markers of interest on EXOs. This method was tested with different surface markers on EXOs from cell-derived EXOs in the breast cancer model. Using the method, we demonstrated that HER2-positive breast cancer can be diagnosed with exosome HER2 with high diagnostic power. Due to advantages in simplicity, speed, and low sample consumption, our QD-based method with magnetic separation holds strong promises for molecular detection of EXOs for basic vesicle research and clinical applications.

2. Materials and Methods

2.1 Materials

All reagents were purchased from Sigma-Aldrich (St. Louis, MO) unless otherwise specified. Anti-rabbit CD81 antibody was purchased from Boster Biological Technology (Pleasanton, CA). Antibodies targeting HER2, epidermal cell adhesion molecule (EpCAM), CD24, CD44, CD9, and CD63 were purchased from Biolegend (San Diego, CA). Breast cancer cell lines SkBR3, MDA-MB 231, MCF7, and normal breast cell line MCF12A were purchased

from ATCC (Manassas, VA). PRMI and high glucose DMEM media were purchased from VWR (Radnor, PA). NHS-activated MBs, QD655 with secondary antibodies, fetal bovine serum (FBS), and BCA kit were purchased from Fisher Scientific (Waltham, MA).

2.2 Conjugation of Capture Antibody to MB

Prior to the conjugation, 20 µL of 10 mg/mL NHS-activated MBs were washed with 200 µL of ice-cold hydrochloric acid (1 mM) for 15 sec. The beads were then collected using Qiagen 12-tube magnets and mixed with 200 µL of anti-rabbit CD81 antibodies (50 µg/mL) for 2 h at room temperature (RT). During the first 30 minutes, the mixture was vortexed every 5 minutes for 15 seconds. Then, the mixture was vortexed every 15 minutes for 15 seconds. After 2 h, CD81 antibody-conjugated MBs were collected with magnetic stand, the flow-through was saved for BCA analysis and the pellet was washed twice with 400 µL of Glycine (0.1 M, pH 2.0) and once with 400 µL of UP water. The CD81-MBs were then quenched for 2 h on a rotator at RT using 400 µL of Ethanolamine (3M, pH 9.0). At the end of the 2 h, CD81-MBs were collected and washed once with 400 µL of UP water followed by three consecutive washes with 400 µL of DPBS 1x. 200 µL of DPBS 1x with 0.05% Sodium azide was then used as a storage buffer and CD81-MBs were stored at 4 ºC until use.

2.3 Collection and Purification of Cell-derived EXOs

Breast carcinoma cells MDA-MB-231 (MM231), MCF7, and SKBR3 were cultured in Dulbecco's Modified Eagle Medium (DMEM) (MM231, MCF7) and RPMI 1640 medium (SKBR3) supplemented with 10% FBS, 1% penicillin-streptomycin, 1% NEAA at 5% CO_2 and 37 ºC. Human breast normal cells MCF12A were cultured in DMEM: Nutrient Mixture F-12 with 5% fetal horse serum, 1% penicillin-streptomycin, 1% NEAA, 100 ng/mL cholera toxin, 0.5

mg/mL hydrocortisone, 10 µg/mL bovine insulin, and 20 ng/mL epidermal growth factor. When cells reached a confluency of approximately 70%, the medium was exchanged with serum-free medium and incubated for 48 h. Then, EXOs were isolated by differential centrifugation, as described previously.[146] Briefly, the culture medium was collected and centrifuged at 430g for 10 min at RT. The supernatant was collected and centrifuged at 16,500g for 30 minutes at 4 ºC followed by 90 min centrifugation at 100,000g at 4 ºC. The supernatant was discarded, and the pellet was redispersed in ice-cold sterile Dulbecco's phosphate buffer solution (DPBS), filtered with a 0.22 µm polyethersulfone (PES) filter (Millipore Express), and centrifuged again at 100,000g for 90 minutes at 4 ºC. The final exosome pellet was resuspended in 1 mL of ice-cold sterile DPBS and stored at -80 ºC until use.

2.4 Source of EXOs from Patients and Human Donors

Plasma samples from human epidermal growth factor receptor 2 (HER2)-positive breast cancer patients were obtained from BioIVT (Westbury, NY). The samples were not specifically collected for our proposed research and we did not have access to the identifying information of the subjects. Whole blood samples from different healthy donors were purchased Research Blood Components (Watertown, MA). To obtain plasma from whole blood samples, whole blood was centrifuged at 2,500g for 15 minutes. The supernatant was collected and centrifuged again to obtain the plasma. Both collected and purchased plasma samples were diluted with sterile PBS and filtered with a 0.2 µm PES syringe filter (VWR) before use.

2.5 Characterization of EXOs with Nanoparticle Tracking Analysis (NTA)

Plasma and cell-derived EXOs were characterized with NTA using a NanoSight LM10 microscope (Malvern Instruments, Inc) to determine the concentration and size of EXOs. The samples were diluted to keep exosome concertation within the range of 10^6 to 10^9 EXOs per mL in accordance with the manufacturer's recommendations. All samples were analyzed in triplicate of 40-s videos with camera level set at 12 and detection threshold set at 10.

2.6 EXOs capture and fluorescent detection

50 μL of EXOs at concertation $1.00x10^9$/mL from breast cancer cells or human plasma were added to 10 μL of CD81 antibody-conjugated MBs (1 mg/mL) and mixed on a rotator for 1.5 h at RT. The MBs were then washed with DPBS and collected on the 12-tube magnets. The beads were resuspended with 50 μL PBS containing 2 ug/mL of target-specific antibodies. The mixture was mixed on a rotator for 2 h at RT and washed twice with sterile DPBS and magnetic separation. At last, the beads were resuspended with 50 μL of QD655 linked with secondary antibody (Invitrogen, 10 nM in BlockAid) and incubated on a rotator for 1 h at RT. After four times washing with DPBS and magnetic separation, the sample was resuspended in 50 μL of DPBS and transferred into a micro-quartz cuvette for fluorescence characterization. The fluorescence spectra were measured using a HITACHI F-2710 Fluorescence Spectrophotometer, with an excitation wavelength of 375.0 nm and emission from 600.0 to 700.0 nm. All the spectra were measured with the same instrumentation parameters including scanning speed (300 nm/min) and PMT voltage (400 V). A sample without a primary antibody was used as a negative control for background subtraction.

2.7 Enzyme-linked immunosorbent assay (ELISA)

50 µL of cell-derived EXOs (1.0×10^9/mL) were added into a 96-well polystyrene plate (Nunc MaxiSorp) and incubated at 4 ºC overnight. Captured EXOs were washed 3 times with DPBS followed by blocking with 200 µL of 1% BSA at RT for 2 h. EXOs were then washed three times with DPBS and treated sequentially with following solutions: 50 µL of 2 µg/mL of target-specific antibodies (2 h, RT), 50 µL of anti-mouse secondary antibody conjugated with horseradish peroxidase (HRP, 1:3400 dilution in 1% BSA, 2 h, RT), 100 µL of 3,3′,5,5′ -tetramethylbenzidine (TMB, 30 min, RT). Oxidation of TMB was stopped with 100 µL of 2 M sulfuric acid (H_2SO_4). Each step was followed by three times washing with DPBS containing 0.1% tween 20 (DPBST) and two times with DPBS. The optical density was measured at 450 nm using a BioTEK ELx800 microplate reader. DPBS without primary antibody was used as the negative control.

2.8 Micro BCA Assay

To confirm successful conjugation of CD81 antibodies to MBs, the unreacted antibodies were quantitatively measured using micro BCA assay. The assay was performed according to the standard manufacturer protocol. Briefly, 150 µL of Working Reagent (WR, 25:24:1 MA:MB:MC) was added into each well together with 150 uL of each standard in a range from 0.0-1.0 µg/mL. The microplate was incubated at 37 ºC for 2 h. Absorbance was measured with BioTEK ELx800 microplate reader at 540 nm.

2.9 Statistical Analysis

Statistical analysis was performed to compare the expression levels of target proteins across different cell lines or between cancer patients and healthy controls using analysis of variance (ANOVA) with post hoc Scheffe method. A p-value ≤ 0.01 was considered significantly different.

The mean difference between different groups was considered to be significant if the absolute value was greater than the minimum significant difference derived from the Scheffe method. The marker difference between breast cancer patients and healthy donors was evaluated from generalized estimation equations (geepack v1.2-1 in R) to account for the measurement correlation within each individual. The diagnostic value of identified markers in breast cancer patients was evaluated by receiver operation characteristic (ROC) curve analysis using R packages.

3. Results and Discussion

3.1 Design of the Methodology

Figure 3.1.a shows the schematic design of exosomal surface marker detection using QDs in conjunction with magnetic separation with immuno-MBs. The method involves three straightforward steps: (1) capturing cell-derived or plasma EXOs with anti-CD81 antibody-conjugated MBs; (2) labeling surface cancer markers of interest on the captured EXOs with specific primary antibodies; (3) detecting the target-specific primary antibodies with secondary antibody-conjugated QD655 with fluorescence spectroscopy. To facilitate comparison between different samples, we use EXOs of the same concentration ($1x10^9$/mL). EXOs were pre-filtered with a 0.2 μm filter to get rid of cell debris or other impurities. Thus, the MBs can capture EXOs directly from the filtered plasma without further pre-purification due to the specificity of CD81 antibodies to EXOs.

We took advantage of exosomal marker CD81 from the tetraspanin family and used it as a selective way to capture EXOs to the surface of the beads. CD81 is proven to be the most reliable marker to differentiate EXOs from other types of EVs.[146] Our previous studies have shown that CD81 is highly expressed on EXOs from different breast cancer cell lines, breast cancer patients, and healthy donors [146]. The anti-CD81 anti-rabbit antibodies were linked to MBs via amide bonds

between the NHS-activated beads and the amine groups on the antibodies. The MBs also enrich EXOs onto the bead surface to improve detection sensitivity. Based on the size of the MB (1 μm) and EXOs (~100 nm), we estimate at least 300 EXOs can be concentrated onto each bead.

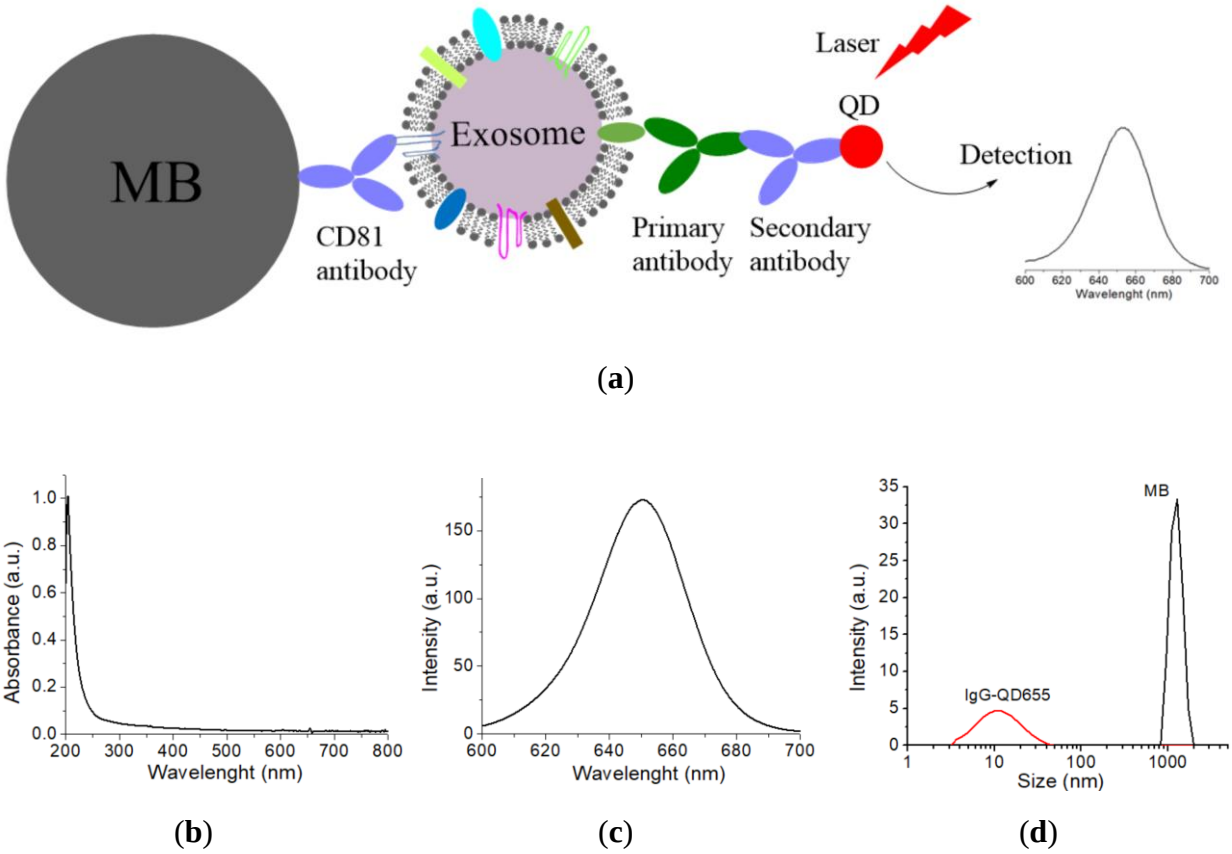

Figure 3.1. Schematic of the QD-based EXO assay (**a**) and characterization of QDs (**b**-**d**). EXOs were captured from biofluids with MB via CD81 monoclonal antibodies. Targeted surface cancer marker was recognized with primary antibody and then detected with secondary antibody-conjugated QD655. Signals were measured with fluorescence spectroscopy to quantify the QDs and correspondingly the surface protein markers on EXOs. (**b**) Absorption spectrum and (**c**) emission spectrum of IgG-QD655. (**d**) DLS characterization of the hydrodynamic size of IgG-QD655 and MB.

To further improve detection sensitivity, we chose commercially available far red-fluorescent QD655 (emission peak around 655 nm) (Figure 3.1.b&c). This QD655 is one of the brightest QDs, with quantum yield of 0.6. Especially, the size of QDs is small, usually 2-10 nm.

Even after conjugation with secondary antibody, the mean hydrodynamic size is only approximately 12 nm (Figure 3.1.d). For signal readout, a regular fluorescence spectrometer is used to measure the exosome solution in a microliter cuvette (50 μL). This capture, labeling, and detection method is extremely simple and easy to operate, practical for use in research and clinic labs.

3.2 Characterization of the Specificity and Sensitivity

Using MM231 EXOs as the model, we examined the specificity of the QD-based EXO assay. Figure 3.2.a shows the fluorescence spectrum of EXOs targeting high expression marker CD44 (olive), in comparison to three controls: EXOs targeting negative marker EpCAM (blue), absence of CD44 primary antibody (red), and absence of both EXOs and CD44 primary antibody (black). Figure 3.2.b shows the intensity plot of Figure 3.2.a. The results show that a strong fluorescence peak from QD655 was observed for EXOs targeting CD44 whereas fluorescence signals from QD655 were not detected for the three negative controls, suggesting the high specificity of our QD-based EXO assay. The three controls gave similar background signals that were most likely due to the scattering of the MBs and EXOs as well as instrumental noise.

Using SKBR3 EXOs as the model, we examined the sensitivity of our assay using high expression HER2 as the protein marker. A series of dilutions of SKBR3 EXOs were made to determine the limit of detection (LOD). Figure 3.2.c shows a mean of fluorescence spectra (n=3) of different EXO concentrations and Figure 3.2.d shows the dose-response curve of data from the fluorescence peak at 655 nm.

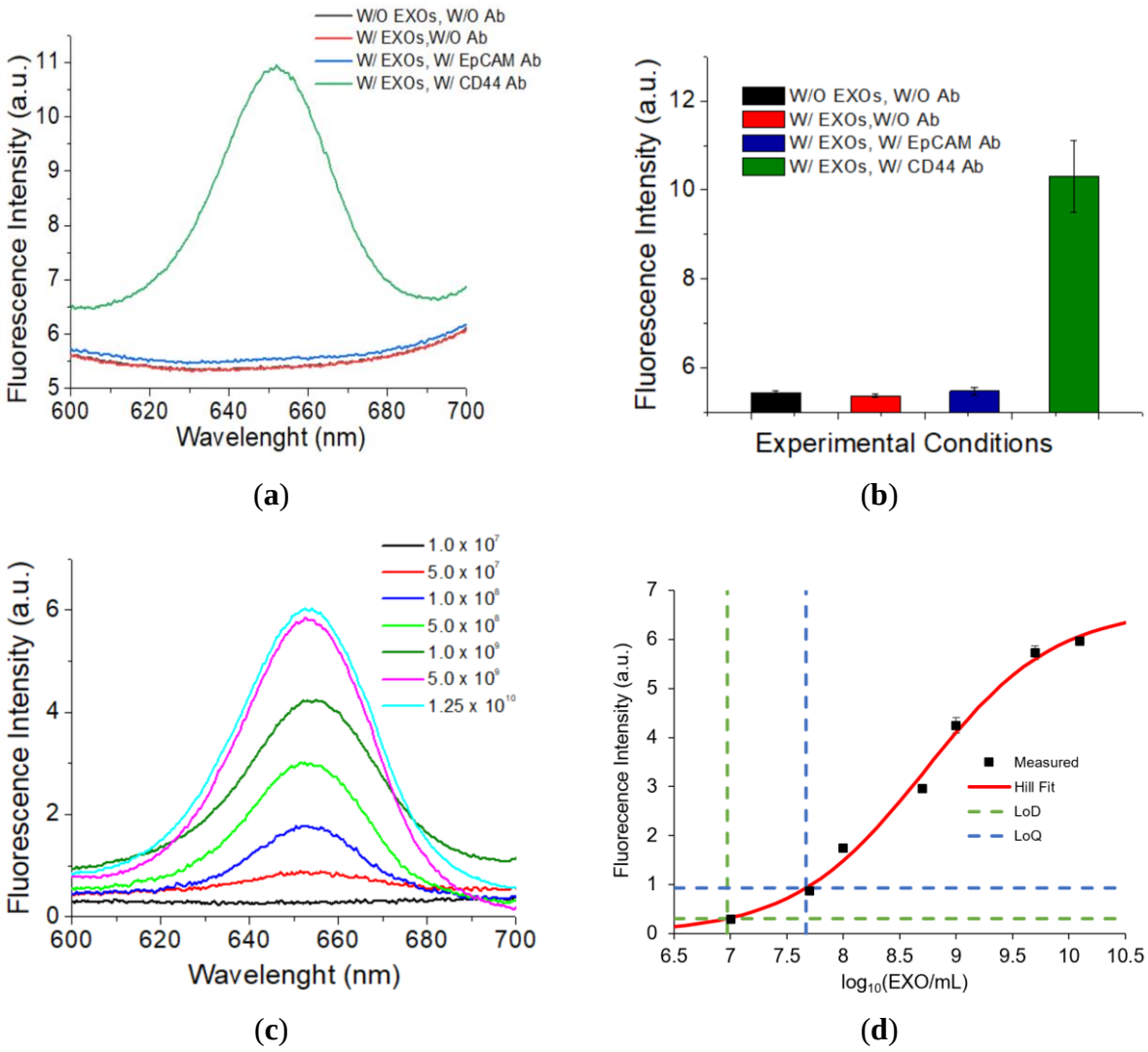

Figure 3.2. Examination of the specificity (**a**,**b**) and sensitivity (**c**,**d**) of the QD-based EXO assay. (a) Fluorescence spectra of MM231 EXOs treated under four different conditions. (**b**) Intensity plot of (**a**) using the fluorescence intensity at 655 nm. (**c**) Fluorescence spectra of SKBR3 EXOs targeting HER2 at different concentrations. (**g**) Dose-response curve based on data in (**c**) using the fluorescence intensity at 655 nm. Signals were background corrected using the signals without the presence of HER2 primary antibody. Error bar is the standard deviation from triplicate experiments. Ab: antibody.

All data were background corrected using the signals at 655 nm without the presence of a HER2 primary antibody. The results showed that the intensity of QD655 fluorescence signals increased with the increase of the EXO concentration. Signals reach saturation after $1x10^{10}$ EXOs/mL. The studies showed that the LOD was 9.3×10^{6} EXOs/mL. The concentration of

exosomes in human plasma is $>10^9$/mL.[146] Thus, our assay can detect exosomes at a concentration at least 107 times lower than a typical concentration of exosomes in plasma. This sensitivity was achieved using an excitation wavelength of 375 nm, scanning speed of 300 nm per min, and voltage at 400V. The limit of quantification (LOQ) was determined to be 4.7×10^7 EXOs/mL. The working concertation for the rest of the studies was set to 1.00 x 10^9 EXO/mL.

3.3 Validation with ELISA

To examine the feasibility of our assay for the detection of proteins on the surface of EXOs, we analyzed six surface markers on SKBR3 EXOs and compared them with ELISA (Figure 3.3.). The six proteins were from three different categories: epithelial marker EpCAM, breast cancer markers HER2, CD24 and CD44, and exosome markers CD9 and CD63. These markers have a varied expression on the SKBR3 cells, with high expression of HER2, moderate to high EpCAM and CD24, and low expression of CD44.[215–217] Figure 3a shows the mean fluorescence spectra of all the markers (n=3) and Figure 3.3.b shows the expression profile of these markers on the SKBR3 EXOs based on the data from Figure 3.3.a. The results show that SKBR3 EXOs have a high expression HER2 marker, moderate to high expression of CD9, CD63, CD24, and EpCAM, and very low expression of CD44 marker. These results are consistent with our previous reports using a Raman-based assay.[146]

To further validate our results, we measured the expression of the six markers on SKBR3 EXOs using ELISA (Figure 3.3.c&d). ELISA was performed in an indirect mode, in which EXOs were adsorbed onto a 96-well plate, labeled with primary antibodies, and detected with HRP-conjugated secondary antibodies. Similar to our QD-based method, the ELISA results showed high expression HER2, moderate to high expression of CD9, CD63, CD24, and EpCAM, and very low expression of CD44. A side-by-side comparison (Figure 3.3.d) shows a strong correlation of the

two methods, with a correlation coefficient of 0.972. Compared to ELISA, our QD-based assay is much quicker, with a turnaround time of 4.5 h in contrast to 2 days for ELISA.

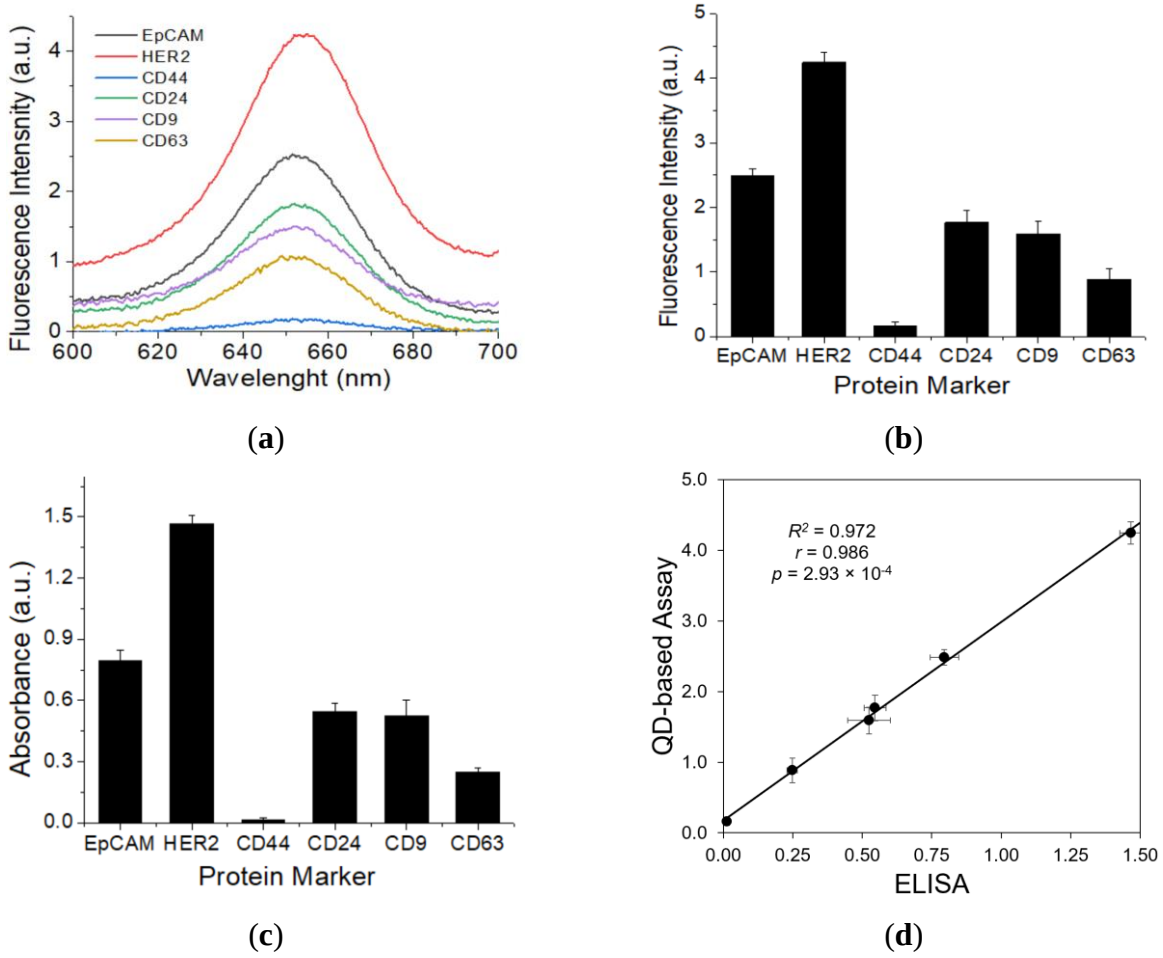

Figure 3.3. Comparison of QD-based assay and ELISA for the detection of exosome surface protein markers. (**a**) Fluorescence spectra of targeted markers on the surface of SKBR3 EXOs using the QD-based method. (**b**) Protein expression profile based on data in (**a**) at the mean intensity of 655 nm. (**c**) Protein expression profile of targeted surface markers on the surface of SKBR3 EXOs determined using ELISA. Error bar is the standard deviation from triplicate experiments.

3.4 Detection of Different Protein Markers on EXOs Derived from Different Cell Lines

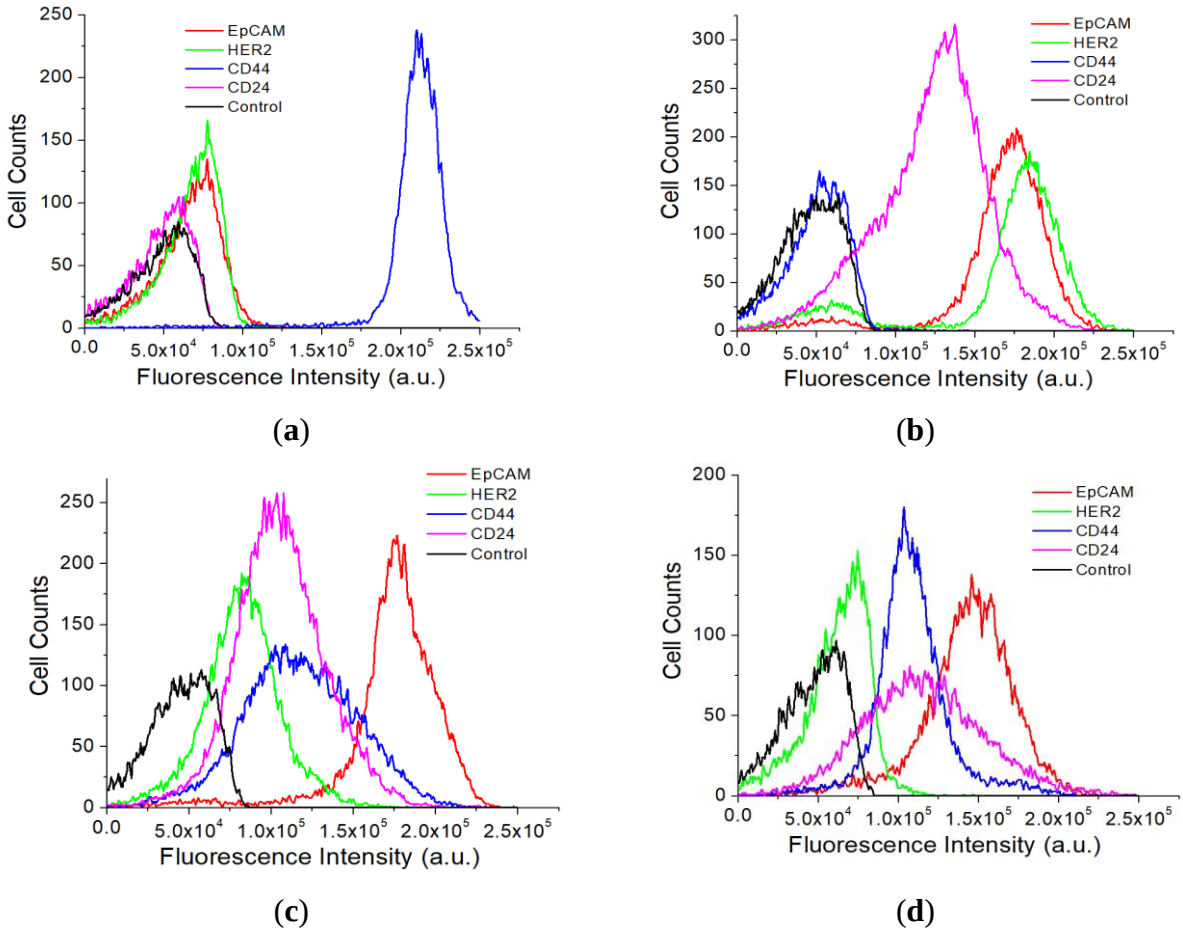

Figure 3.4. Flow cytometry analysis of different cell surface protein markers for SKBR3 (**a**), MM231 (**b**), and MCF7(**c**) breast cancer cell lines and normal breast cell line MCF12A (**d**).

Using the QD-based assay, we compared the expression of four common breast cancer-associated surface protein markers EpCAM, HER2, CD44, and CD24 on three breast cancer cell lines, SKBR3, MM231, and MCF7, and compared with those from a normal breast cell line MCF12A. Flow cytometry shows distinct expression patterns of these markers on these cell lines (Figure 3.4.). SKBR3 is a HER2-positive breast cancer cell line. It also has a strong expression of EpCAM and moderate expression of CD24. MM231 is a triple-negative-

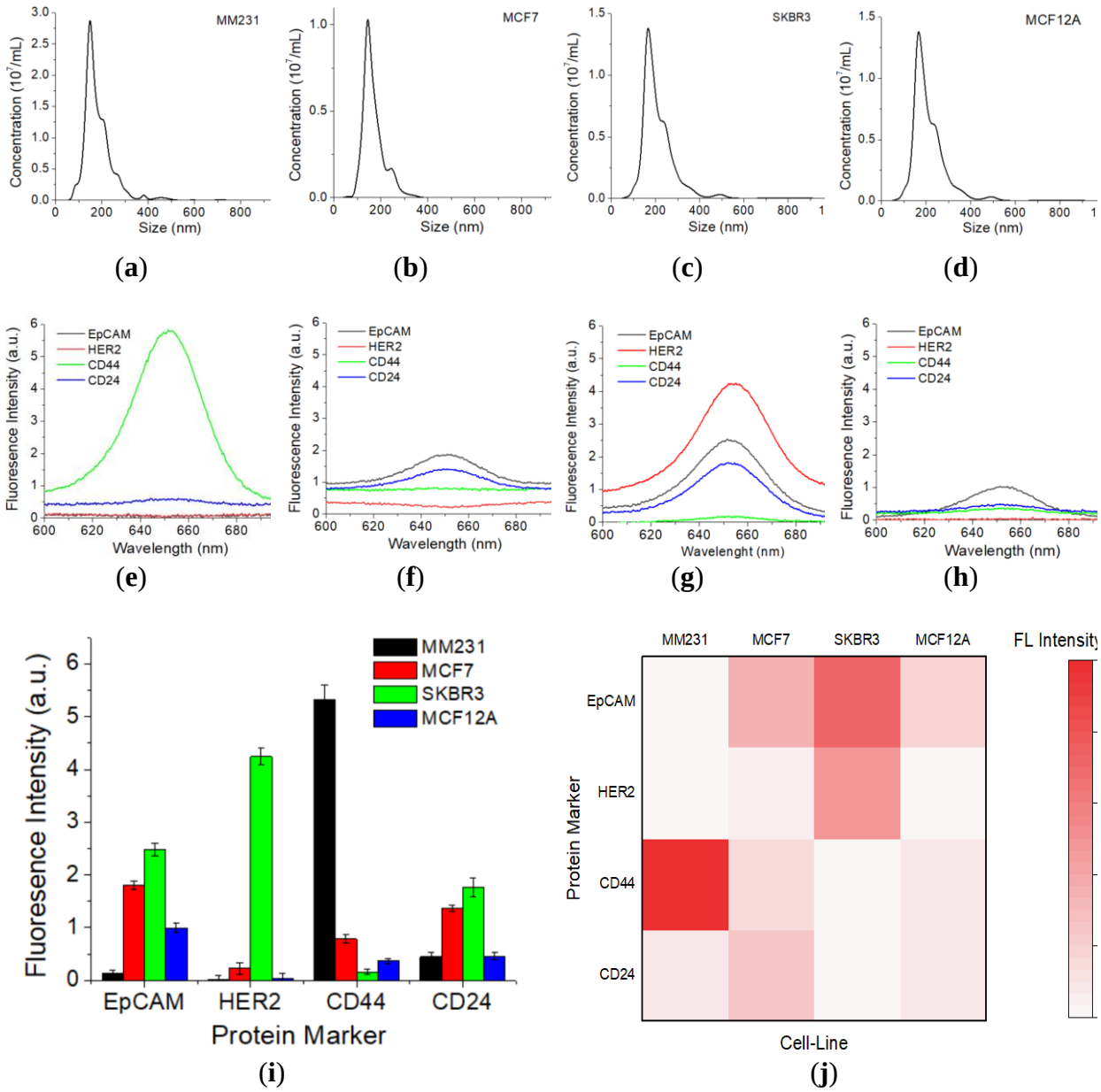

Figure 3.5. Detection of surface protein markers on EXOs derived from different breast cancer cells (MM231, MCF7, and SKBR3) in comparison to normal cells (MCF12A). (**a-d**) Size distribution of EXOs measured with NTA. (**e-f**) Fluorescence spectra of EXOs targeting different surface markers. (**i**) Comparison of protein marker expressions based on the fluorescence mean intensity at 655 nm. The p-values among the four cell-lines for markers EpCAM, HER2, CD44, and CD24 are 2.3×10^{-8}, 6.2×10^{-10}, 1.3×10^{-9}, and 3.0×10^{-6}, respectively. (**j**) Heatmap comparison of protein expression based on data in (**i**). Error bar is the standard deviation from triplicate experiments.

metastatic breast cancer cell line. It is known to have extremely high expression of CD44, but not CD24. The MCF cells have strong expression of EpCAM and moderate expression of CD44 and CD24. The MCF12A normal cells have a weak expression of EpCAM, HER2, CD44, and CD24.

NTA characterization (Figure 3.5.a-d) shows the size of EXOs derived from SKBR3, MM231, MCF7, and MCF12A was 167 ± 80, 149 ± 65, 145 ± 45, 138 ± 71 nm, respectively. Figure 3.5.e-h show fluorescence spectra of each marker on EXOs derived from each cell line. Signals were corrected with the background, the fluorescence spectrum without primary antibody. Figure 3.5.i is a quantitative comparison of the background-corrected fluorescence intensity at 655 nm. Figure 3.5.j is a heatmap comparison using the data from Figure 3.5.i. Compared to the protein expression of these markers on cells (Figure 3.4.), it is clear that EXOs reflect the surface protein expression of their originating cells. For example, CD44 is highly expressed on MM231 EXOs. HER2 is highly expressed on SKBR3 EXOs but it is negative on MM231 EXOs and MCF12A normal exosomes. It has a low expression on MCF7 exosomes. Expression of EpCAM follows a decreased order of SKBR3, MCF7, MCF12A, and MM231. The normal MCF12A EXOs are negative for HER2 but have low expression of CD44 and CD24.

3.5 Detection of Breast Cancer via Plasma EXOs

The clinical potential of our QD-based EXO method for cancer diagnostics was evaluated using HER2-positive breast cancer as the disease model. HER2- positive BC is one of the major BC subtypes. Identification of HER2 overexpression directs effective treatment with trastuzumab. For proof-of-concept studies, we analyzed plasma from eight HER2-positive breast cancer patients and eight healthy donors. All plasma samples in this study were diluted with 1x PBS and filtered through a 0.2 μm PES filter. No further purification was performed. Figure 3.6. shows the size of plasma samples from all the human subjects. The size of EXOs ranged from 107 ± 35 to 189 ± 48

nm, without statistically significant differences between healthy donors and cancer patients. Based on the concentrations determined by NTA, all samples were further diluted to a concentration of 1.00×10^9 EXOs/mL before use.

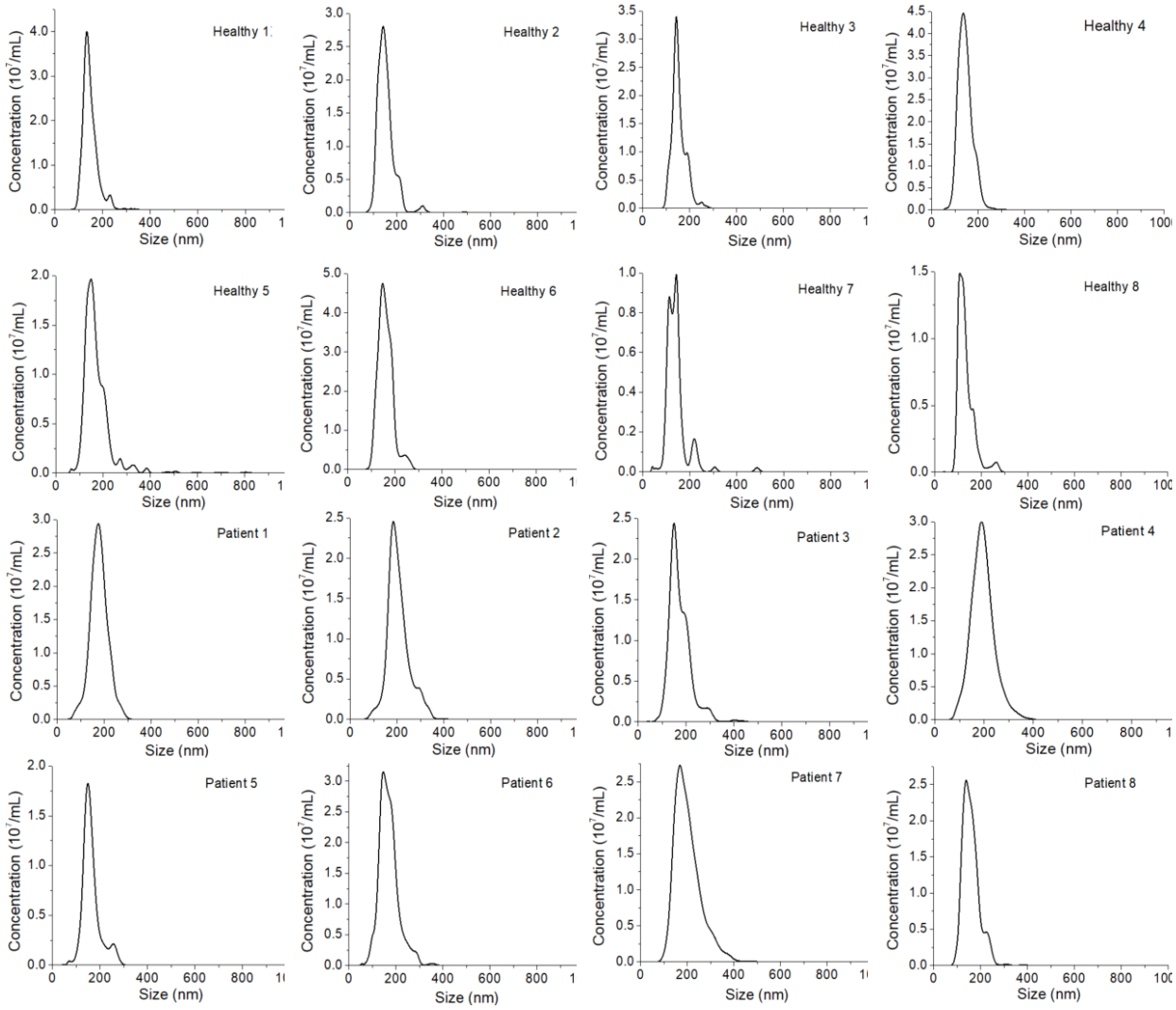

Figure 3.6. Size distribution of EXOs in plasma from HER2-positive breast cancer patients and healthy donors measured by NTA.

Figure 3.7.a&b show the fluorescence spectrum of EXOs from patients (a) and healthy controls (b). The results showed that six cancer patients (75%) showed fluorescence signals from 0.5 to 2.4 while all eight healthy controls gave signals lower than 0.45. Statistical analysis with

ANOVA showed that the mean fluorescence intensity of HER2 expression on the plasma EXOs from the cancer patients was significantly different from that of healthy control, with a p-value of 6.44×10^{-3} (Figure 3.7.c). The HER2 expression was approximately five times higher than that of healthy control (1.24±0.74 for patient versus 0.25±0.12 for healthy control). Further ROC analysis with sensitivity and specificity showed that exosomal HER2 expression was a strong diagnostic marker for HER-positive patients, with AUC = 0.96875. This is consistent with previous studies by our group using the Raman method,[146] and other groups using surface plasm resonance.[126] The studies showed our QD-based exosome assay can detect breast cancer via HER2 detection and quantification using plasma exosomes from patients.

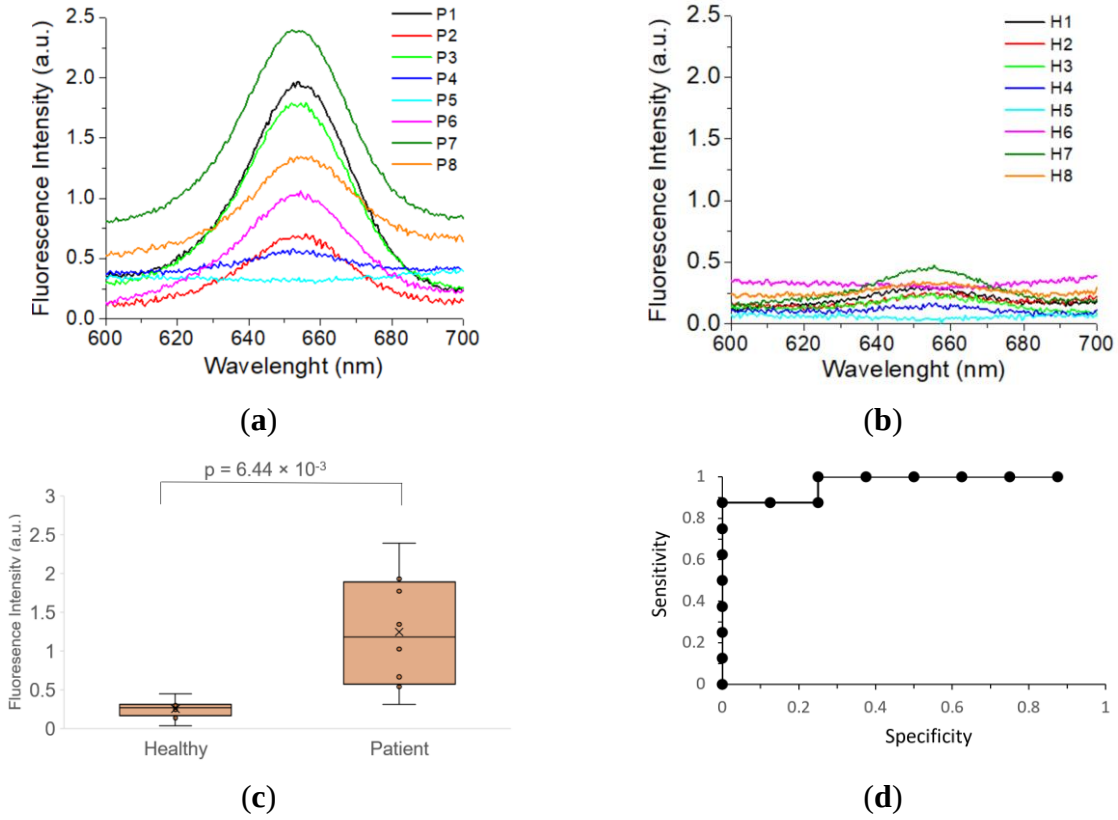

Figure 3.7. Detection of HER2-positive breast cancer using QD-based EXO assay. (**a**) Average fluorescence spectra (n=3) of HER2-targeted EXOs from each patient with HER2-positive breast cancer. (**b**) Average fluorescence spectra (n=3) of HER2-targeted EXOs from each healthy donor. (**c**) Comparison of the exosomal HER2 expression between patient and healthy control. (**d**) ROC curve for detecting HER2-positive breast cancer by QD-based EXO assay.

4. Conclusion

In conclusion, we have demonstrated that exosomal surface markers can be quantitatively detected using QDs in conjunction with magnetic separation with microbeads. In this method, exosomes were captured and concentrated onto magnetic microbeads followed by recognition of targeted surface markers with primary antibody and then detection with secondary antibody-conjugated QDs. Using this QD-based method, we can specifically and quantitatively detect different surface protein markers on exosomes from different breast cancer cell lines. We can also differentiate cancer exosomes from normal exosomes using cancer-associated surface protein markers. Using pilot clinical samples, we have shown that HER2-positive breast cancer can be detected by analysis of HER2 expression on plasma exosomes using QDs in conjunction with magnetic separation and enrichment. Cancer patients show about five times higher HER2 expression than healthy donors. The high AUC value (AUC = 0.96875) suggests exosomal HER2 as a strong diagnostic marker for HER2-positive patients.

Compared to previous methods using QDs, our method is simple and rapid. Our method follows a straightforward capture, labeling, and measurement methodology, requiring only 4-5 h total time. It does not require extensive pre-preparation of plasma samples and sophisticated instrumentation. Detection was simply performed with bulk fluorescence measurement with a routine fluorescence spectrometer. The method is also highly sensitive, with LOD of 9.3×10^6 EXOs/mL that is over 100 times lower than a typical exosome concentration in plasma. Due to the advantages in simplicity, high sensitivity, and widely accessible instrumentation, our method can be widely used in research and clinical laboratory. We would like to point out that our research results need to be further validated with a larger cohort before clinical applications. The throughput at the current stage is also limited. However, the method can be adapted for simultaneous analysis

of multiple samples using multi-well magnetic microplates such as the EpiMag HT magnetic separator. For signal readout, a portable fluorescence spectrometer may be used to measure samples directly in the microplates in the absence of the magnets.

Chapter 4: PURIFICATION-FREE SINGLE EXOSOMES PROTEIN PROFILING WITH FLUORESCENCE AND DARKFIELD IMAGING FOR EARLY CANCER DETECTION

1. Introduction

A critical step towards successful cancer treatment is undoubtedly an early diagnosis.[218] Therefore, there has been an ongoing search for a way to quickly and non-invasively take action to detect this disease in time.[219–222] One of the possible approaches to achieve this end is the relatively new field of extracellular vesicles (EVs). EVs, especially their subgroup known as exosomes, appear to be ideal biomarkers that could allow early detection, characterization, and treatment monitoring in cancer patients, but also other diseases such as Alzheimer's disease or Frontotemporal dementia.[223–225] The significance of EV's composition in biological function motivated the development of various analytical methods to detect proteins, lipids, and genetic material. However, it is very challenging to detect these molecular contents. This is mainly because of i) small size of vesicles contributing to the low amount of the protein content, ii) interference caused by aggregates of proteins, lipoproteins and overall complexity of the sample, iii) refractive index that is approximately the same as water and thus complicates direct detection in aqueous solution.[226,227]

Moreover, the concentration of exosomes in the bloodstream and other body fluids is dependent on the number of cells that produce these vesicles, it can be concluded that during the early stages there is only a small fraction of EVs from cancer cells in the bloodstream.[228] Exosomes of cancer origin are thus masked by many non-tumor exosomes from various tissues and hematopoietic cells. The heterogeneous composition of exosomes in clinical samples thus further limits the sensitivity of the bulk analytical approaches which are in most cases already very sample

demanding. In an example, ELISA or Western Blotting requires a minimum of 10^5-10^6 EVs to measure a single biomarker and more sensitive methods such as nPLEX or μNMR require 10^2-10^3 EVs.[72,128] For this reason, there is a need for a detection approach that can detect small amounts of cancer cell-derived exosomes that are mixed with a vast majority of non-tumor exosomes and can even operate at the single-molecule level in a reasonable amount of time without the need of large sample size, labor-intensive purification, and complex sample labeling.

Current attempts on a single vesicle technology (SVT) are mainly focused on modifications of high-resolution flow cytometry-based methods coupled with fluorescent amplification labeling.[113,121,229–235] However, the small size of EVs causes two major complications i) difficulty or literally impossibility to distinguish such small particles from the background, ii) scarcity of antigens on EVs' small surface. Progress to achieve this goal is therefore very slow and limited. Löf et al. addressed these limitations by using multiplex and multicolor in situ proximity ligation assays (PLA).[236] In this study they employed a very complex procedure of a rolling circle replication of DNA combined with detection oligonucleotides coupled to fluorophores. The growing chain of DNA with the incorporated detection oligonucleotides amplified the signal for each targeted protein. Although, this method has proven to be successful and very specific, it is a too complex method for general clinical conditions. Further, the method struggles with optical cooperation of PLA probes in multi-color application which may cause some EVs to fall below a threshold and thus not be correctly detected. Lee et al. waived flow cytometry as a method of choice for SVT and constructed a microfluidic device for exosome immobilization and on-chip immune-staining and fluorescence imaging.[128] Their procedure was based on the subsequent addition of three different fluorochromes. After labeling and detecting the first targeted protein with the first applied fluorochrome, the signal was quenched before targeting another protein with

a second fluorochrome. This way they achieve a method that could detect three different proteins simultaneously, and they could potentially increase this number by employing more fluorochromes. However, this on-chip method can analyze only one sample at a time and has no potential to be scaled up for mass use. Thus, the need for efficient, scalable, and reliable SVT that could apply to the general clinical environment is still present.

In this chapter, we report progress towards an SVT that is capable of sensitive, specific, and efficient surface protein profiling of exosomes directly captured from biofluids. Exosomes were directly captured from culture medium or plasma based on their CD81 expression, a biomarker that differentiates exosomes from other types of extracellular vesicles. We localized the captured exosomes by staining their phospholipid membrane with fluorescent dyes and we define their positions by fluorescence imaging. Additionally, we targeted surface proteins on individual exosomes using either a fluorescent tag coupled with fluorescence imaging or a nanosphere tag coupled with darkfield imaging. By combining both images, we thus obtained both the position of the individual exosomes and the relative expression of proteins on the exosome surface. Single exosome profiling data were then generated within minutes via dual imaging analysis. Our SVT is simple and fast and requires only microliters of diluted (typically 20-fold dilution) plasma samples, making single exosome molecular analysis easy and practical for clinical use. It would accelerate the progress in the exosome field in terms of biomarker discovery and clinical translation.

2. Materials and Methods

2.1 Materials

All reagents were purchased from Sigma-Aldrich (St. Louis, MO) unless otherwise specified. Antibodies were purchased from Biolegend (San Diego, CA). Cholesterol-PEG-Cy5 fluorescence dye was purchased from Nanocs, Inc (Natick, MA). Gold colloid nanospheres 60 nm were purchased from BBI solutions (Portland, ME). Epoxy resin was purchased from Epoxy Technology, Inc. (Billerica, MA) and gold coated silicon wafer was purchased from Angstrom Engineering (Kitchener Ontario, Canada). All cell lines were purchased from ATCC (Manassas, VA). Cell culture media were purchased from VWR (Radnor, PA). Organic fluorophores, quantum dots, BlockAid and FBS were purchased from Fisher Scientific (Waltham, MA).

2.2 Fabrication of Au Multi-well Chip

Gold was strip down from gold coated silicon wafer disk (100 mm Dia. x 0.525 mm thick) using glass slide chips (12.5 x 12.5 x 1 mm) and a heat curing epoxy resin. Briefly, after combining epoxy part A and B, a thin layer of the mixture was applied to glass chips and the chips were pressed on gold surface of the silicon wafer. The wafer with chips was cured at 150 ^{o}C for 2h. Individual chips were carefully peeled off with a gold layer pasted on their surface. A piece of an electrical tape (12.5 x 12.5 x 0.5 mm) was perforated with 4 mm holes (4 holes per chip) and was used as a sample-well template. The surface of each chip was cleaned with nitrogen gas, the template was firmly pressed against it, and chamber chip was ready to use.

2.3 Preparation of AuNP Tags

Antibodies of interest were linked with PEG-linker by incubating 20 µg of antibody with 100-fold molar excess of NHS-PEG-SH (MW 1000) for 2 h at 37 ºC. The reaction was quench with 50 mM Tris Buffer pH 8 for 5 minutes at RT and then purified three times by a centrifuge filtration through a 10 kD filter. The filter content was redispersed with 20 mM HEPES buffer pH 7. To make 43 pM of AuNP tags, 14,000-fold excess of Ab-PEG-SH is added and vortexed for 1,5 h at RT. Then 30,000-fold excess of mPEG-SH (MW: 2,000) were added and vortexed for another 1,5 h at RT. The final mixture is purified three times by centrifugation at 10,000 x rpm for 6 minutes. The pellet was redispersed in PBST 0.01% with 0.05% Sodium azide and stored at 4 ºC for later use.

2.4 Collection of Exosomes from Cell Lines

Cells were cultured in their respective media with 10% FBS and 1% Pen/Strep (100×) at 37 °C under 5% CO_2. The medium was RPMI 1640 for SKBR3 and Dulbecco's Modified Eagle Medium (DMEM) with high glucose for MDA-MB-231. To collect exosomes, cells were grown in conditioned cell culture media (media + 10% exosome-free FBS) for 48 h. To purify exosomes, culture supernatant was collected and centrifuged at 430 ×g at RT for 10 min. The supernatant was collected and centrifuged at 16,500 ×g at 4 °C for 30 min. The supernatant was collected and centrifuged at 100,000 ×g at 4 °C for 70 min. After removing the supernatant, the exosome pellet was resuspended in cold sterile PBS and centrifuged again at 100,000 ×g at 4 °C for 70 min. The exosome pellet was resuspended in cold sterile PBS and stored at -80 °C until use. The concentration and size distribution of exosomes were characterized using NTA with a NanoSight LM10 microscope (Malvern Instruments, Inc).

2.5 Exosome Capture to Au Substrate

Anti-CD81 rabbit monoclonal antibody was linked with PEG linker by incubating 20 µg of the antibody with 100-fold molar excess of NHS-PEG-SH (MW 1000) for 2 h at 37 ^{o}C and then purified by centrifugation filtration with a 10KD filter. To capture exosomes, the chamber slide was incubated with 25 µg/mL PEG-linked anti-CD81 antibodies in 5% BSA (8 µL for each well) for 12 h and then 0.1 mM MU-TEG for 1 h. Then, exosome solutions were added and incubated for 3 h, while after first and second hour of incubation the solution was removed and replaced with a fresh drop of exosome solution. A combination of washings with PBS-Tween 0.01-0.05% and PBS was used for washing after each step, except for the last step when only PBS was used to avoid disruption in exosome-cholesterol labeling.

2.6 Exosome Labeling

2.6.1 SVT Using Two Organic Fluorophores

To label targeted protein on exosomes, the surface was block with BlockAid solution for 30 min at RT. After the blocking step, 5 µg/ml of primary antibody in 1x PBS were added and incubated for 2 h at RT followed by addition of a secondary antibody conjugated to organic fluorophores (1-5 µg/mL, 1.5-2 h, RT). For amplified labeling, the biotinylated IgG was used as a secondary antibody (2-5 µg/mL, 1.5-2 h, RT) followed by addition of fluorophore-streptavidin conjugates (2-5 µg/mL, 1 h, RT). To fluorescently label exosome membrane, 5 µM lipophilic dye was added for 30 minutes at RT. Sample was washed with 1x PBS 3-5 times after each step.

2.6.2 SVT Using Quantum Dot 655 in Conjunction with Organic Fluorophore

To label targeted protein on exosomes, the surface was block with BlockAid solution for 30 min at RT. After the blocking step, 5 µg/ml of primary antibody in 1x PBS were added and incubated for 2 h at RT followed by addition of a secondary antibody IgG-QDot 655 (1-5 µg/mL, 1.5-2 h, RT). For amplified labeling, the biotinylated IgG was used as a secondary antibody (2-5 µg/mL, 1.5-2 h, RT) followed by addition of QDot 655-streptavidin conjugates (2-5 µg/mL, 1 h, RT). To fluorescently label exosome membrane, 5 µM lipophilic dye was added for 30 minutes at RT. Sample was washed with 1x PBS 3-5 times after each step.

2.6.3 SVT Using AuNPs in Conjunction with Organic Fluorophore

To label targeted protein on exosomes, 20 pM of AuNP target-specific tags in 2.5% BSA were added and incubated with the captured exosomes for 2 h, while after first hour of incubation the solutions were removed and replaced with fresh drops of AuNP tag solutions. To fluorescently label exosomes, 5 nM Cholestorol-PEG-Cy5 was added for 15 minutes at 37 ^{o}C. A combination of washings with PBS-Tween 0.01-0.05% and PBS was used for washing after each step, except for the last step when only PBS was used to avoid disruption in exosome-cholesterol labeling.

2.7 SVT Microscopy Instrumentation

2.7.1 Nikon Eclipse Ti A1Plus Confocal Microscope

The microscope is equipped with four lasers made by Coeherent: DAPI (λ = 403.4 nm, Cube), FITC (λ = 488.0 nm, Sapphire), TRITC (λ = 561.3 nm, Sapphire), and Cy5 (λ = 647.0 nm, Cube). Laser filter channels: DAPI 425-475 nm (PMT, blue), FITC 500-550 nm (GaAsP, green), TRITC 575-625 nm (GaAsP, red), Cy5 650-720 nm (PMT, far red). The fluorescence images were

taken under 20x objective (0.45 S plan Fluor ELWD, air immersion). The image was detected by a Andor DU-897 EM-CCD camera.

2.7.2 Custom Nikon LV 150N Microscope for FL and Dark-field Imaging

The system was constructed on a customized Nikon LV 150N microscope. A halogen lamp was used for bright and dark field imaging. A Melles Griot continuous-wave He laser (Model 05-LPH-925, λ = 632.8 nm) was used to excite a fluorescent dye. The laser beam, after being filtered by a band-pass filter, is defocused by a lens so a large area of the sample (192 μm in diameter) was homogenously illuminated. The fluorescence signal was detected by a Photometrics CoolSnap DYNO camera to image single exosomes. Thus, the same area of exosome samples on the chamber slide can be simultaneously detected with dark field light scattering imaging and fluorescence imaging.

2.7.3 Image Acquisition with Customized Nikon LV 150N Microscope

First, the microscope was set to florescence mode and exosomes labeled with Cy5 FL dye were excited with a He laser at 632.8 nm. The florescence image was taken under 50x objective (WD = 10 mm, air immersion). This image served as the “target” to provide information on level of targeted protein expression on surface of exosome. The setup was then switched to a dark field mode and an image of same area was captured. The dark field light scattering image served as the “mask” to provide the exact location of exosomes.

2.8 Imaging Processing and Analysis

Each set of images, "mask" and target", is analyzed for a single exosome protein expression via Python-based analysis method developed by Dr. Wang's group. The image processing follows three major steps: 1) subtraction of background and large bright areas caused by surface imperfections and reagent aggregates 2) conversion of both images into binary images 3) overlay of two images to determine locations of exosomes and to extract light scatter intensity signals over exosome spot automatically to build a histogram. To analyze the data, the mPEG-AuNP control was used to establish the cutoff value of the light scatter signals which was used to identify protein-positive exosomes and calculate the fraction of protein-positive exosomes *Fp*.

2.9 Enzyme-linked Immunosorbent Assay (ELISA)

50 µL of 2 ug/mL exosomes-capture antibodies (anti-CD81) were added to a 96-well polystyrene plate (Nunc MaxiSorp) and incubated at 4 ºC overnight. The wells were washed 3 times with DPBS-Tween 0.2% (DPBS-T) and twice with DPBS 1x. The surface was blocked with 100 µL of 1% BSA in DPBS at RT for 2 h followed by washing three times with DPBS-T and twice with DPBS 1x. 50 µL of $1.00x10^9$/mL isolated exosomes from cell-culture media were added into each well for 2 h at RT. After washing 3 times with PBS 1x each well was treated with following solution in the order listed: 50 µL of 2 ug/mL of target-specific antibodies (2 h, RT), 50 µL of anti-mouse IgG Ab conjugated with horseradish peroxidase (HRP, 1:60 dilution in 1% BSA, 2 h, RT), 100 µL of 3,3′,5,5′ -tetramethylbenzidine (TMB, 30 min, RT). After each step each well was washed three times with DPBS 1x, and final oxidation of TMB was stopped with 100 µL of 2 M sulfuric acid (H_2SO_4). The absorbance was measured at 450 nm using a BioTEK ELx800 microplate reader. DPBS with no exosomes was used as the control.

3. Results and Discussion

Figure 4.1. shows an overview of exosome capture on a gold chip. Each gold chip was fabricated by a striping method from a gold-coated silicon wafer and was subsequently glued to a multi-well template made of an array of perforations with a diameter of 4 mm (~0.5 mm height) allowing for each well to hold 8.0 µL of working volume. To capture exosomes, we functionalized the gold surface with a long chain of polyethylene glycol-thiol (NH2-PEG-SH, MW 5000) conjugated to anti-CD81 antibodies. As previously mentioned CD81 belongs to a tetraspanin family and represents an exosomal marker that has been proven to differentiate exosomes from other extracellular vesicles.[15,237] Although CD81 is not invariably expressed on all exosomes, the presence of CD81 positive exosomes is abundant in all exosomes of various cellular origins.

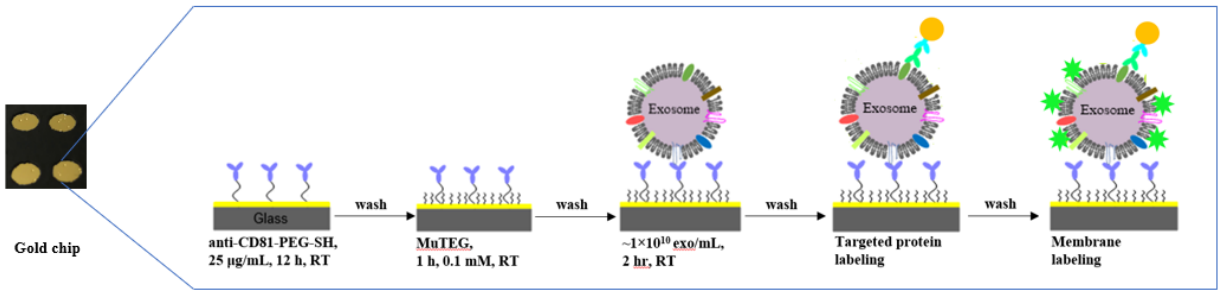

Figure 4.1. Schematic of SVT strategy for exosomes capture and labeling on a multi-well gold chip.

To prevent cross-talking between free binding sites of CD81 capture antibody and secondary antibody used in protein labeling step, we used antibodies raised in different hosts. CD81 antibody was raised in rabbit, while secondary antibody was raised in goat. To fully saturate the functionalized surface and thus prevent non-specific interactions between the exposed gold surface and applied molecules (exosomes, antibodies, labeling probes, etc.), we used the short hydrophilic polymer 11-mercaptoundecyl tetra (ethylene glycol) (MU-TEG). As we have already

demonstrated in our previous studies, this method of surface functionalization appears to be very specific and proven for exosome capture.[146]

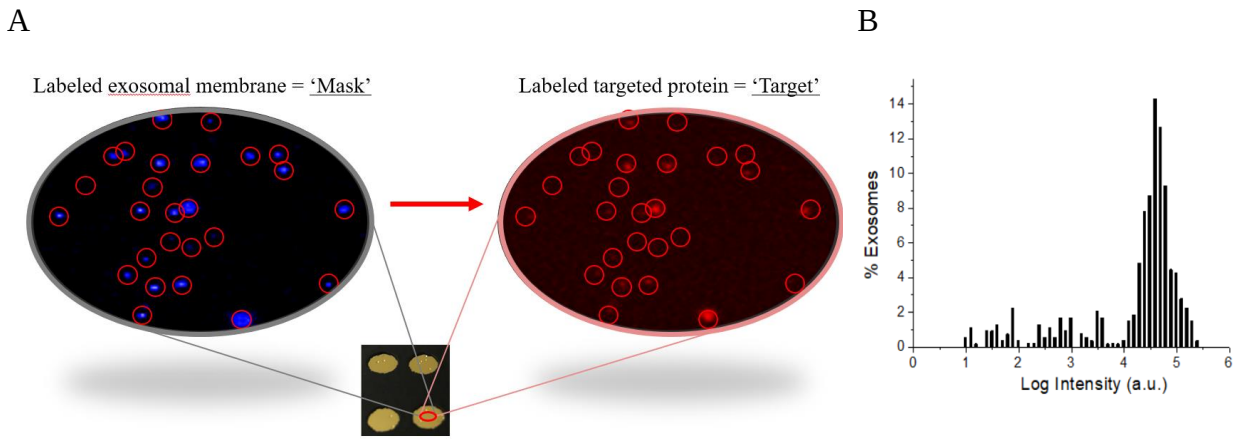

Figure 4.2. Design of exosome protein profiling from dual image strategy. (A) Transfer of the exosomes location from "mask" image to "target" image. (B) Histogram of protein expression based on intensity values measured from each exosome location.

Our SVT is based on the idea of a dual imaging approach (Figure 4.2.). Each selected area of functionalized gold surface and captured exosomes captured on it is subjected to two detection images using microscopy. The first image, which we call the "mask", is designed to detect the exact position, quantity, and quality of captured exosomes. To achieve this goal exosomes are stained with lipophilic fluorescence dyes and are detected with a fluorescence microscope. The organic dyes we used are the very same which are widely used in the fields of biology and medical histology for tissue staining and cellular staining and have been proven to a some extend work for exosomes as well.[238,239] The types of images we call "target" are designed to record the presence and relative amounts of proteins on the surface of individual vesicles, using an antibody conjugated detection tag. To reach this goal we tested multiple different approaches including fluorescent imaging and dark-field imaging coupled with protein tags such as 1) organic fluorophores 2)

quantum dots, and 3) Au nanospheres. Each approach is individually described in the sections below.

When both images were acquired, the exact location of each exosome was transferred as a circular area from the "mask" image onto the "target" image. Intensity per area can then be measured from the "target" image based on the amount of protein tag bound to the individual exosome corresponding to protein expression. Obtained results can be read as exosome count vs intensity per area (Figure 4.2.B).

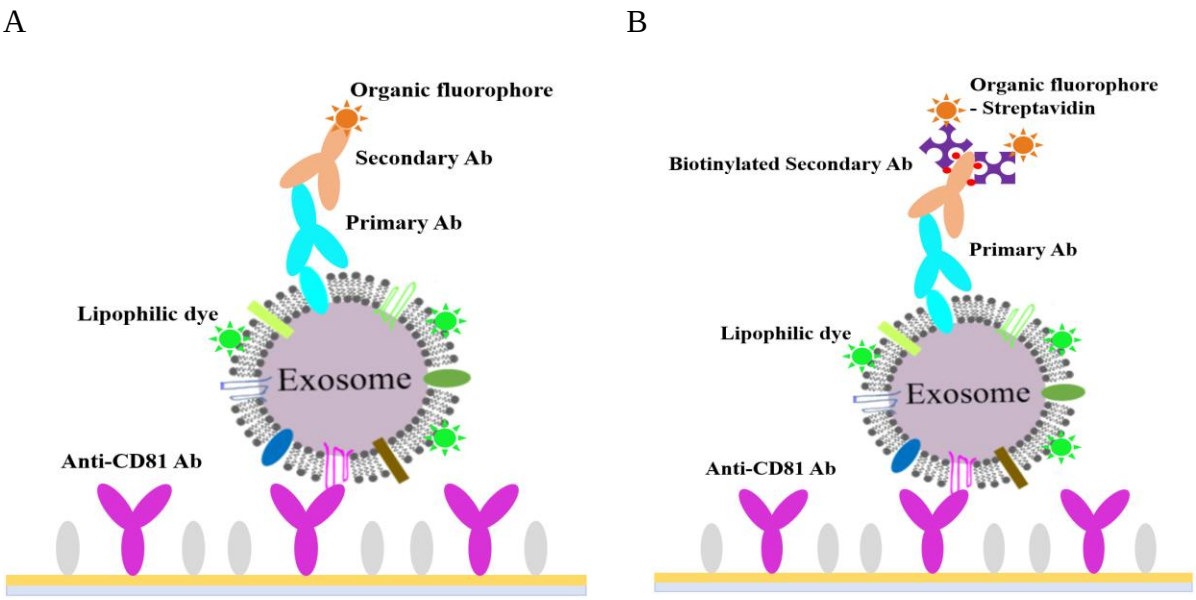

Figure 4.3. Schematic of molecular exosome detection with two organic fluorophores. (A) Indirect protein labeling with standard (unamplified) approach using secondary antibody directly coupled to an organic fluorophore. (B) Indirect protein labeling with amplified approach using biotinylated secondary antibody and streptavidin coupled to an organic fluorophore.

3.1 SVT Using Two Organic Fluorophores

The initial approach towards the development of a single vesicle technology was with the help of confocal microscopy and two organic fluorophores with different emission wavelengths. The labeling with organic fluorophores represents a very common and practical way of fluorescent

staining, which has been used in the field of biology for decades and are currently used to detect exosomes as well.[130,240–252] The main advantages of organic fluorophores include a wide spectral range of available dyes, relatively good photostability, small size, and high brightness.

Proteins on the surface of exosomes were labeled with an indirect approach using targeted primary antibodies and secondary antibodies linked to fluorophores (Figure 4.3.A). A lipophilic fluorophore with a different emission wavelength was then used to stain the exosomal membranes (Figure 4.4.). Every area on the sample was imaged twice under two different channels corresponding to distinct excitation and emission spectra of each dye. Since organic dyes pose narrow absorption and excitation bands, the theory suggests that if absorption bands for two fluorophores do not overlay each other they can be used simultaneously. However, since exosomes are only 40 to 200 nm in diameter, we suggest that their small surface area limits the number of individual surface proteins to only a few (~ 1-5 proteins per exosome). The very low number of targeted proteins thus limits the number of fluorescent tags. This weak FL signal required many times higher levels of laser power than it would be used for cell or tissue imaging. Nevertheless, higher excitation power caused fluorescent bleeding between membrane stain and protein tag and hence limited what would be a requisite instrument setting as well as narrowed down fluorophore that could be coupled together (Figure 4.5.A1,2).

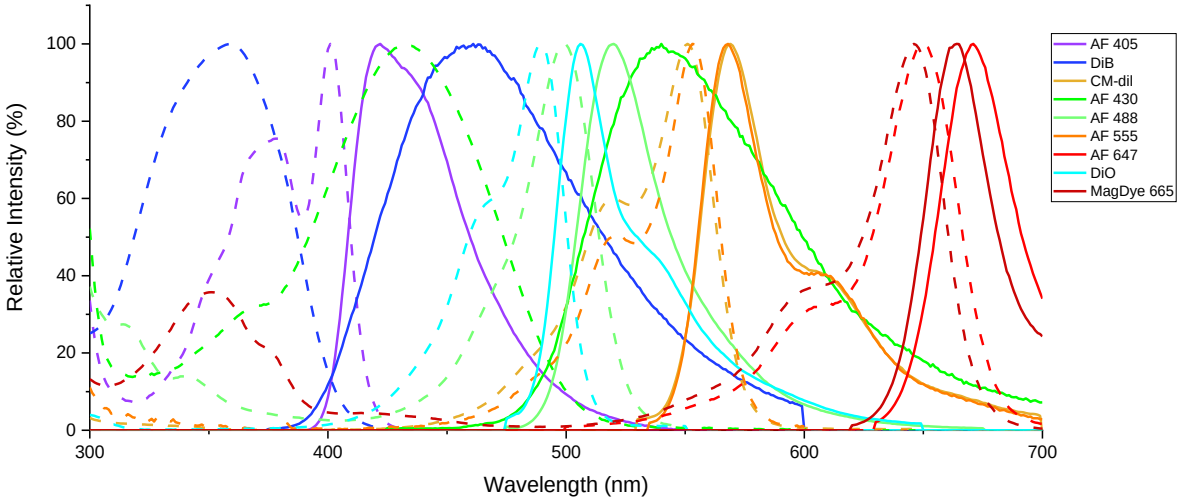

Membrane dye		Protein dye	
Name	$\lambda_{Ex}/\lambda_{Em}$	Name	$\lambda_{Ex}/\lambda_{Em}$
DiB	353/442 nm	Alexa Fluor 405 - streptavidin	401/421 nm
DiO	484/501 nm	Alexa Fluor 430 - IgG	433/541 nm
CM-Dil	553/570 nm	Alexa Fluor 488 - IgG	496/519 nm
		Alexa Fluor 555 - IgG	555/565 nm
		Alexa Fluor 647 - IgG	650/665 nm
		MagDye 665	~640/665 nm

Figure 4.4. List of tested organic FL dyes. On the spectrogram, the excitation spectra are depicted with dashed lines and the emission spectra are depicted with solid lines.

Another pitfall of organic dyes for SVT application is linked to the physical property of these molecules. FL organic dyes are in general hydrophobic and readily aggregate into crystals of size 100-500 nm.[207] These aggregates tend to adhere to the substrate and mimic the shape and size of the exosome (Figure 4.5.B1,2). This phenomenon of organic fluorophores causes false-positive results in acquired images. Interestingly, aggregation of organic fluorophores is more common for red dyes like cyanines and rhodamines due to their poor solubility.[253–255] Blue and green dyes such as Alexa Fluor 405, 430, and 488 would be more adequate for time-

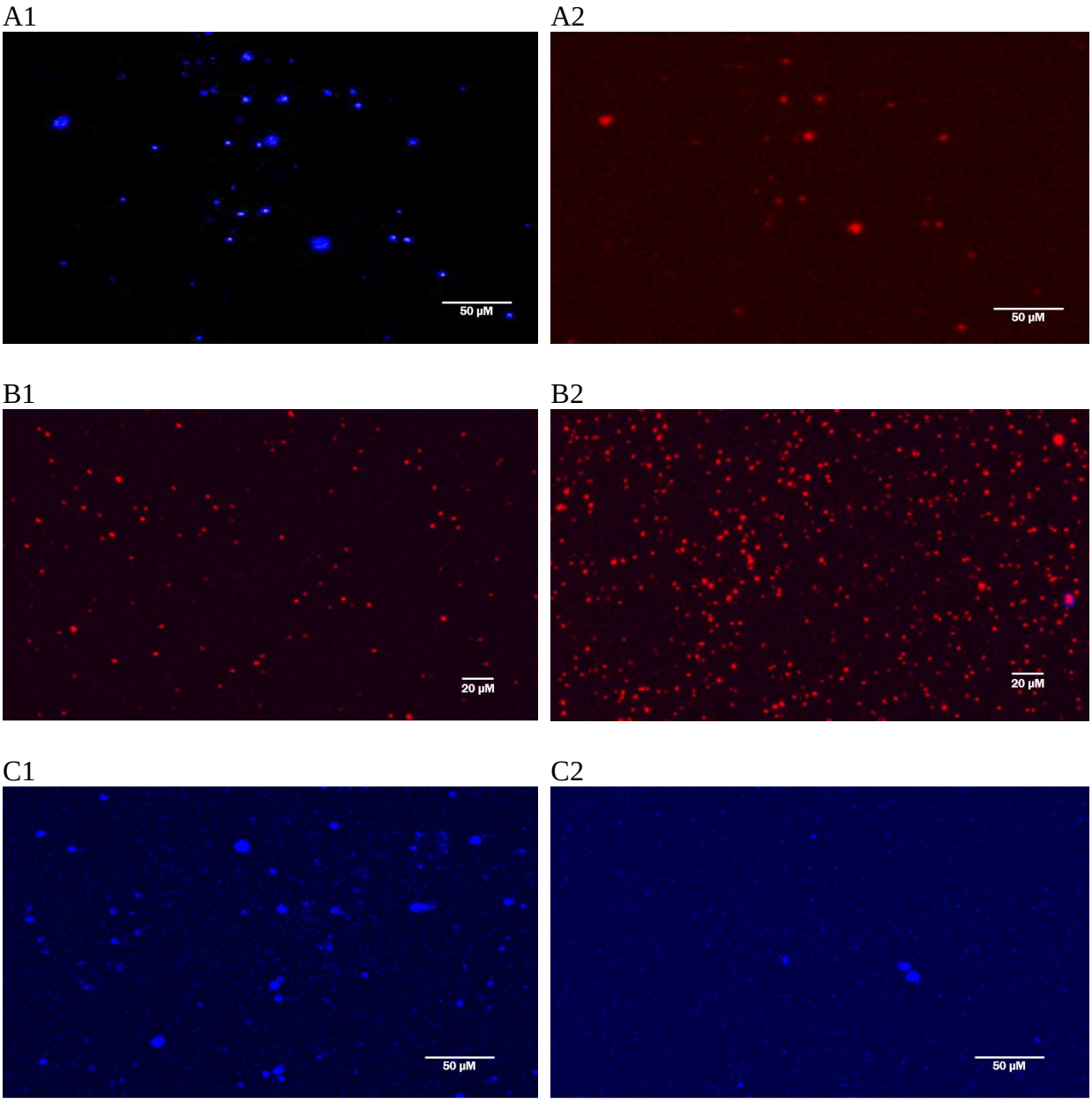

Figure 4.5. FL images of labeled exosomes. (A1-2) Set of images taken from same area using two different channels – blue and red for exosomes labeled with DiB lipophilic dye (λ_{Ex}353/ λ_{Em}442 nm). DiB bleeding into red channel when exited with 640 nm laser (right). (B1-2) Dye aggregation of CM-dil dye. Negative control without exosomes (left) vs positive control with exosomes (right). (C1-2) Loss of FL signal during long sample processing period. Before amplified protein labeling (left), after amplified protein labeling (right).

intensive protein labeling, but they are not bright enough in comparison to orange and red dyes.

To address this issue, we tried FL signal amplification using biotinylated secondary antibody and

fluorophore streptavidin conjugates Alexa Fluor 405 (Figure 4.3.B). Each biotinylated antibody provides ~7-10 binding sites for streptavidin, thus giving room for signal amplification. However, this approach was significantly longer in sample processing, which resulted in a loss of binding of either captured vesicles or the FL stain (Figure 4.5.C1,2).

Even though the method combining two organic fluorophores and confocal microscopy seemed to be a promising solution for SVT development, the negative aspects of organic FL dyes outweighed their positives. The difficulties associated with organic fluorophores such as photo-bleeding, insufficient brightness of blue and green dyes, and dye aggregations yield this approach unreproducible and elusive. It is also important to note that organic fluorophores are much more prone to photo-bleaching, in our case conditions such as a high laser power could negatively affect the interpretation of fluorescence intensity between individual images. Organic FL dyes designed specifically for EV research thus far still represent a niche in the market.

3.2 SVT Using Quantum Dot 655 in Conjunction with Organic Fluorophore

Our next solution to achieve SVT using fluorescent labeling and confocal microscopy was to replace organic fluorophore with quantum dots Qdot 655 for protein labeling (Figure 4.6.A). As mentioned in Chapter 3, quantum dots are inorganic fluorophore with greater photostability, higher signal-to-noise ratio, and 10-20 times higher brightness compared to organic fluorophores.[256,257] The absorption properties of these semiconductors dictate that their highest excitation point on the spectrum of visible light is near the UV region (~ 380-400 nm). For this reason, we were using two sources of light to excite Qdots 655 either with a DAPI laser (~ 407 nm) or a FITC laser (~ 488 nm), depending on which organic fluorophore was used as the second dye for membrane staining (DiB - Exλ / Emλ: 353/442 nm or CM-dil Exλ / Emλ: 553/570 nm) (Figure 4.6.B).

Photomultipliers (PMTs) and filters were set for emission collection from 600 to 700 nm to avoid the collection of emissions from the organic fluorescent dyes.

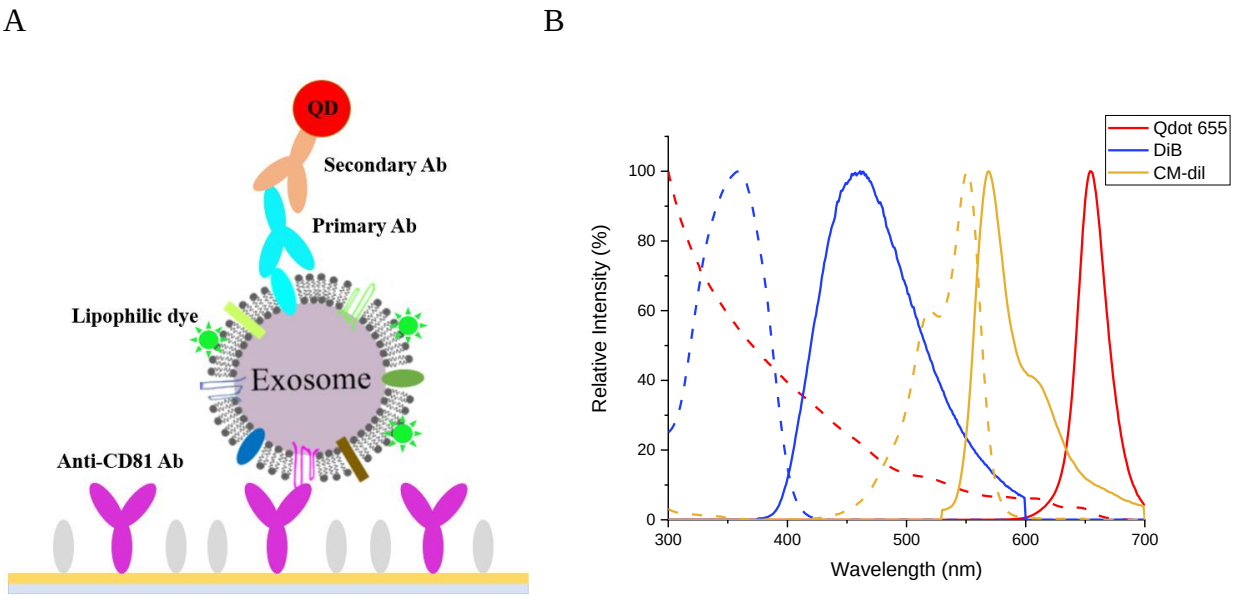

Figure 4.6. (A) Schematic of molecular exosome detection with QDot 655. (B) Spectrogram of tested FL dyes.

With this approach, we found several limitations of the Nikon A1 confocal microscope in our intended application. Firstly, Nikon recommended PMT mode significantly increased the background noise coming from the gold surface and incorrectly subtracted the signal from quantum dots leaving dark dots in theirs place instead (Figure 4.7.A2). Furthermore, in the standard FL mode, the membrane dye was FL bleeding into a custom QDot channel. To test for FL bleeding, we labeled captured exosomes with membrane dye only (no quantum dots were used) and took images in both channels (Figure 4.7.B1,2). The main cause of FL bleeding was most likely the connection of two factors a) limited effectiveness of the filters that were supposed to block the signal lower than 600 nm b) organic dyes which, when sufficiently excited, emitted a fluorescent light out of their expected emission spectra. We addressed this problem by using different membrane staining dye CM-dil, which had an absorption range placed farther away from

the absorption range of the quantum dots. Replacing DiB with CM-dil significantly reduced FL bleeding and thus reduced the false positive signal. However, despite solving this complication associated with FL bleeding the signal from quantum dots was not strong and detectable under 20x dry objective, which was the highest magnification with this instrument (Figure 4.7.D1,2). The same conclusion was reached even when protein labeling was amplified via biotinylated secondary antibody paired with QDot 655-streptavidin (Figure 4.7.E).

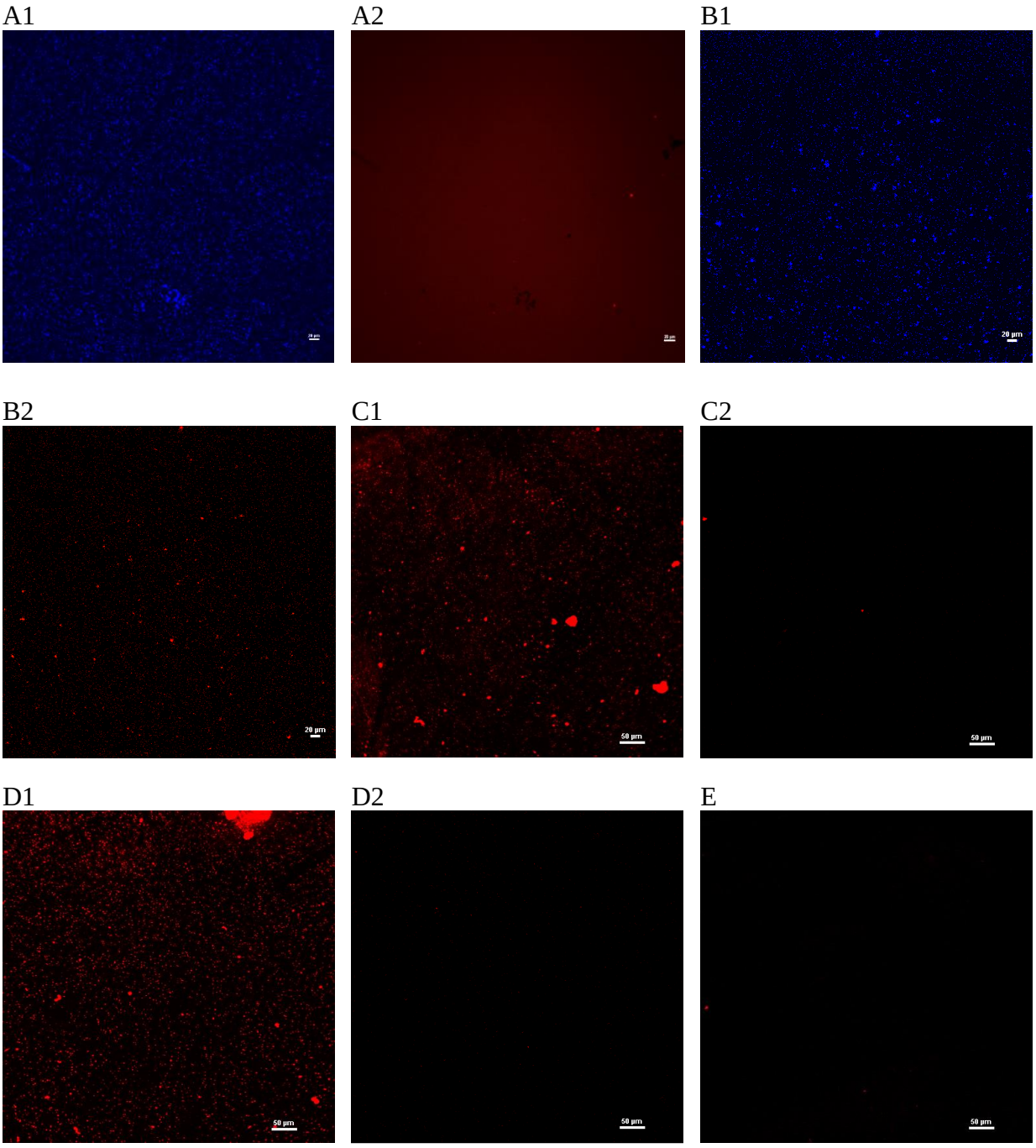

Figure 4.7. Sets of images depicting areas under two different FL channels. (A1) Exosome membrane stained with DiB. (A2) Nikon recommended PMT mode. Qdot labeled a highly expressed protein on surface of exosome. (B1) Exosome membrane stained with DiB. (B2) No Qdot control. FL bleeding of DiB into 'Qdot channel'. (C1) Exosome membrane stained with CM-dil. (C2) No Qdot control. FL bleeding of CM-dil into 'Qdot channel'. (D1) Exosome membrane stained with CM-Dil. (D2) Highly expressed protein on surface of exosome labeled with QDot 655. (E) Highly expressed protein on surface of exosomes labeled via amplification method.

The limitations associated with instrument setting and effectiveness of the filters and PMTs of the Nikon A1 confocal microscope did not allow us to achieve the required detection range, which would effectively eliminate the emission signal from organic fluorophore DiB. We found that replacing DiB dye with CM-dil, and thus completely avoiding an overlap of excitation spectra between quantum dots and membrane dye, provides a solution that can significantly eliminate a false positive signal. Nevertheless, after further testing, we found that the 20x dry objective does not allow for sufficient magnification of quantum dot-based SVT with Nikon A1 set up and higher magnification would be needed for accurate imaging of single vesicles.

3.3 SVT Using AuNPs in Conjunction with Organic Fluorophore

Our final strategy for achieving SVT through dual imaging technology was based on knowledge from the previous two approaches. To avoid previous complications that occurred when we tried relying solely on fluorescence imaging including dye aggregations over longer periods, FL bleeding between various dyes, and insufficiently strong signal from a protein label, we addressed most of those complications by combining fluorescent microscopy with dark field imagining. Figure 4.8.A depicts a schematic of an exosome labeled with a fluorescence dye and AuNP.

To fluorescently label exosome membrane we used Cy5-PEG-Cholesterol. Cyanine5 (Cy5) is a near-infrared dye with Exλ / Emλ: 646/660 nm. Cy5 is linked to cholesterol with Polyethylene glycol (2,000 Da) which serves as a hydrophilic spacer and mitigates hydrophobicity of cholesterol moiety making the overall molecule readily water-soluble. In comparison to lipophilic dyes we tested in previous approaches, Cy5-PEG-Chol is much more specific in membrane staining and retains longer on the plasma membrane before being partially internalized.[258] Under right

conditions (~ 37ºC, 15 min) cholesterol easily fuse with the semifluid lipid bilayer of exosomes and functions here as a dye anchor for membrane insertion.

A B

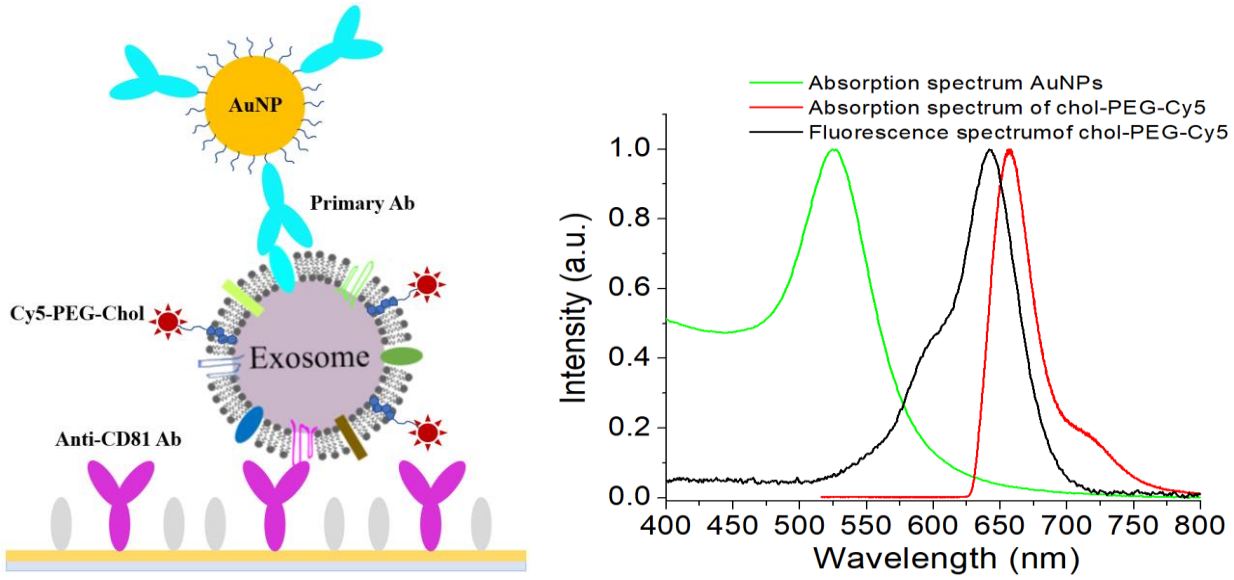

Figure 4.8. (A) Schematic of molecular exosome detection with AuNP and Cy5-PEG-CLS. (B) Spectrogram of AuNP and Cy5-PEG-CLS.

To find ideal conditions we initial incubated Cy5-PEG-Chol for 45 min at RT according to He et al.,[259] however, cholesterol fusion depends on the fluidity of the lipid bilayer, which directly increases with increasing temperature. Thus, incubation at 37ºC not only significantly increase cholesterol fusion, but also decrease incubation time to one third and positively increase the solubility of Cy5 in PBS solution. The difference in exosomes staining at RT vs 37ºC is shown in Figure 4.9.A-C.

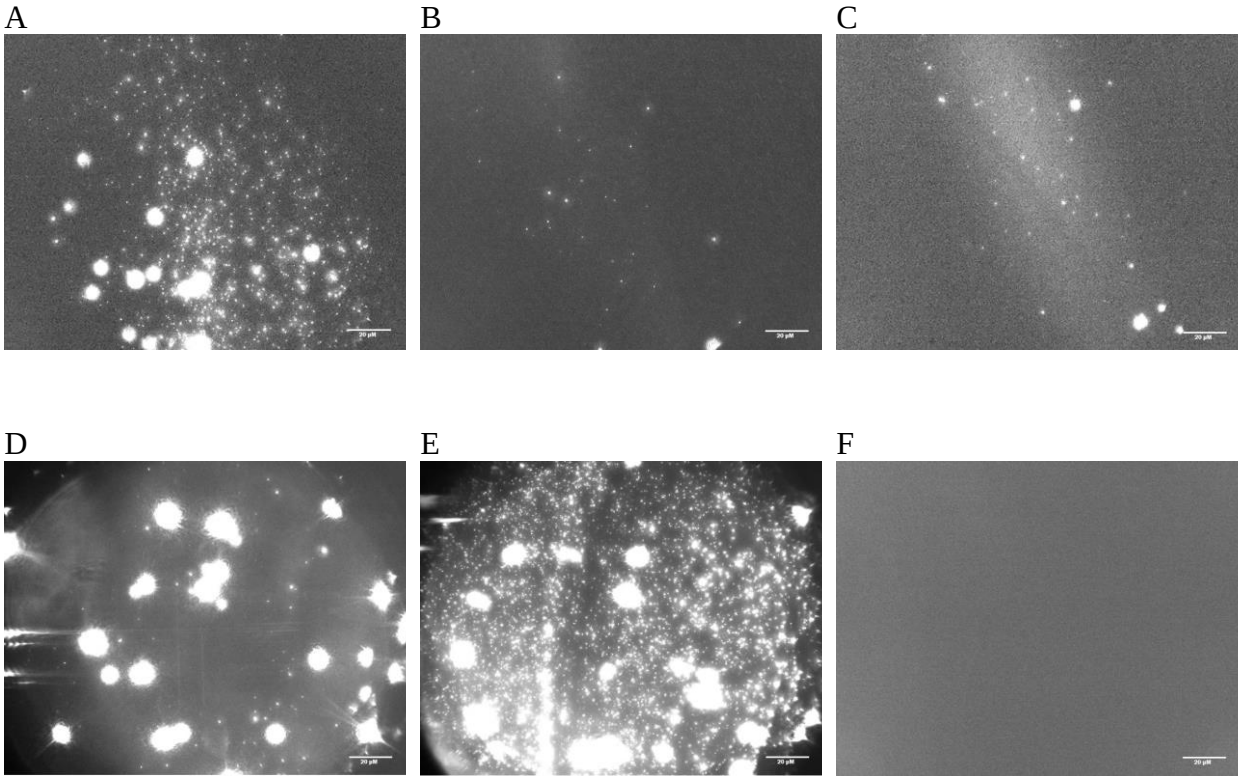

Figure 4.9. Evaluation of FL/DF SVT labeling and imaging (A) Cy5 labeled exosomes at 37ºC (FL image). (B) Cy5 negative control without exosomes (FL image). (C) Cy5 labeling of exosomes done at RT (FL image). (D) Dark-field image of (A). (E) CD44-AuNP labeled exosomes (DF image). (F) Fluorescence image of (E). Exosomes were derived from MM231 cells.

To label surface proteins of interested we conjugated selected antibodies to Au nanosphere (Ø = 60 nm). The conjugated antibodies were stabilized with mPEG-SH (2,000 Da). We tested various sizes including 40 nm, 50 nm, and 60 nm to find out which size scatters the light most and thus provides highest intensity signal on the dark field image under 50x dry objective (Figure 4.10.). We also had to keep in mind that exosomes are only 40-200 nm so the AuNP cannot be too large to prevent other spheres from binding to multiple proteins on the same exosome. By conjugating selected antibodies directly to the nanosphere we eliminated otherwise two-step process of indirect labeling, which is known to be prone to cross reactivity and nonspecific binding, and we reduced the time for protein labeling from 4 h to 3 h.[260]

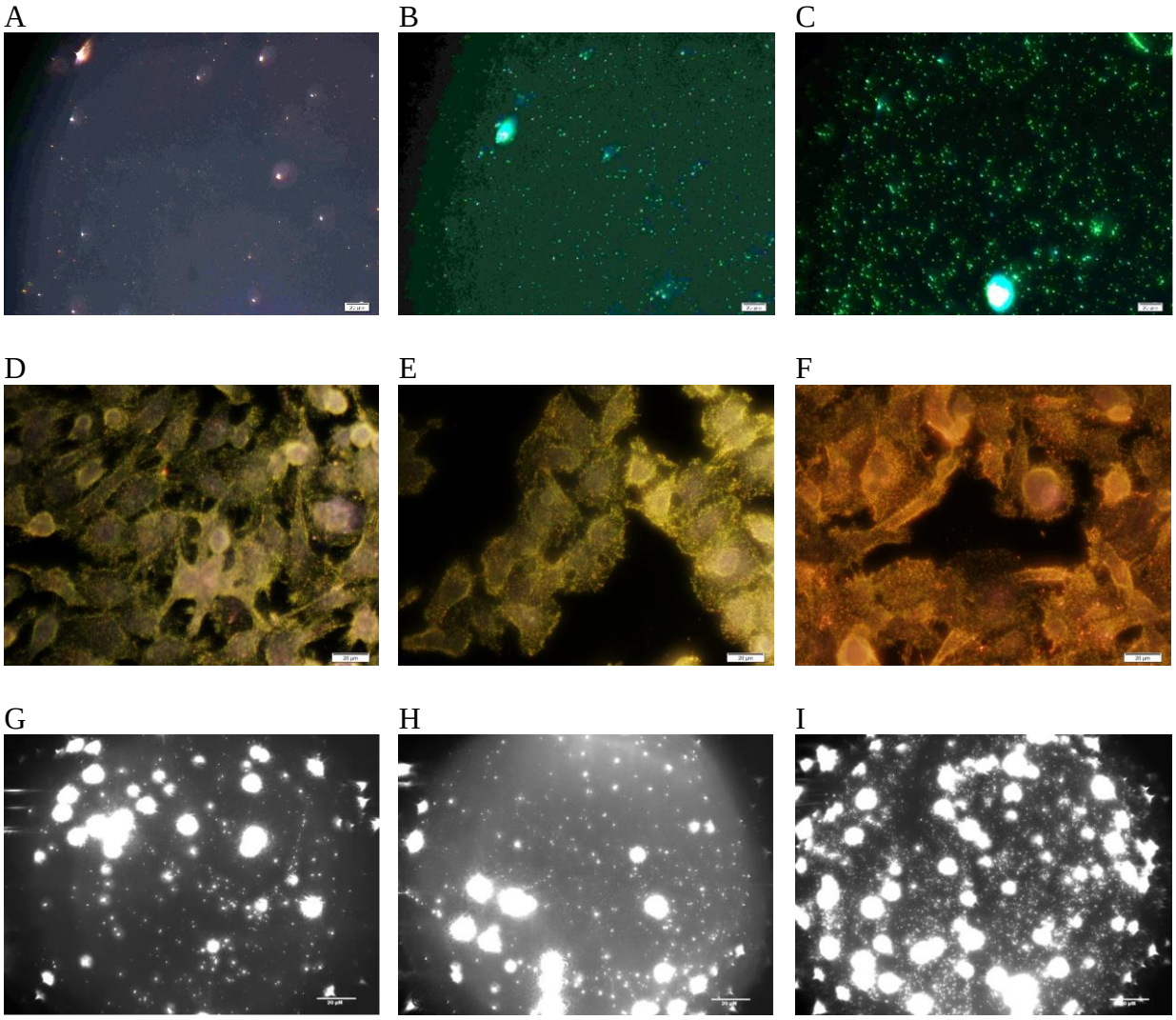

Figure 4.10. Evaluation of various sizes of AuNP based on light scattering under DF. (A, D, G) 40 nm AuNP. (B, E, H) 50 nm AuNP. (C, F, I) 60 nm AuNP. Individual particles (A-C) and labeled cells (D-F), images were taken with Olympus IX 71 microscope. Labeled exosomes (G-I) images were taken with the custom Nikon LV 150N.

We believe that the size of individual population pools for our SVT approach must be greater than 1000 exosomes to accurately assess the marker expression for each sample. Thus, since previous two approaches, we have further explored the ideal conditions for capturing exosomes to always achieve such large sample pools. We discovered that, unlike one addition of an exosome sample, multiple additions significantly increased the number of captured exosomes. This can be explained by the relatively rapid sedimentation of the exosomes in the undisturbed

liquid and thus reduction of the chances for exosomes to interacting with the anti-CD81 capture antibody. We tested our theory with one, two, and three additions of exosomes within a total of 3 hours of incubation time (Figure 4.11.)

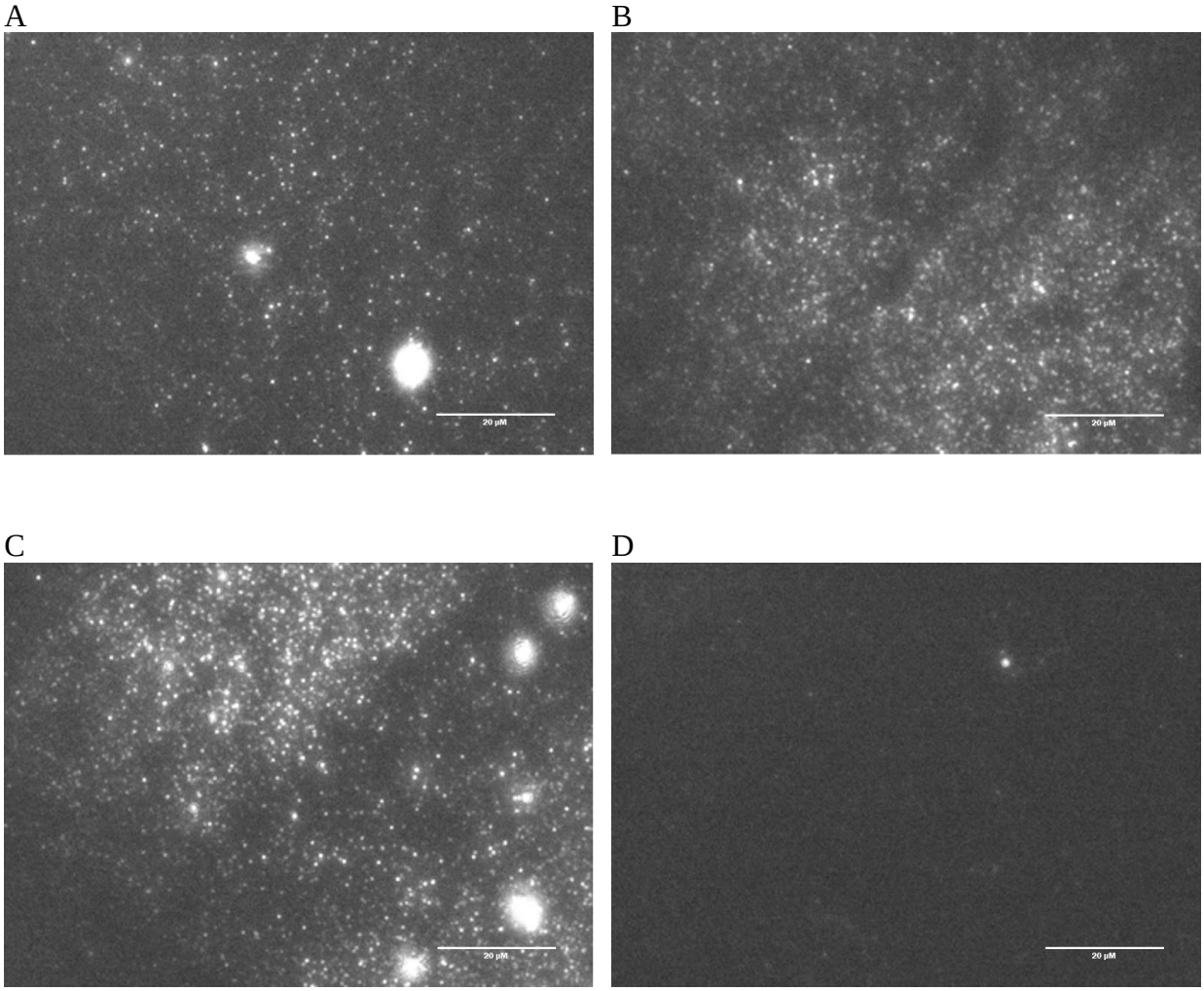

Figure 4.11. Effect of multiple additions on exosomes capture. (A) Single addition (3 h incubation time for each addition). (B) Two additions (1,5 h incubation time for each addition). (C) Three additions (1 h incubation time for each addition). (D) No exosomes control.

Labeled exosomes were imaged by a custom multifunctional system composed of Nikon microscope and optical components for bright field, dark field, and fluorescence imaging under near-infrared excitation (He laser: 632.8 nm) developed by Dr. Hoang. First, localized exosomes were captured by fluorescence imaging to obtain a “mask” image, and then the same area was

captured by light scattering dark field imaging to obtain a "target" image. To verify that Cy5-PEG-CLS or AuNP does not interfere with each other and can be used simultaneously we tested membrane labeled and protein labeled exosomes separately under both fluorescence and dark-field setting (Figure 4.9.D-F).

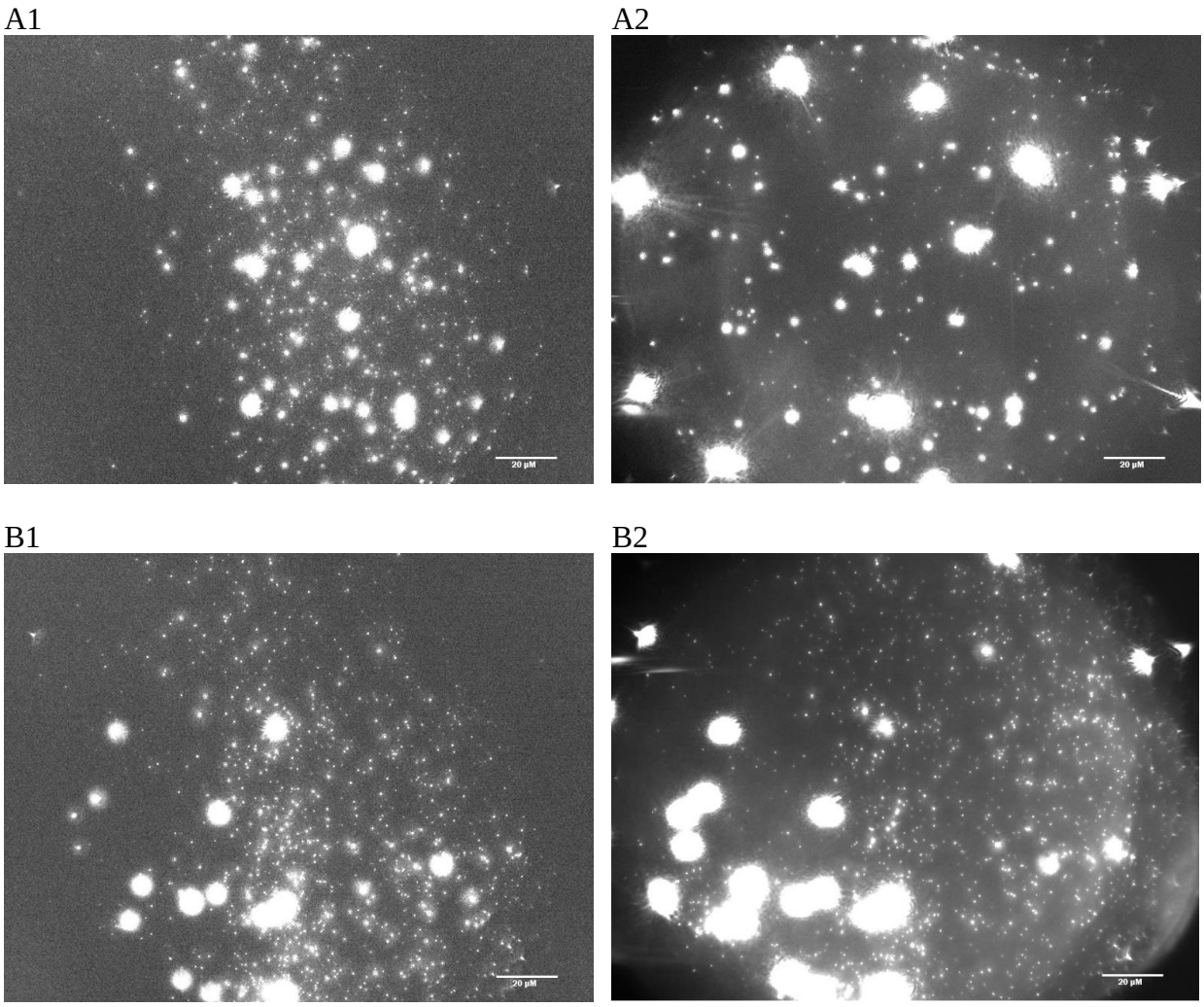

Figure 4.12. FL/DF dual imaging strategy. (A1, B1) Cy5 labeled exosomes (mask). (A2) mPEG-AuNP labeled exosomes (negative control, target for A1). (B2) CD44-AuNP labeled exosomes (highly expressed marker, target for B2). Exosomes were derived from MM231 cells.

To further verify the FL/DF dual imaging strategy we tested the methodology on MM231 exosomes by using CD44-AuNP (CD44 is a highly expressed marker in MM231) and we

compared it with mPEG-AuNP negative control (Figure 4.12.). A high amount of binding can be seen in Figure 4.12.B2 proving the specificity of AuNP conjugates.

After acquiring "mask" and target" image, both images were analyzed for a single exosome protein expression via Python-based analysis method developed by Dr. Wang's group. Briefly, software first subtracts background and large bright areas caused by surface imperfections and reagent aggregates. Both images are then turned into binary images. The position of individual exosome is automatically detected from the mask image and the signal intensity from target image is integrated over the exosome area. The obtained light scattering intensity values were plotted as a histogram of exosomes count vs protein expression. To validate our SVT approach, we tested it on exosomes collected from model breast cancer cell-lines SKBR3. The exosomes were harvested from FBS free media via multistep centrifuge method and size/concertation was determined with NTA (SKBR3 exosomes Ø = 165 ± 38). For our proof of concept, we targeted three different surface proteins, epithelia cell adhesion molecule (EpCAM) and cancer markers HER2, and CD44. According to our flow cytometry data on cells SKBR3 cell-line (Chapter 3, Figure 3.4.) is known to have high expression of EpCAM and HER2 and low expression of CD44. The resulting density histograms clearly indicate that protein expression on exosomes correlates with protein expression of cells (Figure 4.13.A-D). Exosomes derived from SKBR3 shows high expression of EpCAM and HER2 (Figure 4.13.F). The F_{HER2}, F_{EpCAM}, and F_{CD44} for SKBR3 exosomes was 70.3%, 67.6%, and 11.0%, respectively.

Our method was further validated with a sandwich ELISA. We correlated fraction positive exosomes (*Fp*) from Figure 11 to a bulk measurement by ELISA. To stay consistent with the FL/DF-SVT and CD81-positive sample population, we performed a sandwich ELISA approach in which anti-CD81 antibodies were used to capture exosomes. ELISA measurement also showed the

high expression of EpCAM and HER2. A further quantitative comparison of the two methods is shown in Figure 4.13.H**.** The two methods showed a high correlation, with a correlation coefficient $R^2 = 0.98$.

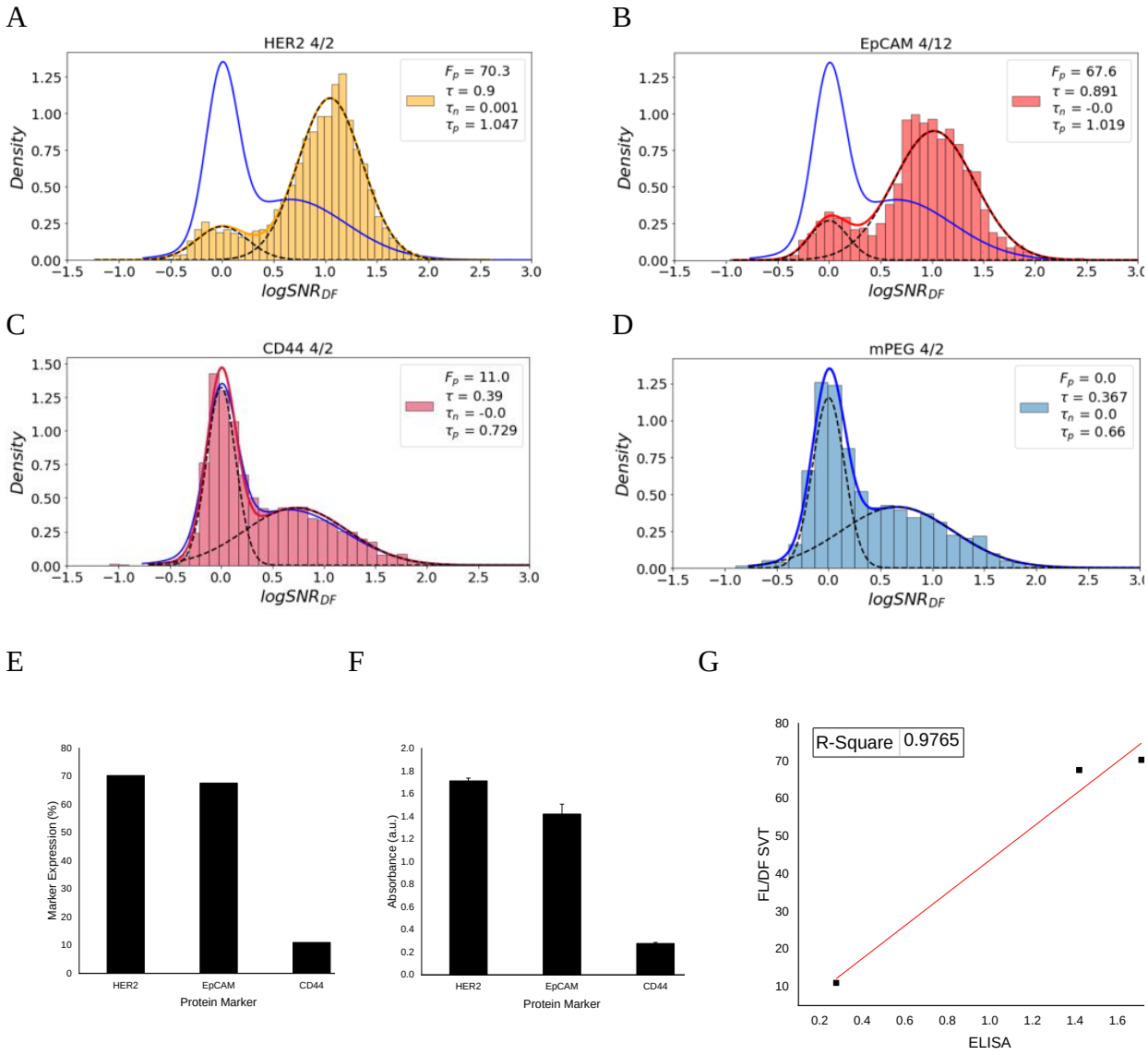

Figure 4.13. Protein profiling of SKBR3 exosomes. (A) HER2. (B) EpCAM. (C) CD44. (D) mPEG. (E) Protein expression profile based on data in (A-D). (F) Protein expression profile of targeted surface markers on the surface of SKBR3 EXOs determined using ELISA. Error bar is the standard deviation from triplicate experiments. (G) Correlation of the FL/DF SVT assay with sandwich ELISA.

4. Conclusion and Future Outlook

Protein analysis of exosomes on a single vesicle level opens door to new advancements in exosomal research and clinical application, arguably surpassing bulk analytical methods that are commonly used in academic research today. The proteins on the surface of the exosome are the key contact point for cell-to-cell communication and represent invaluable insight into biological events including oncogenesis, proliferation, and metastasis. Furthermore, given that liquid biopsy utilizes protein biomarkers that can be easily obtained from body fluids, this method appears highly preferable to costly, impractical, and in many cases dangerously invasive tissue biopsies.

This chapter expanded on our ideas and approaches that led towards a novel single vesicle technology with a great clinical potential. Here we reported a protein analysis assay of CD81 positive exosomes on a single vesicle level using fluorescence and dark-field microscopy and subsequent dual image profiling. To reach our goal, we tested many different strategies for exosome capture, membrane staining, protein labeling, and image acquisition, before we achieved technology that overcomes the challenges associated with a single exosome molecular analysis. Our technology is sensitive, simple, efficient, considered of sample consumption and has plenty of room for modification and expansion. The technology quantifies the fraction of exosome subtypes based on surface marker expression, which provides great value in informing the number of tumor-derived exosomes in biofluids. With proof-of-concept studies we demonstrated the technology on two populations of exosomes derived from our model breast cancer cell-lines SKBR3 and MDA-MB-231. Further, we validated our findings with widely used methods such as flow cytometry and sandwich ELISA. Great attribute of our SVT method is that it can be adjusted for any protein marker or cancer cell-line without need of changing the methodology.

Further testing and improvement of the DF/FL-SVT will continue in the future by my colleagues and research collaborators. The next goal of this project is to demonstrate efficacy and clinical potential of our SVT on plasma samples collected from breast cancer patients at all stages of cancer progression. The exosomes from HER2-positive BC plasma samples will be profiled for the cancer marker HER2 and results will be statistically compared with a profile of exosomes from healthy donors. These studies should provide us with a clear answer to whether we are able to detect cancer at early stages based on HER2 expression. The technology itself also has a lot of space for it to be improved, especially in in the automation of sample deposition, processing, and image analysis. The ultimate goal is to turn this SVT into a robust, accessible, and easy to learn tool for routine exosome analysis of various types of cancer.

Chapter 5. CONCLUSION AND FURTHER PERSPECTIVES

In this dissertation, we focused on the possibilities and limitations associated with the protein analysis of exosomes. We explained what pivotal roles exosomes play in the onset and progression of cancer, and why they are considered by many to be a rich source of cancer biomarkers with the potential for non-invasive liquid biopsies. Since oncogenic receptors often reside within regions of the plasma membrane, surface protein analysis is one of the primary approaches for understanding the role of exosomes in cancer. Many studies have described recent advances in the development of a new generation of liquid biopsies through the usage of exosomes. However, despite all efforts, the progress is indolent due to conventional technologies not being yet fully adapted for the detection of exosomal content, which puts us still in the early stages of exosomal research before we can transfer it from academia to the medical setting.

In Chapter 3, we demonstrated 3D printing as an effective tool for creating custom devices and modifiers for traditional analytical methods. Using the free web software TinkerCAD, we designed several custom micro-array templates, which served as the main building blocks for a miniaturized device used in exosome detection. Thanks to easy-to-use TinkerCAD software and affordable printing method, we were able to redesign and modify our final layout in a very short time, which would not be possible using conventional lithography. Our final micro-array device allowed us to detect 85 samples simultaneously on a single gold slide, which is 5.8 times more effective in terms of sample per area than ELISA plate. We validated our miniaturized device by using it in our SERS-based assay designed for protein marker analysis on the surface of the exosome in cancer detection.[146]

In Chapter 4, we reported a simple and rapid method for exosome surface protein detection using quantum dot coupled with immunomagnetic capture and enrichment. In this method, exosomes were captured by magnetic beads based on CD81 protein expression. Surface protein markers of interest were recognized by primary antibody and then detected by secondary antibody-conjugated quantum dot with fluorescent spectroscopy. Validated by ELISA, our method can specifically detect different surface markers on exosomes from different cancer cell lines and differentiate cancer exosomes from normal exosomes. The clinical potential was demonstrated with pilot plasma samples using HER2-positive breast cancer as the disease model. The results show that exosomes from HER2-positive breast cancer patients exhibited a five times higher level of HER2 expression than healthy controls. Exosomal HER2 showed strong diagnostic power for HER2-positive patients, with the area under the curve of 0.969. This quantum dot-based exosome method is rapid (about 4h turnaround time) and only requires microliters of diluted plasma without pre-purification, practical for routine use for basic vesicle research and clinical applications.

In Chapter 5, we discussed the difficulties associated with the detection of cancer-derived exosomes at an early stage of cancer and how these difficulties could be overcome by molecular detection at the single vesicle level. We reported progress toward a simple, efficient, and clinically practical single vesicle technology (SVT) for exosome surface protein profiling using a dual imaging approach in combination with a purification-free capture platform. The exosomes were first captured based on their CD81 expression, their position was detected by staining their membrane with an organic fluorophore, and surface proteins of interest were detected with AuNP antibody conjugate. Across three different strategies we tested, we found that the vast majority of fluorescent dyes are not suitable for use in single exosome applications

due to low brightness, low specificity, high hydrophobicity, and associated aggregation. We demonstrated our technology on exosomes derived from SKBR3 model cell line by profiling them for EpCAM, HER2, and CD44 markers, and we validated our results with conventional ELISA. We found high expression of EpCAM and HER2 and low expression of CD44 (Fp = 70.3%, 67.6%, and 11.0%, respectively), which based on our flow cytometry data also closely resembles protein expression on cells. We are aware that our SVT method still needs to be further improved and validated. However, meeting our technical needs, the FL / DF-SVT has great potential to become a routine analytical technology for exosomal content detection in fundamental exosome research or biomarker detection in clinical care.

REFERENCES

(1) Whitehead, C. A.; Luwor, R. B.; Morokoff, A. P.; Kaye, A. H.; Stylli, S. S. Cancer Exosomes in Cerebrospinal Fluid. *Translational Cancer Research* **2017**, *6* (8). https://doi.org/10.21037/15519.

(2) Raposo, G.; Stoorvogel, W. Extracellular Vesicles: Exosomes, Microvesicles, and Friends. *Journal of Cell Biology* **2013**, *200* (4), 373–383. https://doi.org/10.1083/jcb.201211138.

(3) Lowry, M. C.; Gallagher, W. M.; O'Driscoll, L. The Role of Exosomes in Breast Cancer. *Clinical Chemistry* **2015**, *61* (12), 1457–1465. https://doi.org/10.1373/clinchem.2015.240028.

(4) Battistelli, M.; Falcieri, E. Apoptotic Bodies: Particular Extracellular Vesicles Involved in Intercellular Communication. *Biology* **2020**, *9* (1), 21. https://doi.org/10.3390/biology9010021.

(5) Kalra, H.; Drummen, G.; Mathivanan, S. Focus on Extracellular Vesicles: Introducing the Next Small Big Thing. *IJMS* **2016**, *17* (2), 170. https://doi.org/10.3390/ijms17020170.

(6) Yang, W.; Pan, X.; Ma, A. The Potential of Exosomal RNAs in Atherosclerosis Diagnosis and Therapy. *Front. Neurol.* **2021**, *11*, 572226. https://doi.org/10.3389/fneur.2020.572226.

(7) Yu, L.-L.; Zhu, J.; Liu, J.-X.; Jiang, F.; Ni, W.-K.; Qu, L.-S.; Ni, R.-Z.; Lu, C.-H.; Xiao, M.-B. A Comparison of Traditional and Novel Methods for the Separation of Exosomes from Human Samples. *BioMed Research International* **2018**, *2018*, 1–9. https://doi.org/10.1155/2018/3634563.

(8) Sidhom, K.; Obi, P. O.; Saleem, A. A Review of Exosomal Isolation Methods: Is Size Exclusion Chromatography the Best Option? *Int J Mol Sci* **2020**, *21* (18). https://doi.org/10.3390/ijms21186466.

(9) Kalluri, R. The Biology and Function of Exosomes in Cancer. *Journal of Clinical Investigation* **2016**, *126* (4), 1208–1215. https://doi.org/10.1172/JCI81135.

(10) Patil, A. A.; Rhee, W. J. Exosomes: Biogenesis, Composition, Functions, and Their Role in Pre-Metastatic Niche Formation. *Biotechnol Bioproc E* **2019**, *24* (5), 689–701. https://doi.org/10.1007/s12257-019-0170-y.

(11) Théry, C.; Zitvogel, L.; Amigorena, S. Exosomes: Composition, Biogenesis and Function. *Nature Reviews Immunology* **2002**, *2* (8), 569–579. https://doi.org/10.1038/nri855.

(12) Choi, D.-S.; Kim, D.-K.; Kim, Y.-K.; Gho, Y. S. Proteomics of Extracellular Vesicles: Exosomes and Ectosomes. *Mass Spectrom Rev* **2015**, *34* (4), 474–490. https://doi.org/10.1002/mas.21420.

(13) Wyciszkiewicz, A.; Kalinowska-Łyszczarz, A.; Nowakowski, B.; Kaźmierczak, K.; Osztynowicz, K.; Michalak, S. Expression of Small Heat Shock Proteins in Exosomes from

Patients with Gynecologic Cancers. *Sci Rep* **2019**, *9* (1), 9817. https://doi.org/10.1038/s41598-019-46221-9.

(14) Simpson, R. J.; Jensen, S. S.; Lim, J. W. E. Proteomic Profiling of Exosomes: Current Perspectives. *Proteomics* **2008**, *8* (19), 4083–4099. https://doi.org/10.1002/pmic.200800109.

(15) Andreu, Z.; Yanez-Mo, M. Tetraspanins in Extracellular Vesicle Formation and Function. *Front. Immunol.* **2014**, *5*. https://doi.org/10.3389/fimmu.2014.00442.

(16) Subra, C.; Laulagnier, K.; Perret, B.; Record, M. Exosome Lipidomics Unravels Lipid Sorting at the Level of Multivesicular Bodies. *Biochimie* **2007**, *89* (2), 205–212. https://doi.org/10.1016/j.biochi.2006.10.014.

(17) Zhang, Y.; Liu, Y.; Liu, H.; Tang, W. H. Exosomes: Biogenesis, Biologic Function and Clinical Potential. *Cell Biosci* **2019**, *9* (1), 19. https://doi.org/10.1186/s13578-019-0282-2.

(18) Balaj, L.; Lessard, R.; Dai, L.; Cho, Y.-J.; Pomeroy, S. L.; Breakefield, X. O.; Skog, J. Tumour Microvesicles Contain Retrotransposon Elements and Amplified Oncogene Sequences. *Nat Commun* **2011**, *2*, 180. https://doi.org/10.1038/ncomms1180.

(19) Kahlert, C.; Melo, S. A.; Protopopov, A.; Tang, J.; Seth, S.; Koch, M.; Zhang, J.; Weitz, J.; Chin, L.; Futreal, A.; Kalluri, R. Identification of Double-Stranded Genomic DNA Spanning All Chromosomes with Mutated KRAS and P53 DNA in the Serum Exosomes of Patients with Pancreatic Cancer. *J Biol Chem* **2014**, *289* (7), 3869–3875. https://doi.org/10.1074/jbc.C113.532267.

(20) Trajkovic, K.; Hsu, C.; Chiantia, S.; Rajendran, L.; Wenzel, D.; Wieland, F.; Schwille, P.; Brügger, B.; Simons, M. Ceramide Triggers Budding of Exosome Vesicles into Multivesicular Endosomes. *Science* **2008**, *319* (5867), 1244–1247. https://doi.org/10.1126/science.1153124.

(21) Menck, K.; Sönmezer, C.; Worst, T. S.; Schulz, M.; Dihazi, G. H.; Streit, F.; Erdmann, G.; Kling, S.; Boutros, M.; Binder, C.; Gross, J. C. Neutral Sphingomyelinases Control Extracellular Vesicles Budding from the Plasma Membrane. *Journal of Extracellular Vesicles* **2017**, *6* (1), 1378056. https://doi.org/10.1080/20013078.2017.1378056.

(22) Villarroya-Beltri, C.; Baixauli, F.; Mittelbrunn, M.; Fernández-Delgado, I.; Torralba, D.; Moreno-Gonzalo, O.; Baldanta, S.; Enrich, C.; Guerra, S.; Sánchez-Madrid, F. ISGylation Controls Exosome Secretion by Promoting Lysosomal Degradation of MVB Proteins. *Nature Communications* **2016**, *7* (1), 13588. https://doi.org/10.1038/ncomms13588.

(23) Hsu, C.; Morohashi, Y.; Yoshimura, S.; Manrique-Hoyos, N.; Jung, S.; Lauterbach, M. A.; Bakhti, M.; Grønborg, M.; Möbius, W.; Rhee, J.; Barr, F. A.; Simons, M. Regulation of Exosome Secretion by Rab35 and Its GTPase-Activating Proteins TBC1D10A–C. *Journal of Cell Biology* **2010**, *189* (2), 223–232. https://doi.org/10.1083/jcb.200911018.

(24) Ostrowski, M.; Carmo, N. B.; Krumeich, S.; Fanget, I.; Raposo, G.; Savina, A.; Moita, C. F.; Schauer, K.; Hume, A. N.; Freitas, R. P.; Goud, B.; Benaroch, P.; Hacohen, N.; Fukuda, M.;

Desnos, C.; Seabra, M. C.; Darchen, F.; Amigorena, S.; Moita, L. F.; Thery, C. Rab27a and Rab27b Control Different Steps of the Exosome Secretion Pathway. *Nature Cell Biology* **2010**, *12* (1), 19–30. https://doi.org/10.1038/ncb2000.

(25) Fader, C. M.; Sánchez, D. G.; Mestre, M. B.; Colombo, M. I. TI-VAMP/VAMP7 and VAMP3/Cellubrevin: Two v-SNARE Proteins Involved in Specific Steps of the Autophagy/Multivesicular Body Pathways. *Biochimica et Biophysica Acta (BBA) - Molecular Cell Research* **2009**, *1793* (12), 1901–1916. https://doi.org/10.1016/j.bbamcr.2009.09.011.

(26) Chahar, H. S.; Bao, X.; Casola, A. Exosomes and Their Role in the Life Cycle and Pathogenesis of RNA Viruses. *Viruses* **2015**, *7* (6), 3204–3225. https://doi.org/10.3390/v7062770.

(27) Zöller, M. Tetraspanins: Push and Pull in Suppressing and Promoting Metastasis. *Nature Reviews Cancer* **2009**, *9* (1), 40–55. https://doi.org/10.1038/nrc2543.

(28) Kim, J.; Song, Y.; Park, C. H.; Choi, C. Platform Technologies and Human Cell Lines for the Production of Therapeutic Exosomes. *Extracellular Vesicles and Circulating Nucleic Acids* **2021**, *2* (1), 3–17. https://doi.org/10.20517/evcna.2020.01.

(29) Johnstone, R. M.; Adam, M.; Hammond, J. R.; Orr, L.; Turbide, C. Vesicle Formation during Reticulocyte Maturation. Association of Plasma Membrane Activities with Released Vesicles (Exosomes). *J Biol Chem* **1987**, *262* (19), 9412–9420.

(30) Hessvik, N. P.; Llorente, A. Current Knowledge on Exosome Biogenesis and Release. *Cell Mol Life Sci* **2018**, *75* (2), 193–208. https://doi.org/10.1007/s00018-017-2595-9.

(31) Valadi, H.; Ekström, K.; Bossios, A.; Sjöstrand, M.; Lee, J. J.; Lötvall, J. O. Exosome-Mediated Transfer of MRNAs and MicroRNAs Is a Novel Mechanism of Genetic Exchange between Cells. *Nature Cell Biology* **2007**, *9* (6), 654–659. https://doi.org/10.1038/ncb1596.

(32) Nolte-'t Hoen, E. N. M.; Buschow, S. I.; Anderton, S. M.; Stoorvogel, W.; Wauben, M. H. M. Activated T Cells Recruit Exosomes Secreted by Dendritic Cells via LFA-1. *Blood* **2009**, *113* (9), 1977–1981. https://doi.org/10.1182/blood-2008-08-174094.

(33) Pant, S.; Hilton, H.; Burczynski, M. E. The Multifaceted Exosome: Biogenesis, Role in Normal and Aberrant Cellular Function, and Frontiers for Pharmacological and Biomarker Opportunities. *Biochem Pharmacol* **2012**, *83* (11), 1484–1494. https://doi.org/10.1016/j.bcp.2011.12.037.

(34) Prada, I.; Meldolesi, J. Binding and Fusion of Extracellular Vesicles to the Plasma Membrane of Their Cell Targets. *Int J Mol Sci* **2016**, *17* (8). https://doi.org/10.3390/ijms17081296.

(35) Siegel, R. L.; Miller, K. D.; Fuchs, H. E.; Jemal, A. Cancer Statistics, 2021. *CA: A Cancer Journal for Clinicians* **2021**, *71* (1), 7–33. https://doi.org/10.3322/caac.21654.

(36) Försti, A.; Luo, L.; Vorechovsky, I.; Söderberg, M.; Lichtenstein, P.; Hemminki, K. Allelic Imbalance on Chromosomes 13 and 17 and Mutation Analysis of BRCA1 and BRCA2

Genes in Monozygotic Twins Concordant for Breast Cancer. *Carcinogenesis* **2001**, *22* (1), 27–33. https://doi.org/10.1093/carcin/22.1.27.

(37) Ganguly, A.; Leahy, K.; Marshall, A. M.; Dhulipala, R.; Godmilow, L.; Ganguly, T. Genetic Testing for Breast Cancer Susceptibility: Frequency of BRCA1 and BRCA2 Mutations. *Genet Test* **1997**, *1* (2), 85–90. https://doi.org/10.1089/gte.1997.1.85.

(38) Hulka, B. S.; Moorman, P. G. Breast Cancer: Hormones and Other Risk Factors. *Maturitas* **2001**, *38* (1), 103–113; discussion 113-116. https://doi.org/10.1016/s0378-5122(00)00196-1.

(39) Millikan, R. C.; Schroeder, J. C.; Barnholtz-Sloan, J. S.; Levine, B. J. Reproductive and Hormonal Risk Factors for Ductal Carcinoma in Situ of the Breast. *Cancer Epidemiol Biomarkers Prev* **2009**, *18* (5), 1507–1514. https://doi.org/10.1158/1055-9965.EPI-08-0967.

(40) Lambe, M.; Hsieh, C.; Trichopoulos, D.; Ekbom, A.; Pavia, M.; Adami, H.-O. Transient Increase in the Risk of Breast Cancer after Giving Birth. *New England Journal of Medicine* **1994**, *331* (1), 5–9. https://doi.org/10.1056/NEJM199407073310102.

(41) Sczaniecka, A. K.; Brasky, T. M.; Lampe, J. W.; Patterson, R. E.; White, E. Dietary Intake of Specific Fatty Acids and Breast Cancer Risk among Postmenopausal Women in the VITAL Cohort. *Nutr Cancer* **2012**, *64* (8), 1131–1142. https://doi.org/10.1080/01635581.2012.718033.

(42) Chiriac, V.-F.; Baban, A.; Dumitrascu, D. L. PSYCHOLOGICAL STRESS AND BREAST CANCER INCIDENCE: A SYSTEMATIC REVIEW. *Medicine and Pharmacy Reports* **2018**, *91* (1), 18–26. https://doi.org/10.15386/cjmed-924.

(43) Anders, C. K.; Johnson, R.; Litton, J.; Phillips, M.; Bleyer, A. Breast Cancer Before Age 40 Years. *Semin Oncol* **2009**, *36* (3), 237–249. https://doi.org/10.1053/j.seminoncol.2009.03.001.

(44) Winkler, J.; Abisoye-Ogunniyan, A.; Metcalf, K. J.; Werb, Z. Concepts of Extracellular Matrix Remodelling in Tumour Progression and Metastasis. *Nature Communications* **2020**, *11* (1), 5120. https://doi.org/10.1038/s41467-020-18794-x.

(45) O'Brien, K.; Rani, S.; Corcoran, C.; Wallace, R.; Hughes, L.; Friel, A. M.; McDonnell, S.; Crown, J.; Radomski, M. W.; O'Driscoll, L. Exosomes from Triple-Negative Breast Cancer Cells Can Transfer Phenotypic Traits Representing Their Cells of Origin to Secondary Cells. *European Journal of Cancer* **2013**, *49* (8), 1845–1859. https://doi.org/10.1016/j.ejca.2013.01.017.

(46) Giordano, C.; La Camera, G.; Gelsomino, L.; Barone, I.; Bonofiglio, D.; Andò, S.; Catalano, S. The Biology of Exosomes in Breast Cancer Progression: Dissemination, Immune Evasion and Metastatic Colonization. *Cancers* **2020**, *12* (8), 2179. https://doi.org/10.3390/cancers12082179.

(47) Clayton, A.; Mason, M. D. Exosomes in Tumour Immunity. *Curr Oncol* **2009**, *16* (3), 46–49.

(48) Whiteside, T. L. Exosomes and Tumor-Mediated Immune Suppression. *J Clin Invest 126* (4), 1216–1223. https://doi.org/10.1172/JCI81136.

(49) Xu, Z.; Zeng, S.; Gong, Z.; Yan, Y. Exosome-Based Immunotherapy: A Promising Approach for Cancer Treatment. *Molecular Cancer* **2020**, *19* (1), 160. https://doi.org/10.1186/s12943-020-01278-3.

(50) RONG, L.; LI, R.; LI, S.; LUO, R. Immunosuppression of Breast Cancer Cells Mediated by Transforming Growth Factor-β in Exosomes from Cancer Cells. *Oncol Lett* **2016**, *11* (1), 500–504. https://doi.org/10.3892/ol.2015.3841.

(51) Jang, J.-Y.; Lee, J.-K.; Jeon, Y.-K.; Kim, C.-W. Exosome Derived from Epigallocatechin Gallate Treated Breast Cancer Cells Suppresses Tumor Growth by Inhibiting Tumor-Associated Macrophage Infiltration and M2 Polarization. *BMC Cancer* **2013**, *13* (1), 421. https://doi.org/10.1186/1471-2407-13-421.

(52) Gomes, F. G.; Sandim, V.; Almeida, V. H.; Rondon, A. M. R.; Succar, B. B.; Hottz, E. D.; Leal, A. C.; Verçoza, B. R. F.; Rodrigues, J. C. F.; Bozza, P. T.; Zingali, R. B.; Monteiro, R. Q. Breast-Cancer Extracellular Vesicles Induce Platelet Activation and Aggregation by Tissue Factor-Independent and -Dependent Mechanisms. *Thromb Res* **2017**, *159*, 24–32. https://doi.org/10.1016/j.thromres.2017.09.019.

(53) Shi, J.; Ren, Y.; Zhen, L.; Qiu, X. Exosomes from Breast Cancer Cells Stimulate Proliferation and Inhibit Apoptosis of CD133+ Cancer Cells in Vitro. *Mol Med Rep* **2015**, *11* (1), 405–409. https://doi.org/10.3892/mmr.2014.2749.

(54) Dong, H.; Wang, W.; Chen, R.; Zhang, Y.; Zou, K.; Ye, M.; He, X.; Zhang, F.; Han, J. Exosome-Mediated Transfer of LncRNA-SNHG14 Promotes Trastuzumab Chemoresistance in Breast Cancer. *Int J Oncol* **2018**, *53* (3), 1013–1026. https://doi.org/10.3892/ijo.2018.4467.

(55) Mashouri, L.; Yousefi, H.; Aref, A. R.; Ahadi, A. mohammad; Molaei, F.; Alahari, S. K. Exosomes: Composition, Biogenesis, and Mechanisms in Cancer Metastasis and Drug Resistance. *Mol Cancer* **2019**, *18* (1), 75. https://doi.org/10.1186/s12943-019-0991-5.

(56) Azmi, A. S.; Bao, B.; Sarkar, F. H. Exosomes in Cancer Development, Metastasis, and Drug Resistance: A Comprehensive Review. *Cancer Metastasis Rev* **2013**, *32* (3), 623–642. https://doi.org/10.1007/s10555-013-9441-9.

(57) Dong, X.; Bai, X.; Ni, J.; Zhang, H.; Duan, W.; Graham, P.; Li, Y. Exosomes and Breast Cancer Drug Resistance. *Cell Death Dis* **2020**, *11* (11), 987. https://doi.org/10.1038/s41419-020-03189-z.

(58) Dutta, S.; Warshall, C.; Bandyopadhyay, C.; Dutta, D.; Chandran, B. Interactions between Exosomes from Breast Cancer Cells and Primary Mammary Epithelial Cells Leads to Generation of Reactive Oxygen Species Which Induce DNA Damage Response, Stabilization of P53 and Autophagy in Epithelial Cells. *PLOS ONE* **2014**, *9* (5), e97580. https://doi.org/10.1371/journal.pone.0097580.

(59) English, D. P.; Roque, D. M.; Santin, A. D. HER2 Expression Beyond Breast Cancer: Therapeutic Implications for Gynecologic Malignancies. *Mol Diagn Ther* **2013**, *17* (2), 85–99. https://doi.org/10.1007/s40291-013-0024-9.

(60) Wang, J.; Xu, B. Targeted Therapeutic Options and Future Perspectives for HER2-Positive Breast Cancer. *Signal Transduction and Targeted Therapy* **2019**, *4* (1), 1–22. https://doi.org/10.1038/s41392-019-0069-2.

(61) Zhou, B.; Xu, K.; Zheng, X.; Chen, T.; Wang, J.; Song, Y.; Shao, Y.; Zheng, S. Application of Exosomes as Liquid Biopsy in Clinical Diagnosis. *Sig Transduct Target Ther* **2020**, *5* (1), 144. https://doi.org/10.1038/s41392-020-00258-9.

(62) Lee, M.; Ban, J.-J.; Im, W.; Kim, M. Influence of Storage Condition on Exosome Recovery. *Biotechnol Bioproc E* **2016**, *21* (2), 299–304. https://doi.org/10.1007/s12257-015-0781-x.

(63) Yu, W.; Hurley, J.; Roberts, D.; Chakrabortty, S. K.; Enderle, D.; Noerholm, M.; Breakefield, X. O.; Skog, J. K. Exosome-Based Liquid Biopsies in Cancer: Opportunities and Challenges. *Annals of Oncology* **2021**, *32* (4), 466–477. https://doi.org/10.1016/j.annonc.2021.01.074.

(64) Xu, R.; Greening, D. W.; Zhu, H.-J.; Takahashi, N.; Simpson, R. J. Extracellular Vesicle Isolation and Characterization: Toward Clinical Application. *J Clin Invest* **2016**, *126* (4), 1152–1162. https://doi.org/10.1172/JCI81129.

(65) Sun, B.; Li, Y.; Zhou, Y.; Ng, T. K.; Zhao, C.; Gan, Q.; Gu, X.; Xiang, J. Circulating Exosomal CPNE3 as a Diagnostic and Prognostic Biomarker for Colorectal Cancer: SUN ET AL. *J Cell Physiol* **2019**, *234* (2), 1416–1425. https://doi.org/10.1002/jcp.26936.

(66) Szatanek, R.; Baj-Krzyworzeka, M.; Zimoch, J.; Lekka, M.; Siedlar, M.; Baran, J. The Methods of Choice for Extracellular Vesicles (EVs) Characterization. *Int J Mol Sci* **2017**, *18* (6). https://doi.org/10.3390/ijms18061153.

(67) Filipe, V.; Hawe, A.; Jiskoot, W. Critical Evaluation of Nanoparticle Tracking Analysis (NTA) by NanoSight for the Measurement of Nanoparticles and Protein Aggregates. *Pharm Res* **2010**, *27* (5), 796–810. https://doi.org/10.1007/s11095-010-0073-2.

(68) Maguire, C. M.; Rösslein, M.; Wick, P.; Prina-Mello, A. Characterisation of Particles in Solution – a Perspective on Light Scattering and Comparative Technologies. *Sci Technol Adv Mater* **2018**, *19* (1), 732–745. https://doi.org/10.1080/14686996.2018.1517587.

(69) Gurunathan, S.; Kang, M.-H.; Jeyaraj, M.; Qasim, M.; Kim, J.-H. Review of the Isolation, Characterization, Biological Function, and Multifarious Therapeutic Approaches of Exosomes. *Cells* **2019**, *8* (4), 307. https://doi.org/10.3390/cells8040307.

(70) Akers, J. C.; Ramakrishnan, V.; Nolan, J. P.; Duggan, E.; Fu, C.-C.; Hochberg, F. H.; Chen, C. C.; Carter, B. S. Comparative Analysis of Technologies for Quantifying Extracellular

Vesicles (EVs) in Clinical Cerebrospinal Fluids (CSF). *PLoS One* **2016**, *11* (2). https://doi.org/10.1371/journal.pone.0149866.

(71) Taylor, D. D.; Zacharias, W.; Gercel-Taylor, C. Exosome Isolation for Proteomic Analyses and RNA Profiling. *Methods Mol Biol* **2011**, *728*, 235–246. https://doi.org/10.1007/978-1-61779-068-3_15.

(72) Shao, H.; Im, H.; Castro, C. M.; Breakefield, X.; Weissleder, R.; Lee, H. New Technologies for Analysis of Extracellular Vesicles. *Chem. Rev.* **2018**, *118* (4), 1917–1950. https://doi.org/10.1021/acs.chemrev.7b00534.

(73) Witwer, K. W.; Buzás, E. I.; Bemis, L. T.; Bora, A.; Lässer, C.; Lötvall, J.; Nolte-'t Hoen, E. N.; Piper, M. G.; Sivaraman, S.; Skog, J.; Théry, C.; Wauben, M. H.; Hochberg, F. Standardization of Sample Collection, Isolation and Analysis Methods in Extracellular Vesicle Research. *J Extracell Vesicles* **2013**, *2*. https://doi.org/10.3402/jev.v2i0.20360.

(74) Rupp, A.-K.; Rupp, C.; Keller, S.; Brase, J. C.; Ehehalt, R.; Fogel, M.; Moldenhauer, G.; Marmé, F.; Sültmann, H.; Altevogt, P. Loss of EpCAM Expression in Breast Cancer Derived Serum Exosomes: Role of Proteolytic Cleavage. *Gynecol Oncol* **2011**, *122* (2), 437–446. https://doi.org/10.1016/j.ygyno.2011.04.035.

(75) Runz, S.; Keller, S.; Rupp, C.; Stoeck, A.; Issa, Y.; Koensgen, D.; Mustea, A.; Sehouli, J.; Kristiansen, G.; Altevogt, P. Malignant Ascites-Derived Exosomes of Ovarian Carcinoma Patients Contain CD24 and EpCAM. *Gynecol Oncol* **2007**, *107* (3), 563–571. https://doi.org/10.1016/j.ygyno.2007.08.064.

(76) Szajnik, M.; Derbis, M.; Lach, M.; Patalas, P.; Michalak, M.; Drzewiecka, H.; Szpurek, D.; Nowakowski, A.; Spaczynski, M.; Baranowski, W.; Whiteside, T. L. Exosomes in Plasma of Patients with Ovarian Carcinoma: Potential Biomarkers of Tumor Progression and Response to Therapy. *Gynecol Obstet (Sunnyvale)* **2013**, *Suppl 4*, 3. https://doi.org/10.4172/2161-0932.S4-003.

(77) Yoshioka, Y.; Konishi, Y.; Kosaka, N.; Katsuda, T.; Kato, T.; Ochiya, T. Comparative Marker Analysis of Extracellular Vesicles in Different Human Cancer Types. *J Extracell Vesicles* **2013**, *2*. https://doi.org/10.3402/jev.v2i0.20424.

(78) Ruiz-Martinez, M.; Navarro, A.; Marrades, R. M.; Viñolas, N.; Santasusagna, S.; Muñoz, C.; Ramírez, J.; Molins, L.; Monzo, M. YKT6 Expression, Exosome Release, and Survival in Non-Small Cell Lung Cancer. *Oncotarget* **2016**, *7* (32), 51515–51524. https://doi.org/10.18632/oncotarget.9862.

(79) Beckham Carla J.; Olsen Jayme; Yin Peng-Nien; Wu Chia-Hao; Ting Huei-Ju; Hagen Fred K.; Scosyrev Emelian; Messing Edward M.; Lee Yi-Fen. Bladder Cancer Exosomes Contain EDIL-3/Del1 and Facilitate Cancer Progression. *Journal of Urology* **2014**, *192* (2), 583–592. https://doi.org/10.1016/j.juro.2014.02.035.

(80) Liu, C.; Xu, X.; Li, B.; Situ, B.; Pan, W.; Hu, Y.; An, T.; Yao, S.; Zheng, L. Single-Exosome-Counting Immunoassays for Cancer Diagnostics. *Nano Lett.* **2018**, *18* (7), 4226–4232. https://doi.org/10.1021/acs.nanolett.8b01184.

(81) Hannafon, B. N.; Trigoso, Y. D.; Calloway, C. L.; Zhao, Y. D.; Lum, D. H.; Welm, A. L.; Zhao, Z. J.; Blick, K. E.; Dooley, W. C.; Ding, W. Q. Plasma Exosome MicroRNAs Are Indicative of Breast Cancer. *Breast Cancer Research* **2016**, *18* (1), 90. https://doi.org/10.1186/s13058-016-0753-x.

(82) Li, C.; Liu, D.-R.; Li, G.-G.; Wang, H.-H.; Li, X.-W.; Zhang, W.; Wu, Y.-L.; Chen, L. CD97 Promotes Gastric Cancer Cell Proliferation and Invasion through Exosome-Mediated MAPK Signaling Pathway. *World J Gastroenterol* **2015**, *21* (20), 6215–6228. https://doi.org/10.3748/wjg.v21.i20.6215.

(83) Pan, L.; Liang, W.; Fu, M.; Huang, Z.; Li, X.; Zhang, W.; Zhang, P.; Qian, H.; Jiang, P.; Xu, W.; Zhang, X. Exosomes-Mediated Transfer of Long Noncoding RNA ZFAS1 Promotes Gastric Cancer Progression. *J Cancer Res Clin Oncol* **2017**, *143* (6), 991–1004. https://doi.org/10.1007/s00432-017-2361-2.

(84) Wang, L.; Skotland, T.; Berge, V.; Sandvig, K.; Llorente, A. Exosomal Proteins as Prostate Cancer Biomarkers in Urine: From Mass Spectrometry Discovery to Immunoassay-Based Validation. *European Journal of Pharmaceutical Sciences* **2017**, *98*, 80–85. https://doi.org/10.1016/j.ejps.2016.09.023.

(85) Mahmood, T.; Yang, P.-C. Western Blot: Technique, Theory, and Trouble Shooting. *N Am J Med Sci* **2012**, *4* (9), 429–434. https://doi.org/10.4103/1947-2714.100998.

(86) Chiriacò, M. S.; Bianco, M.; Nigro, A.; Primiceri, E.; Ferrara, F.; Romano, A.; Quattrini, A.; Furlan, R.; Arima, V.; Maruccio, G. Lab-on-Chip for Exosomes and Microvesicles Detection and Characterization. *Sensors (Basel)* **2018**, *18* (10). https://doi.org/10.3390/s18103175.

(87) Nguyen, H.-Q.; Lee, D.; Kim, Y.; Paek, M.; Kim, M.; Jang, K.-S.; Oh, J.; Lee, Y.-S.; Yeon, J. E.; Lubman, D. M.; Kim, J. Platelet Factor 4 as a Novel Exosome Marker in MALDI-MS Analysis of Exosomes from Human Serum. *Anal. Chem.* **2019**, *91* (20), 13297–13305. https://doi.org/10.1021/acs.analchem.9b04198.

(88) Maji, S.; Chaudhary, P.; Akopova, I.; Nguyen, P. M.; Hare, R. J.; Gryczynski, I.; Vishwanatha, J. K. Exosomal Annexin A2 Promotes Angiogenesis and Breast Cancer Metastasis. *Mol Cancer Res* **2017**, *15* (1), 93–105. https://doi.org/10.1158/1541-7786.MCR-16-0163.

(89) Sakamoto, S.; Putalun, W.; Vimolmangkang, S.; Phoolcharoen, W.; Shoyama, Y.; Tanaka, H.; Morimoto, S. Enzyme-Linked Immunosorbent Assay for the Quantitative/Qualitative Analysis of Plant Secondary Metabolites. *J Nat Med* **2018**, *72* (1), 32–42. https://doi.org/10.1007/s11418-017-1144-z.

(90) Baker, H. N.; Murphy, R.; Lopez, E.; Garcia, C. Conversion of a Capture ELISA to a Luminex XMAP Assay Using a Multiplex Antibody Screening Method. *J Vis Exp* **2012**, No. 65. https://doi.org/10.3791/4084.

(91) Khan, S.; Bennit, H. F.; Turay, D.; Perez, M.; Mirshahidi, S.; Yuan, Y.; Wall, N. R. Early Diagnostic Value of Survivin and Its Alternative Splice Variants in Breast Cancer. *BMC Cancer* **2014**, *14*, 176. https://doi.org/10.1186/1471-2407-14-176.

(92) Logozzi, M.; De Milito, A.; Lugini, L.; Borghi, M.; Calabrò, L.; Spada, M.; Perdicchio, M.; Marino, M. L.; Federici, C.; Iessi, E.; Brambilla, D.; Venturi, G.; Lozupone, F.; Santinami, M.; Huber, V.; Maio, M.; Rivoltini, L.; Fais, S. High Levels of Exosomes Expressing CD63 and Caveolin-1 in Plasma of Melanoma Patients. *PLoS One* **2009**, *4* (4), e5219. https://doi.org/10.1371/journal.pone.0005219.

(93) Logozzi, M.; Di Raimo, R.; Mizzoni, D.; Fais, S. Immunocapture-Based ELISA to Characterize and Quantify Exosomes in Both Cell Culture Supernatants and Body Fluids. In *Methods in Enzymology*; Elsevier, 2020; Vol. 645, pp 155–180. https://doi.org/10.1016/bs.mie.2020.06.011.

(94) Breuninger, S.; Erl, J. Quantitative Analysis of Liposomal Heat Shock Protein 70 (Hsp70) in the Blood of Tumor Patients Using a Novel LipHsp70 ELISA. *J Clin Cell Immunol* **2014**, *05* (05). https://doi.org/10.4172/2155-9899.1000264.

(95) Zlotogorski-Hurvitz, A.; Dayan, D.; Chaushu, G.; Salo, T.; Vered, M. Morphological and Molecular Features of Oral Fluid-Derived Exosomes: Oral Cancer Patients versus Healthy Individuals. *J Cancer Res Clin Oncol* **2016**, *142* (1), 101–110. https://doi.org/10.1007/s00432-015-2005-3.

(96) Sharma, R.; Huang, X.; Brekken, R. A.; Schroit, A. J. Detection of Phosphatidylserine-Positive Exosomes for the Diagnosis of Early-Stage Malignancies. *British Journal of Cancer* **2017**, *117* (4), 545–552. https://doi.org/10.1038/bjc.2017.183.

(97) Hong, C.-S.; Muller, L.; Whiteside, T. L.; Boyiadzis, M. Plasma Exosomes as Markers of Therapeutic Response in Patients with Acute Myeloid Leukemia. *Front. Immunol.* **2014**, *5*. https://doi.org/10.3389/fimmu.2014.00160.

(98) Moon, P.-G.; Lee, J.-E.; Cho, Y.-E.; Lee, S. J.; Chae, Y. S.; Jung, J. H.; Kim, I.-S.; Park, H. Y.; Baek, M.-C. Fibronectin on Circulating Extracellular Vesicles as a Liquid Biopsy to Detect Breast Cancer. *Oncotarget* **2016**, *7* (26), 40189–40199. https://doi.org/10.18632/oncotarget.9561.

(99) Bandu, R.; Oh, J. W.; Kim, K. P. Mass Spectrometry-Based Proteome Profiling of Extracellular Vesicles and Their Roles in Cancer Biology. *Exp Mol Med* **2019**, *51* (3), 30. https://doi.org/10.1038/s12276-019-0218-2.

(100) Brown, B. A.; Zeng, X.; Todd, A. R.; Barnes, L. F.; Winstone, J. M. A.; Trinidad, J. C.; Novotny, M. V.; Jarrold, M. F.; Clemmer, D. E. Charge Detection Mass Spectrometry

Measurements of Exosomes and Other Extracellular Particles Enriched from Bovine Milk. *Anal. Chem.* **2020**, *92* (4), 3285–3292. https://doi.org/10.1021/acs.analchem.9b05173.

(101) Rosa-Fernandes, L.; Rocha, V. B.; Carregari, V. C.; Urbani, A.; Palmisano, G. A Perspective on Extracellular Vesicles Proteomics. *Front. Chem.* **2017**, *5*, 102. https://doi.org/10.3389/fchem.2017.00102.

(102) Palazzolo, G.; Albanese, N. N.; Cara, G. D.; Gygax, D.; Vittorelli, M. L.; Pucci-Minafra, I. Proteomic Analysis of Exosome-like Vesicles Derived from Breast Cancer Cells. *ANTICANCER RESEARCH* **2012**, 14.

(103) Chen, I.-H.; Xue, L.; Hsu, C.-C.; Paez, J. S. P.; Pan, L.; Andaluz, H.; Wendt, M. K.; Iliuk, A. B.; Zhu, J.-K.; Tao, W. A. Phosphoproteins in Extracellular Vesicles as Candidate Markers for Breast Cancer. *Proc Natl Acad Sci U S A* **2017**, *114* (12), 3175–3180. https://doi.org/10.1073/pnas.1618088114.

(104) Willms, E.; Johansson, H. J.; Mäger, I.; Lee, Y.; Blomberg, K. E. M.; Sadik, M.; Alaarg, A.; Smith, C. I. E.; Lehtiö, J.; EL Andaloussi, S.; Wood, M. J. A.; Vader, P. Cells Release Subpopulations of Exosomes with Distinct Molecular and Biological Properties. *Scientific Reports* **2016**, *6* (1), 22519. https://doi.org/10.1038/srep22519.

(105) Duijvesz, D.; Burnum-Johnson, K. E.; Gritsenko, M. A.; Hoogland, A. M.; Berg, M. S. V. den; Willemsen, R.; Luider, T.; Paša-Tolić, L.; Jenster, G. Proteomic Profiling of Exosomes Leads to the Identification of Novel Biomarkers for Prostate Cancer. *PLOS ONE* **2013**, *8* (12), e82589. https://doi.org/10.1371/journal.pone.0082589.

(106) Hosseini-Beheshti, E.; Pham, S.; Adomat, H.; Li, N.; Tomlinson Guns, E. S. Exosomes as Biomarker Enriched Microvesicles: Characterization of Exosomal Proteins Derived from a Panel of Prostate Cell Lines with Distinct AR Phenotypes. *Mol Cell Proteomics* **2012**, *11* (10), 863–885. https://doi.org/10.1074/mcp.M111.014845.

(107) Risha, Y.; Minic, Z.; Ghobadloo, S. M.; Berezovski, M. V. The Proteomic Analysis of Breast Cell Line Exosomes Reveals Disease Patterns and Potential Biomarkers. *Sci Rep* **2020**, *10* (1), 13572. https://doi.org/10.1038/s41598-020-70393-4.

(108) Görgens, A. Webinar | Analysis of Extracellular Vesicles Including Exosomes by Imaging Flow Cytometry. *Science* **2016**, *352* (6292), 1479–1479. https://doi.org/10.1126/science.352.6292.1479-b.

(109) Jara, R.; Campos, C.; María, M.; Vales, M. Exosome Detection and Characterization Based on Flow Cytometry. 8.

(110) Theodoraki, M.-N.; Hong, C.-S.; Donnenberg, V. S.; Donnenberg, A. D.; Whiteside, T. L. Evaluation of Exosome Proteins by On-Bead Flow Cytometry. *Cytometry Part A* **2021**, *99* (4), 372–381. https://doi.org/10.1002/cyto.a.24193.

(111) Escrevente, C.; Keller, S.; Altevogt, P.; Costa, J. Interaction and Uptake of Exosomes by Ovarian Cancer Cells. *BMC Cancer* **2011**, *11* (1), 108. https://doi.org/10.1186/1471-2407-11-108.

(112) Welton, J. L.; Khanna, S.; Giles, P. J.; Brennan, P.; Brewis, I. A.; Staffurth, J.; Mason, M. D.; Clayton, A. Proteomics Analysis of Bladder Cancer Exosomes*. *Molecular & Cellular Proteomics* **2010**, *9* (6), 1324–1338. https://doi.org/10.1074/mcp.M000063-MCP201.

(113) Tian, Y.; Ma, L.; Gong, M.; Su, G.; Zhu, S.; Zhang, W.; Wang, S.; Li, Z.; Chen, C.; Li, L.; Wu, L.; Yan, X. Protein Profiling and Sizing of Extracellular Vesicles from Colorectal Cancer Patients via Flow Cytometry. *ACS Nano* **2018**, *12* (1), 671–680. https://doi.org/10.1021/acsnano.7b07782.

(114) Theodoraki, M.-N.; Matsumoto, A.; Beccard, I.; Hoffmann, T. K.; Whiteside, T. L. CD44v3 Protein-Carrying Tumor-Derived Exosomes in HNSCC Patients' Plasma as Potential Noninvasive Biomarkers of Disease Activity. *OncoImmunology* **2020**, *9* (1), 1747732. https://doi.org/10.1080/2162402X.2020.1747732.

(115) Xiao, Y.; Li, Y.; Yuan, Y.; Liu, B.; Pan, S.; Liu, Q.; Qi, X.; Zhou, H.; Dong, W.; Jia, L. The Potential of Exosomes Derived from Colorectal Cancer as a Biomarker. *Clinica Chimica Acta* **2019**, *490*, 186–193. https://doi.org/10.1016/j.cca.2018.09.007.

(116) Cumba Garcia, L. M.; Peterson, T. E.; Cepeda, M. A.; Johnson, A. J.; Parney, I. F. Isolation and Analysis of Plasma-Derived Exosomes in Patients With Glioma. *Front. Oncol.* **2019**, *9*. https://doi.org/10.3389/fonc.2019.00651.

(117) Rim, K.-T.; Kim, S.-J. Quantitative Analysis of Exosomes From Murine Lung Cancer Cells by Flow Cytometry. *J Cancer Prev* **2016**, *21* (3), 194–200. https://doi.org/10.15430/JCP.2016.21.3.194.

(118) Nolan, J.; Sarimollaoglu, M.; Nedosekin, D. A.; Jamshidi-Parsian, A.; Galanzha, E. I.; Kore, R. A.; Griffin, R. J.; Zharov, V. P. In Vivo Flow Cytometry of Circulating Tumor-Associated Exosomes. *Analytical Cellular Pathology* **2016**, *2016*, e1628057. https://doi.org/10.1155/2016/1628057.

(119) O'Donnell, E. A.; Ernst, D. N.; Hingorani, R. Multiparameter Flow Cytometry: Advances in High Resolution Analysis. *Immune Netw* **2013**, *13* (2), 43–54. https://doi.org/10.4110/in.2013.13.2.43.

(120) Inglis, H.; Norris, P.; Danesh, A. Techniques for the Analysis of Extracellular Vesicles Using Flow Cytometry. *J Vis Exp* **2015**, No. 97. https://doi.org/10.3791/52484.

(121) Kibria, G.; Ramos, E. K.; Lee, K. E.; Bedoyan, S.; Huang, S.; Samaeekia, R.; Athman, J. J.; Harding, C. V.; Lötvall, J.; Harris, L.; Thompson, C. L.; Liu, H. A Rapid, Automated Surface Protein Profiling of Single Circulating Exosomes in Human Blood. *Sci Rep* **2016**, *6* (1), 36502. https://doi.org/10.1038/srep36502.

(122) Grasso, L.; Wyss, R.; Weidenauer, L.; Thampi, A.; Demurtas, D.; Prudent, M.; Lion, N.; Vogel, H. Molecular Screening of Cancer-Derived Exosomes by Surface Plasmon Resonance Spectroscopy. *Anal Bioanal Chem* **2015**, *407* (18), 5425–5432. https://doi.org/10.1007/s00216-015-8711-5.

(123) Liu, C.; Zeng, X.; An, Z.; Yang, Y.; Eisenbaum, M.; Gu, X.; Jornet, J. M.; Dy, G. K.; Reid, M. E.; Gan, Q.; Wu, Y. Sensitive Detection of Exosomal Proteins via a Compact Surface Plasmon Resonance Biosensor for Cancer Diagnosis. *ACS Sens.* **2018**, *3* (8), 1471–1479. https://doi.org/10.1021/acssensors.8b00230.

(124) Administrator, E. R. Surface Plasmon Resonance Assay for Exosomes | Exosome RNA, 2020.

(125) Im, H.; Shao, H.; Park, Y. I.; Peterson, V. M.; Castro, C. M.; Weissleder, R.; Lee, H. Label-Free Detection and Molecular Profiling of Exosomes with a Nano-Plasmonic Sensor. *Nat Biotechnol* **2014**, *32* (5), 490–495. https://doi.org/10.1038/nbt.2886.

(126) Sina, A. A. I.; Vaidyanathan, R.; Dey, S.; Carrascosa, L. G.; Shiddiky, M. J. A.; Trau, M. Real Time and Label Free Profiling of Clinically Relevant Exosomes. *Scientific Reports* **2016**, *6* (1), 30460. https://doi.org/10.1038/srep30460.

(127) Park, J.; Im, H.; Hong, S.; Castro, C. M.; Weissleder, R.; Lee, H. Analyses of Intravesicular Exosomal Proteins Using a Nano-Plasmonic System. *ACS Photonics* **2018**, *5* (2), 487–494. https://doi.org/10.1021/acsphotonics.7b00992.

(128) Lee, K.; Fraser, K.; Ghaddar, B.; Yang, K.; Kim, E.; Balaj, L.; Chiocca, E. A.; Breakefield, X. O.; Lee, H.; Weissleder, R. Multiplexed Profiling of Single Extracellular Vesicles. *ACS Nano* **2018**, *12* (1), 494–503. https://doi.org/10.1021/acsnano.7b07060.

(129) Wyss, R.; Grasso, L.; Wolf, C.; Grosse, W.; Demurtas, D.; Vogel, H. Molecular and Dimensional Profiling of Highly Purified Extracellular Vesicles by Fluorescence Fluctuation Spectroscopy. *Anal. Chem.* **2014**, *86* (15), 7229–7233. https://doi.org/10.1021/ac501801m.

(130) Kanwar, S. S.; Dunlay, C. J.; Simeone, D. M.; Nagrath, S. Microfluidic Device (ExoChip) for on-Chip Isolation, Quantification and Characterization of Circulating Exosomes. *Lab Chip* **2014**, *14* (11), 1891–1900. https://doi.org/10.1039/c4lc00136b.

(131) He, M.; Crow, J.; Roth, M.; Zeng, Y.; Godwin, A. K. Integrated Immunoisolation and Protein Analysis of Circulating Exosomes Using Microfluidic Technology. *Lab Chip* **2014**, *14* (19), 3773–3780. https://doi.org/10.1039/c4lc00662c.

(132) Zhao, Z.; Yang, Y.; Zeng, Y.; He, M. A Microfluidic ExoSearch Chip for Multiplexed Exosome Detection Towards Blood-Based Ovarian Cancer Diagnosis. *Lab Chip* **2016**, *16* (3), 489–496. https://doi.org/10.1039/c5lc01117e.

(133) Ko, J.; Hemphill, M. A.; Gabrieli, D.; Wu, L.; Yelleswarapu, V.; Lawrence, G.; Pennycooke, W.; Singh, A.; Meaney, D. F.; Issadore, D. Smartphone-Enabled Optofluidic

Exosome Diagnostic for Concussion Recovery. *Scientific Reports* **2016**, *6* (1), 31215. https://doi.org/10.1038/srep31215.

(134) Kalimuthu, K.; Kwon, W. Y.; Park, K. S. A Simple Approach for Rapid and Cost-Effective Quantification of Extracellular Vesicles Using a Fluorescence Polarization Technique. *Journal of Biological Engineering* **2019**, *13* (1), 31. https://doi.org/10.1186/s13036-019-0160-9.

(135) Daaboul, G. G.; Gagni, P.; Benussi, L.; Bettotti, P.; Ciani, M.; Cretich, M.; Freedman, D. S.; Ghidoni, R.; Ozkumur, A. Y.; Piotto, C.; Prosperi, D.; Santini, B.; Ünlü, M. S.; Chiari, M. Digital Detection of Exosomes by Interferometric Imaging. *Sci Rep* **2016**, *6* (1), 37246. https://doi.org/10.1038/srep37246.

(136) Boriachek, K.; Islam, M. N.; Gopalan, V.; Lam, A. K.; Nguyen, N.-T.; Shiddiky, M. J. A. Quantum Dot-Based Sensitive Detection of Disease Specific Exosome in Serum. *Analyst* **2017**, *142* (12), 2211–2219. https://doi.org/10.1039/C7AN00672A.

(137) Tu, M.; Wei, F.; Yang, J.; Wong, D. Detection of Exosomal Biomarker by Electric Field-Induced Release and Measurement (EFIRM). *J Vis Exp* **2015**, No. 95, 52439. https://doi.org/10.3791/52439.

(138) Doldán, X.; Fagúndez, P.; Cayota, A.; Laíz, J.; Tosar, J. P. Electrochemical Sandwich Immunosensor for Determination of Exosomes Based on Surface Marker-Mediated Signal Amplification. *Anal Chem* **2016**, *88* (21), 10466–10473. https://doi.org/10.1021/acs.analchem.6b02421.

(139) Li, Q.; Tofaris, G. K.; Davis, J. J. Concentration-Normalized Electroanalytical Assaying of Exosomal Markers. *Anal Chem* **2017**, *89* (5), 3184–3190. https://doi.org/10.1021/acs.analchem.6b05037.

(140) Vaidyanathan, R.; Naghibosadat, M.; Rauf, S.; Korbie, D.; Carrascosa, L. G.; Shiddiky, M. J. A.; Trau, M. Detecting Exosomes Specifically: A Multiplexed Device Based on Alternating Current Electrohydrodynamic Induced Nanoshearing. *Anal. Chem.* **2014**, *86* (22), 11125–11132. https://doi.org/10.1021/ac502082b.

(141) Jeong, S.; Park, J.; Pathania, D.; Castro, C. M.; Weissleder, R.; Lee, H. Integrated Magneto–Electrochemical Sensor for Exosome Analysis. *ACS Nano* **2016**, *10* (2), 1802–1809. https://doi.org/10.1021/acsnano.5b07584.

(142) Oliveira-Rodríguez, M.; Serrano-Pertierra, E.; García, A. C.; López-Martín, S.; Yañez-Mo, M.; Cernuda-Morollón, E.; Blanco-López, M. C. Point-of-Care Detection of Extracellular Vesicles: Sensitivity Optimization and Multiple-Target Detection. *Biosens Bioelectron* **2017**, *87*, 38–45. https://doi.org/10.1016/j.bios.2016.08.001.

(143) Shao, H.; Chung, J.; Balaj, L.; Charest, A.; Bigner, D. D.; Carter, B. S.; Hochberg, F. H.; Breakefield, X. O.; Weissleder, R.; Lee, H. Protein Typing of Circulating Microvesicles Allows Real-Time Monitoring of Glioblastoma Therapy. *Nat Med* **2012**, *18* (12), 1835–1840. https://doi.org/10.1038/nm.2994.

(144) Shao, H.; Chung, J.; Issadore, D. Diagnostic Technologies for Circulating Tumour Cells and Exosomes. *Biosci Rep* **2016**, *36* (1). https://doi.org/10.1042/BSR20150180.

(145) Avella-Oliver, M.; Puchades, R.; Wachsmann-Hogiu, S.; Maquieira, A. Label-Free SERS Analysis of Proteins and Exosomes with Large-Scale Substrates from Recordable Compact Disks. *Sensors and Actuators B: Chemical* **2017**, *252*, 657–662. https://doi.org/10.1016/j.snb.2017.06.058.

(146) Kwizera, E. A.; O'Connor, R.; Vinduska, V.; Williams, M.; Butch, E. R.; Snyder, S. E.; Chen, X.; Huang, X. Molecular Detection and Analysis of Exosomes Using Surface-Enhanced Raman Scattering Gold Nanorods and a Miniaturized Device. *Theranostics* **2018**, *8* (10), 2722–2738. https://doi.org/10.7150/thno.21358.

(147) Lee, J. U.; Kim, S.; Sim, S. J. SERS-Based Nanoplasmonic Exosome Analysis: Enabling Liquid Biopsy for Cancer Diagnosis and Monitoring Progression. *BioChip J* **2020**, *14* (3), 231–241. https://doi.org/10.1007/s13206-020-4301-5.

(148) Contreras-Naranjo, J. C.; Wu, H.-J.; Ugaz, V. M. Microfluidics for Exosome Isolation and Analysis: Enabling Liquid Biopsy for Personalized Medicine. *Lab Chip* **2017**, *17* (21), 3558–3577. https://doi.org/10.1039/c7lc00592j.

(149) Zhao, Z.; Wijerathne, H.; Godwin, A. K.; Soper, S. A. Isolation and Analysis Methods of Extracellular Vesicles (EVs). *Extracellular Vesicles and Circulating Nucleic Acids* **2021**, *2* (1), 80–103. https://doi.org/10.20517/evcna.2021.07.

(150) Koritzinsky, E. H.; Street, J. M.; Star, R. A.; Yuen, P. S. T. Quantification of Exosomes. *J Cell Physiol* **2017**, *232* (7), 1587–1590. https://doi.org/10.1002/jcp.25387.

(151) Tayebi, M.; Zhou, Y.; Tripathi, P.; Chandramohanadas, R.; Ai, Y. Exosome Purification and Analysis Using a Facile Microfluidic Hydrodynamic Trapping Device. *Anal. Chem.* **2020**, *92* (15), 10733–10742. https://doi.org/10.1021/acs.analchem.0c02006.

(152) L. Hisey, C.; Priya Dorayappan, K. D.; E. Cohn, D.; Selvendiran, K.; J. Hansford, D. Microfluidic Affinity Separation Chip for Selective Capture and Release of Label-Free Ovarian Cancer Exosomes. *Lab on a Chip* **2018**, *18* (20), 3144–3153. https://doi.org/10.1039/C8LC00834E.

(153) Dorayappan, K. D. P.; Gardner, M. L.; Hisey, C. L.; Zingarelli, R. A.; Smith, B. Q.; Lightfoot, M. D. S.; Gogna, R.; Flannery, M. M.; Hays, J.; Hansford, D. J.; Freitas, M. A.; Yu, L.; Cohn, D. E.; Selvendiran, K. A Microfluidic Chip Enables Isolation of Exosomes and Establishment of Their Protein Profiles and Associated Signaling Pathways in Ovarian Cancer. *Cancer Res* **2019**, *79* (13), 3503–3513. https://doi.org/10.1158/0008-5472.CAN-18-3538.

(154) Fang, S.; Tian, H.; Li, X.; Jin, D.; Li, X.; Kong, J.; Yang, C.; Yang, X.; Lu, Y.; Luo, Y.; Lin, B.; Niu, W.; Liu, T. Clinical Application of a Microfluidic Chip for Immunocapture and Quantification of Circulating Exosomes to Assist Breast Cancer Diagnosis and Molecular Classification. *PLOS ONE* **2017**, *12* (4), e0175050. https://doi.org/10.1371/journal.pone.0175050.

(155) Liu, C.; Guo, J.; Tian, F.; Yang, N.; Yan, F.; Ding, Y.; Wei, J.; Hu, G.; Nie, G.; Sun, J. Field-Free Isolation of Exosomes from Extracellular Vesicles by Microfluidic Viscoelastic Flows. *ACS Nano* **2017**, *11* (7), 6968–6976. https://doi.org/10.1021/acsnano.7b02277.

(156) Xu, H.; Liao, C.; Zuo, P.; Liu, Z.; Ye, B.-C. Magnetic-Based Microfluidic Device for On-Chip Isolation and Detection of Tumor-Derived Exosomes. *Anal. Chem.* **2018**, *90* (22), 13451–13458. https://doi.org/10.1021/acs.analchem.8b03272.

(157) Zhang, P.; He, M.; Zeng, Y. Ultrasensitive Microfluidic Analysis of Circulating Exosomes Using a Nanostructured Graphene Oxide/Polydopamine Coating. *Lab on a Chip* **2016**, *16* (16), 3033–3042. https://doi.org/10.1039/C6LC00279J.

(158) Singh Kanwar, S.; James Dunlay, C.; M. Simeone, D.; Nagrath, S. Microfluidic Device (ExoChip) for on-Chip Isolation, Quantification and Characterization of Circulating Exosomes. *Lab on a Chip* **2014**, *14* (11), 1891–1900. https://doi.org/10.1039/C4LC00136B.

(159) Zhu, Q.; Heon, M.; Zhao, Z.; He, M. Microfluidic Engineering of Exosomes: Editing Cellular Messages for Precision Therapeutics. *Lab Chip* **2018**, *18* (12), 1690–1703. https://doi.org/10.1039/C8LC00246K.

(160) Qi, R.; Zhu, G.; Wang, Y.; Wu, S.; Li, S.; Zhang, D.; Bu, Y.; Bhave, G.; Han, R.; Liu, X. Microfluidic Device for the Analysis of MDR Cancerous Cell-Derived Exosomes' Response to Nanotherapy. *Biomed Microdevices* **2019**, *21* (2), 35. https://doi.org/10.1007/s10544-019-0381-1.

(161) Grimm, T.; Grimm, T. A. FUSED DEPOSITION MODELLING: A TECHNOLOGY EVALUATION. 6.

(162) Melchels, F. P. W.; Feijen, J.; Grijpma, D. W. A Review on Stereolithography and Its Applications in Biomedical Engineering. *Biomaterials* **2010**, *31* (24), 6121–6130. https://doi.org/10.1016/j.biomaterials.2010.04.050.

(163) Gholizadeh, S.; Draz, M.; Zarghooni, M.; Nezhad, A. S.; Ghavami, S.; Shafiee, H.; Akbari, M. Microfluidic Approaches for Isolation, Detection, and Characterization of Extracellular Vesicles: Current Status and Future Directions. *Biosens Bioelectron* **2017**, *91*, 588–605. https://doi.org/10.1016/j.bios.2016.12.062.

(164) Kashefi-Kheyrabadi, L.; Kim, J.; Chakravarty, S.; Park, S.; Gwak, H.; Kim, S.-I.; Mohammadniaei, M.; Lee, M.-H.; Hyun, K.-A.; Jung, H.-I. Detachable Microfluidic Device Implemented with Electrochemical Aptasensor (DeMEA) for Sequential Analysis of Cancerous Exosomes. *Biosensors and Bioelectronics* **2020**, *169*, 112622. https://doi.org/10.1016/j.bios.2020.112622.

(165) Cheung, L. S.; Wei, X.; Martins, D.; Song, Y.-A. Rapid Detection of Exosomal MicroRNA Biomarkers by Electrokinetic Concentration for Liquid Biopsy on Chip. *Biomicrofluidics* **2018**, *12* (1), 014104. https://doi.org/10.1063/1.5009719.

(166) Zhao, Z.; McGill, J.; Gamero-Kubota, P.; He, M. Microfluidic On-Demand Engineering of Exosomes towards Cancer Immunotherapy. *Lab on a Chip* **2019**, *19* (10), 1877–1886. https://doi.org/10.1039/C8LC01279B.

(167) Baghban, R.; Roshangar, L.; Jahanban-Esfahlan, R.; Seidi, K.; Ebrahimi-Kalan, A.; Jaymand, M.; Kolahian, S.; Javaheri, T.; Zare, P. Tumor Microenvironment Complexity and Therapeutic Implications at a Glance. *Cell Commun Signal* **2020**, *18* (1), 59. https://doi.org/10.1186/s12964-020-0530-4.

(168) Langley, R. R.; Fidler, I. J. The Seed and Soil Hypothesis Revisited--the Role of Tumor-Stroma Interactions in Metastasis to Different Organs. *Int J Cancer* **2011**, *128* (11), 2527–2535. https://doi.org/10.1002/ijc.26031.

(169) Wei, R.; Liu, S.; Zhang, S.; Min, L.; Zhu, S. Cellular and Extracellular Components in Tumor Microenvironment and Their Application in Early Diagnosis of Cancers. *Analytical Cellular Pathology* **2020**, *2020*, 1–13. https://doi.org/10.1155/2020/6283796.

(170) Roma-Rodrigues, C.; Mendes, R.; Baptista, P. V.; Fernandes, A. R. Targeting Tumor Microenvironment for Cancer Therapy. *International Journal of Molecular Sciences* **2019**, *20* (4), 840. https://doi.org/10.3390/ijms20040840.

(171) Tan, S.; Xia, L.; Yi, P.; Han, Y.; Tang, L.; Pan, Q.; Tian, Y.; Rao, S.; Oyang, L.; Liang, J.; Lin, J.; Su, M.; Shi, Y.; Cao, D.; Zhou, Y.; Liao, Q. Exosomal MiRNAs in Tumor Microenvironment. *Journal of Experimental & Clinical Cancer Research* **2020**, *39* (1), 67. https://doi.org/10.1186/s13046-020-01570-6.

(172) Liang, W.; Chen, X.; Zhang, S.; Fang, J.; Chen, M.; Xu, Y.; Chen, X. Mesenchymal Stem Cells as a Double-Edged Sword in Tumor Growth: Focusing on MSC-Derived Cytokines. *Cell Mol Biol Lett* **2021**, *26* (1), 3. https://doi.org/10.1186/s11658-020-00246-5.

(173) Cufaro, M. C.; Pieragostino, D.; Lanuti, P.; Rossi, C.; Cicalini, I.; Federici, L.; De Laurenzi, V.; Del Boccio, P. Extracellular Vesicles and Their Potential Use in Monitoring Cancer Progression and Therapy: The Contribution of Proteomics. *Journal of Oncology* **2019**, *2019*, e1639854. https://doi.org/10.1155/2019/1639854.

(174) Liangsupree, T.; Multia, E.; Riekkola, M.-L. Modern Isolation and Separation Techniques for Extracellular Vesicles. *Journal of Chromatography A* **2021**, *1636*, 461773. https://doi.org/10.1016/j.chroma.2020.461773.

(175) Peng, X.; Yang, L.; Ma, Y.; Li, Y.; Li, H. Focus on the Morphogenesis, Fate and the Role in Tumor Progression of Multivesicular Bodies. *Cell Communication and Signaling* **2020**, *18* (1), 122. https://doi.org/10.1186/s12964-020-00619-5.

(176) Tschuschke, M.; Kocherova, I.; Bryja, A.; Mozdziak, P.; Angelova Volponi, A.; Janowicz, K.; Sibiak, R.; Piotrowska-Kempisty, H.; Iżycki, D.; Bukowska, D.; Antosik, P.; Shibli, J. A.; Dyszkiewicz-Konwińska, M.; Kempisty, B. Inclusion Biogenesis, Methods of Isolation and Clinical Application of Human Cellular Exosomes. *Journal of Clinical Medicine* **2020**, *9* (2), 436. https://doi.org/10.3390/jcm9020436.

(177) Cocucci, E.; Meldolesi, J. Ectosomes and Exosomes: Shedding the Confusion between Extracellular Vesicles. *Trends Cell Biol* **2015**, *25* (6), 364–372. https://doi.org/10.1016/j.tcb.2015.01.004.

(178) Kalluri, R.; LeBleu, V. S. The Biology, Function, and Biomedical Applications of Exosomes. *Science* **2020**, *367* (6478). https://doi.org/10.1126/science.aau6977.

(179) Kalluri, R. The Biology and Function of Exosomes in Cancer. *J Clin Invest* **2016**, *126* (4), 1208–1215. https://doi.org/10.1172/JCI81135.

(180) van Niel, G.; Porto-Carreiro, I.; Simoes, S.; Raposo, G. Exosomes: A Common Pathway for a Specialized Function. *The Journal of Biochemistry* **2006**, *140* (1), 13–21. https://doi.org/10.1093/jb/mvj128.

(181) Stoorvogel, W.; Kleijmeer, M. J.; Geuze, H. J.; Raposo, G. The Biogenesis and Functions of Exosomes. *Traffic* **2002**, *3* (5), 321–330. https://doi.org/10.1034/j.1600-0854.2002.30502.x.

(182) Sareyeldin, R. M.; Gupta, I.; Al-Hashimi, I.; Al-Thawadi, H. A.; Al Farsi, H. F.; Vranic, S.; Al Moustafa, A.-E. Gene Expression and MiRNAs Profiling: Function and Regulation in Human Epidermal Growth Factor Receptor 2 (HER2)-Positive Breast Cancer. *Cancers* **2019**, *11* (5), 646. https://doi.org/10.3390/cancers11050646.

(183) Wolff, A. C.; Hammond, M. E. H.; Allison, K. H.; Harvey, B. E.; Mangu, P. B.; Bartlett, J. M. S.; Bilous, M.; Ellis, I. O.; Fitzgibbons, P.; Hanna, W.; Jenkins, R. B.; Press, M. F.; Spears, P. A.; Vance, G. H.; Viale, G.; McShane, L. M.; Dowsett, M. Human Epidermal Growth Factor Receptor 2 Testing in Breast Cancer: American Society of Clinical Oncology/College of American Pathologists Clinical Practice Guideline Focused Update. *JCO* **2018**, *36* (20), 2105–2122. https://doi.org/10.1200/JCO.2018.77.8738.

(184) Freitas, M.; Nouws, H. P. A.; Keating, E.; Fernandes, V. C.; Delerue-Matos, C. Immunomagnetic Bead-Based Bioassay for the Voltammetric Analysis of the Breast Cancer Biomarker HER2-ECD and Tumour Cells Using Quantum Dots as Detection Labels. *Microchim Acta* **2020**, *187* (3), 184. https://doi.org/10.1007/s00604-020-4156-4.

(185) Perrier, A.; Gligorov, J.; Lefèvre, G.; Boissan, M. The Extracellular Domain of Her2 in Serum as a Biomarker of Breast Cancer. *Lab Invest* **2018**, *98* (6), 696–707. https://doi.org/10.1038/s41374-018-0033-8.

(186) Carretero-González, A.; Otero, I.; Carril-Ajuria, L.; de Velasco, G.; Manso, L. Exosomes: Definition, Role in Tumor Development and Clinical Implications. *Cancer Microenvironment* **2018**, *11* (1), 13–21. https://doi.org/10.1007/s12307-018-0211-7.

(187) Tickner, J. A.; Urquhart, A. J.; Stephenson, S.-A.; Richard, D. J.; O'Byrne, K. J. Functions and Therapeutic Roles of Exosomes in Cancer. *Front. Oncol.* **2014**, *4*. https://doi.org/10.3389/fonc.2014.00127.

(188) Sun, W.; Ren, Y.; Lu, Z.; Zhao, X. The Potential Roles of Exosomes in Pancreatic Cancer Initiation and Metastasis. *Molecular Cancer* **2020**, *19* (1), 135. https://doi.org/10.1186/s12943-020-01255-w.

(189) He, M.; Zeng, Y. Microfluidic Exosome Analysis toward Liquid Biopsy for Cancer. *J Lab Autom.* **2016**, *21* (4), 599–608. https://doi.org/10.1177/2211068216651035.

(190) Srivastava, A.; Moxley, K.; Ruskin, R.; Dhanasekaran, D. N.; Zhao, Y. D.; Ramesh, R. A Non-Invasive Liquid Biopsy Screening of Urine-Derived Exosomes for MiRNAs as Biomarkers in Endometrial Cancer Patients. *AAPS J* **2018**, *20* (5), 82. https://doi.org/10.1208/s12248-018-0220-y.

(191) Brock, G.; Castellanos-Rizaldos, E.; Hu, L.; Coticchia, C.; Skog, J. Liquid Biopsy for Cancer Screening, Patient Stratification and Monitoring. *Translational Cancer Research* **2015**, *4* (3). https://doi.org/10.21037/4546.

(192) Giannopoulou, L.; Zavridou, M.; Kasimir-Bauer, S.; Lianidou, E. S. Liquid Biopsy in Ovarian Cancer: The Potential of Circulating MiRNAs and Exosomes. *Transl Res* **2019**, *205*, 77–91. https://doi.org/10.1016/j.trsl.2018.10.003.

(193) Li, S.; Yi, M.; Dong, B.; Tan, X.; Luo, S.; Wu, K. The Role of Exosomes in Liquid Biopsy for Cancer Diagnosis and Prognosis Prediction. *International Journal of Cancer* **2021**, *148* (11), 2640–2651. https://doi.org/10.1002/ijc.33386.

(194) Marrugo-Ramírez, J.; Mir, M.; Samitier, J. Blood-Based Cancer Biomarkers in Liquid Biopsy: A Promising Non-Invasive Alternative to Tissue Biopsy. *International Journal of Molecular Sciences* **2018**, *19* (10), 2877. https://doi.org/10.3390/ijms19102877.

(195) Sunkara, V.; Woo, H.-K.; Cho, Y.-K. Emerging Techniques in the Isolation and Characterization of Extracellular Vesicles and Their Roles in Cancer Diagnostics and Prognostics. *Analyst* **2016**, *141* (2), 371–381. https://doi.org/10.1039/C5AN01775K.

(196) Mader, S.; Pantel, K. Liquid Biopsy: Current Status and Future Perspectives. *Oncol Res Treat* **2017**, *40* (7–8), 404–408. https://doi.org/10.1159/000478018.

(197) Halvaei, S.; Daryani, S.; Eslami-S, Z.; Samadi, T.; Jafarbeik-Iravani, N.; Bakhshayesh, T. O.; Majidzadeh-A, K.; Esmaeili, R. Exosomes in Cancer Liquid Biopsy: A Focus on Breast Cancer. *Mol Ther Nucleic Acids* **2018**, *10*, 131–141. https://doi.org/10.1016/j.omtn.2017.11.014.

(198) Castillo, J.; Bernard, V.; San Lucas, F. A.; Allenson, K.; Capello, M.; Kim, D. U.; Gascoyne, P.; Mulu, F. C.; Stephens, B. M.; Huang, J.; Wang, H.; Momin, A. A.; Jacamo, R. O.; Katz, M.; Wolff, R.; Javle, M.; Varadhachary, G.; Wistuba, I. I.; Hanash, S.; Maitra, A.; Alvarez, H. Surfaceome Profiling Enables Isolation of Cancer-Specific Exosomal Cargo in Liquid Biopsies from Pancreatic Cancer Patients. *Ann Oncol* **2018**, *29* (1), 223–229. https://doi.org/10.1093/annonc/mdx542.

(199) Giallombardo, M.; Chacártegui Borrás, J.; Castiglia, M.; Van Der Steen, N.; Mertens, I.; Pauwels, P.; Peeters, M.; Rolfo, C. Exosomal MiRNA Analysis in Non-Small Cell Lung Cancer

(NSCLC) Patients' Plasma Through QPCR: A Feasible Liquid Biopsy Tool. *J Vis Exp* **2016**, No. 111. https://doi.org/10.3791/53900.

(200) Czystowska-Kuzmicz, M.; Whiteside, T. L. The Potential Role of Tumor-Derived Exosomes in Diagnosis, Prognosis, and Response to Therapy in Cancer. *Expert Opinion on Biological Therapy* **2021**, *21* (2), 241–258. https://doi.org/10.1080/14712598.2020.1813276.

(201) Kairdolf, B. A.; Smith, A. M.; Stokes, T. H.; Wang, M. D.; Young, A. N.; Nie, S. Semiconductor Quantum Dots for Bioimaging and Biodiagnostic Applications. *Annu Rev Anal Chem (Palo Alto Calif)* **2013**, *6*, 143–162. https://doi.org/10.1146/annurev-anchem-060908-155136.

(202) Panagopoulou, M. S.; Wark, A. W.; Birch, D. J. S.; Gregory, C. D. Phenotypic Analysis of Extracellular Vesicles: A Review on the Applications of Fluorescence. *J Extracell Vesicles 9* (1). https://doi.org/10.1080/20013078.2019.1710020.

(203) Madhankumar, A. B.; Mrowczynski, O. D.; Patel, S. R.; Weston, C. L.; Zacharia, B. E.; Glantz, M. J.; Siedlecki, C. A.; Xu, L.-C.; Connor, J. R. Interleukin-13 Conjugated Quantum Dots for Identification of Glioma Initiating Cells and Their Extracellular Vesicles. *Acta Biomater* **2017**, *58*, 205–213. https://doi.org/10.1016/j.actbio.2017.06.002.

(204) Dobhal, G.; Ayupova, D.; Laufersky, G.; Ayed, Z.; Nann, T.; Goreham, R. V. Cadmium-Free Quantum Dots as Fluorescent Labels for Exosomes. *Sensors* **2018**, *18* (10), 3308. https://doi.org/10.3390/s18103308.

(205) Bai, Y.; Lu, Y.; Wang, K.; Cheng, Z.; Qu, Y.; Qiu, S.; Zhou, L.; Wu, Z.; Liu, H.; Zhao, J.; Mao, H. Rapid Isolation and Multiplexed Detection of Exosome Tumor Markers Via Queued Beads Combined with Quantum Dots in a Microarray. *Nano-Micro Lett.* **2019**, *11* (1), 59. https://doi.org/10.1007/s40820-019-0285-x.

(206) Rodrigues, M.; Richards, N.; Ning, B.; Lyon, C. J.; Hu, T. Y. Rapid Lipid-Based Approach for Normalization of Quantum-Dot-Detected Biomarker Expression on Extracellular Vesicles in Complex Biological Samples. *Nano Lett.* **2019**, *19* (11), 7623–7631. https://doi.org/10.1021/acs.nanolett.9b02232.

(207) Zhang, M.; Vojtech, L.; Ye, Z.; Hladik, F.; Nance, E. Quantum Dot Labeling and Visualization of Extracellular Vesicles. *ACS Appl. Nano Mater.* **2020**, *3* (7), 7211–7222. https://doi.org/10.1021/acsanm.0c01553.

(208) Wu, M.; Chen, Z.; Xie, Q.; Xiao, B.; Zhou, G.; Chen, G.; Bian, Z. One-Step Quantification of Salivary Exosomes Based on Combined Aptamer Recognition and Quantum Dot Signal Amplification. *Biosensors and Bioelectronics* **2021**, *171*, 112733. https://doi.org/10.1016/j.bios.2020.112733.

(209) Kim, H.-M.; Oh, C.; An, J.; Baek, S.; Bock, S.; Kim, J.; Jung, H.-S.; Song, H.; Kim, J.-W.; Jo, A.; Kim, D.-E.; Rho, W.-Y.; Jang, J.-Y.; Cheon, G. J.; Im, H.-J.; Jun, B.-H. Multi-Quantum Dots-Embedded Silica-Encapsulated Nanoparticle-Based Lateral Flow Assay for

Highly Sensitive Exosome Detection. *Nanomaterials* **2021**, *11* (3), 768. https://doi.org/10.3390/nano11030768.

(210) Zhang, W.; Peng, P.; Kuang, Y.; Yang, J.; Cao, D.; You, Y.; Shen, K. Characterization of Exosomes Derived from Ovarian Cancer Cells and Normal Ovarian Epithelial Cells by Nanoparticle Tracking Analysis. *Tumour Biol* **2016**, *37* (3), 4213–4221. https://doi.org/10.1007/s13277-015-4105-8.

(211) Thane, K. E.; Davis, A. M.; Hoffman, A. M. Improved Methods for Fluorescent Labeling and Detection of Single Extracellular Vesicles Using Nanoparticle Tracking Analysis. *Scientific Reports* **2019**, *9* (1), 12295. https://doi.org/10.1038/s41598-019-48181-6.

(212) Kowal, J.; Arras, G.; Colombo, M.; Jouve, M.; Morath, J. P.; Primdal-Bengtson, B.; Dingli, F.; Loew, D.; Tkach, M.; Théry, C. Proteomic Comparison Defines Novel Markers to Characterize Heterogeneous Populations of Extracellular Vesicle Subtypes. *PNAS* **2016**, *113* (8), E968–E977. https://doi.org/10.1073/pnas.1521230113.

(213) Tomlinson, M. G. Platelet Tetraspanins: Small but Interesting. *J Thromb Haemost* **2009**, *7* (12), 2070–2073. https://doi.org/10.1111/j.1538-7836.2009.03613.x.

(214) Liang, K.; Liu, F.; Fan, J.; Sun, D.; Liu, C.; Lyon, C. J.; Bernard, D. W.; Li, Y.; Yokoi, K.; Katz, M. H.; Koay, E. J.; Zhao, Z.; Hu, Y. Nanoplasmonic Quantification of Tumour-Derived Extracellular Vesicles in Plasma Microsamples for Diagnosis and Treatment Monitoring. *Nature Biomedical Engineering* **2017**, *1* (4), 1–11. https://doi.org/10.1038/s41551-016-0021.

(215) Sheridan, C.; Kishimoto, H.; Fuchs, R. K.; Mehrotra, S.; Bhat-Nakshatri, P.; Turner, C. H.; Goulet, R.; Badve, S.; Nakshatri, H. CD44+/CD24- Breast Cancer Cells Exhibit Enhanced Invasive Properties: An Early Step Necessary for Metastasis. *Breast Cancer Res* **2006**, *8* (5), R59. https://doi.org/10.1186/bcr1610.

(216) Subik, K.; Lee, J.-F.; Baxter, L.; Strzepek, T.; Costello, D.; Crowley, P.; Xing, L.; Hung, M.-C.; Bonfiglio, T.; Hicks, D. G.; Tang, P. The Expression Patterns of ER, PR, HER2, CK5/6, EGFR, Ki-67 and AR by Immunohistochemical Analysis in Breast Cancer Cell Lines. *Breast Cancer (Auckl)* **2010**, *4*, 35–41.

(217) Soysal, S. D.; Muenst, S.; Barbie, T.; Fleming, T.; Gao, F.; Spizzo, G.; Oertli, D.; Viehl, C. T.; Obermann, E. C.; Gillanders, W. E. EpCAM Expression Varies Significantly and Is Differentially Associated with Prognosis in the Luminal B HER2(+), Basal-like, and HER2 Intrinsic Subtypes of Breast Cancer. *Br J Cancer* **2013**, *108* (7), 1480–1487. https://doi.org/10.1038/bjc.2013.80.

(218) Crosby, D.; Lyons, N.; Greenwood, E.; Harrison, S.; Hiom, S.; Moffat, J.; Quallo, T.; Samuel, E.; Walker, I. A Roadmap for the Early Detection and Diagnosis of Cancer. *The Lancet Oncology* **2020**, *21* (11), 1397–1399. https://doi.org/10.1016/S1470-2045(20)30593-3.

(219) Somigliana, E.; Vercellini, P.; Vigano', P.; Benaglia, L.; Crosignani, P. G.; Fedele, L. Non-Invasive Diagnosis of Endometriosis: The Goal or Own Goal? *Human Reproduction* **2010**, *25* (8), 1863–1868. https://doi.org/10.1093/humrep/deq141.

(220) Li, J.; Guan, X.; Fan, Z.; Ching, L.-M.; Li, Y.; Wang, X.; Cao, W.-M.; Liu, D.-X. Non-Invasive Biomarkers for Early Detection of Breast Cancer. *Cancers* **2020**, *12* (10), 2767. https://doi.org/10.3390/cancers12102767.

(221) Cheng, Y.-S. L.; Rees, T.; Wright, J. A Review of Research on Salivary Biomarkers for Oral Cancer Detection. *Clin Trans Med* **2014**, *3* (1), 3. https://doi.org/10.1186/2001-1326-3-3.

(222) Ng, E. Y.-K. A Review of Thermography as Promising Non-Invasive Detection Modality for Breast Tumor. *International Journal of Thermal Sciences* **2009**, *48* (5), 849–859. https://doi.org/10.1016/j.ijthermalsci.2008.06.015.

(223) Jalalian, S. H.; Ramezani, M.; Jalalian, S. A.; Abnous, K.; Taghdisi, S. M. Exosomes, New Biomarkers in Early Cancer Detection. *Analytical Biochemistry* **2019**, *571*, 1–13. https://doi.org/10.1016/j.ab.2019.02.013.

(224) Dong, X.; Zheng, D.; Nao, J. Circulating Exosome MicroRNAs as Diagnostic Biomarkers of Dementia. *Front Aging Neurosci* **2020**, *12*, 580199. https://doi.org/10.3389/fnagi.2020.580199.

(225) Simpson, R. J.; Lim, J. W.; Moritz, R. L.; Mathivanan, S. Exosomes: Proteomic Insights and Diagnostic Potential. *Expert Rev Proteomics* **2009**, *6* (3), 267–283. https://doi.org/10.1586/epr.09.17.

(226) Im, H.; Lee, K.; Weissleder, R.; Lee, H.; Castro, C. M. Novel Nanosensing Technologies for Exosome Detection and Profiling. *Lab Chip* **2017**, *17* (17), 2892–2898. https://doi.org/10.1039/C7LC00247E.

(227) Buzás, E. I.; Gardiner, C.; Lee, C.; Smith, Z. J. Single Particle Analysis: Methods for Detection of Platelet Extracellular Vesicles in Suspension (Excluding Flow Cytometry). *Platelets* **2017**, *28* (3), 249–255. https://doi.org/10.1080/09537104.2016.1260704.

(228) Gandham, S.; Su, X.; Wood, J.; Nocera, A. L.; Alli, S. C.; Milane, L.; Zimmerman, A.; Amiji, M.; Ivanov, A. R. Technologies and Standardization in Research on Extracellular Vesicles. *Trends in Biotechnology* **2020**, *38* (10), 1066–1098. https://doi.org/10.1016/j.tibtech.2020.05.012.

(229) Görgens, A.; Bremer, M.; Ferrer-Tur, R.; Murke, F.; Tertel, T.; Horn, P. A.; Thalmann, S.; Welsh, J. A.; Probst, C.; Guerin, C.; Boulanger, C. M.; Jones, J. C.; Hanenberg, H.; Erdbrügger, U.; Lannigan, J.; Ricklefs, F. L.; El-Andaloussi, S.; Giebel, B. Optimisation of Imaging Flow Cytometry for the Analysis of Single Extracellular Vesicles by Using Fluorescence-Tagged Vesicles as Biological Reference Material. *J Extracell Vesicles* **2019**, *8* (1). https://doi.org/10.1080/20013078.2019.1587567.

(230) Morales-Kastresana, A.; Telford, B.; Musich, T. A.; McKinnon, K.; Clayborne, C.; Braig, Z.; Rosner, A.; Demberg, T.; Watson, D. C.; Karpova, T. S.; Freeman, G. J.; DeKruyff, R. H.; Pavlakis, G. N.; Terabe, M.; Robert-Guroff, M.; Berzofsky, J. A.; Jones, J. C. Labeling Extracellular Vesicles for Nanoscale Flow Cytometry. *Scientific Reports* **2017**, *7* (1), 1878. https://doi.org/10.1038/s41598-017-01731-2.

(231) Stoner, S. A.; Duggan, E.; Condello, D.; Guerrero, A.; Turk, J. R.; Narayanan, P. K.; Nolan, J. P. High Sensitivity Flow Cytometry of Membrane Vesicles. *Cytometry A* **2016**, *89* (2), 196–206. https://doi.org/10.1002/cyto.a.22787.

(232) Inglis, H. C.; Danesh, A.; Shah, A.; Lacroix, J.; Spinella, P. C.; Norris, P. J. Techniques to Improve Detection and Analysis of Extracellular Vesicles Using Flow Cytometry. *Cytometry A* **2015**, *87* (11), 1052–1063. https://doi.org/10.1002/cyto.a.22649.

(233) van der Vlist, E. J.; Nolte-'t Hoen, E. N. M.; Stoorvogel, W.; Arkesteijn, G. J. A.; Wauben, M. H. M. Fluorescent Labeling of Nano-Sized Vesicles Released by Cells and Subsequent Quantitative and Qualitative Analysis by High-Resolution Flow Cytometry. *Nat Protoc* **2012**, *7* (7), 1311–1326. https://doi.org/10.1038/nprot.2012.065.

(234) Marcoux, G.; Duchez, A.-C.; Cloutier, N.; Provost, P.; Nigrovic, P. A.; Boilard, E. Revealing the Diversity of Extracellular Vesicles Using High-Dimensional Flow Cytometry Analyses. *Sci Rep* **2016**, *6*, 35928. https://doi.org/10.1038/srep35928.

(235) Mastoridis, S.; Bertolino, G. M.; Whitehouse, G.; Dazzi, F.; Sanchez-Fueyo, A.; Martinez-Llordella, M. Multiparametric Analysis of Circulating Exosomes and Other Small Extracellular Vesicles by Advanced Imaging Flow Cytometry. *Front. Immunol.* **2018**, *9*. https://doi.org/10.3389/fimmu.2018.01583.

(236) Löf, L.; Ebai, T.; Dubois, L.; Wik, L.; Ronquist, K. G.; Nolander, O.; Lundin, E.; Söderberg, O.; Landegren, U.; Kamali-Moghaddam, M. Detecting Individual Extracellular Vesicles Using a Multicolor in Situ Proximity Ligation Assay with Flow Cytometric Readout. *Sci Rep* **2016**, *6* (1), 34358. https://doi.org/10.1038/srep34358.

(237) Kumar, D.; Gupta, D.; Shankar, S.; Srivastava, R. K. Biomolecular Characterization of Exosomes Released from Cancer Stem Cells: Possible Implications for Biomarker and Treatment of Cancer. *Oncotarget* **2014**, *6* (5), 3280–3291.

(238) Chuo, S. T.-Y.; Chien, J. C.-Y.; Lai, C. P.-K. Imaging Extracellular Vesicles: Current and Emerging Methods. *J Biomed Sci* **2018**, *25*. https://doi.org/10.1186/s12929-018-0494-5.

(239) Li, X.; Corbett, A. L.; Taatizadeh, E.; Tasnim, N.; Little, J. P.; Garnis, C.; Daugaard, M.; Guns, E.; Hoorfar, M.; Li, I. T. S. Challenges and Opportunities in Exosome Research—Perspectives from Biology, Engineering, and Cancer Therapy. *APL Bioengineering* **2019**, *3* (1), 011503. https://doi.org/10.1063/1.5087122.

(240) Feng, D.; Zhao, W.-L.; Ye, Y.-Y.; Bai, X.-C.; Liu, R.-Q.; Chang, L.-F.; Zhou, Q.; Sui, S.-F. Cellular Internalization of Exosomes Occurs Through Phagocytosis. *Traffic* **2010**, *11* (5), 675–687. https://doi.org/10.1111/j.1600-0854.2010.01041.x.

(241) Morishita, M.; Takahashi, Y.; Nishikawa, M.; Takakura, Y. Pharmacokinetics of Exosomes—An Important Factor for Elucidating the Biological Roles of Exosomes and for the Development of Exosome-Based Therapeutics. *Journal of Pharmaceutical Sciences* **2017**, *106* (9), 2265–2269. https://doi.org/10.1016/j.xphs.2017.02.030.

(242) Tian, T.; Wang, Y.; Wang, H.; Zhu, Z.; Xiao, Z. Visualizing of the Cellular Uptake and Intracellular Trafficking of Exosomes by Live-Cell Microscopy. *Journal of Cellular Biochemistry* **2010**, *111* (2), 488–496. https://doi.org/10.1002/jcb.22733.

(243) Chen, C.; Zong, S.; Wang, Z.; Lu, J.; Zhu, D.; Zhang, Y.; Zhang, R.; Cui, Y. Visualization and Intracellular Dynamic Tracking of Exosomes and Exosomal MiRNAs Using Single Molecule Localization Microscopy. *Nanoscale* **2018**, *10* (11), 5154–5162. https://doi.org/10.1039/C7NR08800K.

(244) Song, S.; Shim, M. K.; Lim, S.; Moon, Y.; Yang, S.; Kim, J.; Hong, Y.; Yoon, H. Y.; Kim, I.-S.; Hwang, K. Y.; Kim, K. In Situ One-Step Fluorescence Labeling Strategy of Exosomes via Bioorthogonal Click Chemistry for Real-Time Exosome Tracking In Vitro and In Vivo. *Bioconjugate Chem.* **2020**, *31* (5), 1562–1574. https://doi.org/10.1021/acs.bioconjchem.0c00216.

(245) Jung, K. O.; Jo, H.; Yu, J. H.; Gambhir, S. S.; Pratx, G. Development and MPI Tracking of Novel Hypoxia-Targeted Theranostic Exosomes. *Biomaterials* **2018**, *177*, 139–148. https://doi.org/10.1016/j.biomaterials.2018.05.048.

(246) Shi, R.; Zhao, L.; Cai, W.; Wei, M.; Zhou, X.; Yang, G.; Yuan, L. Maternal Exosomes in Diabetes Contribute to the Cardiac Development Deficiency. *Biochemical and Biophysical Research Communications* **2017**, *483* (1), 602–608. https://doi.org/10.1016/j.bbrc.2016.12.097.

(247) Chen, L.; Wang, Y.; Pan, Y.; Zhang, L.; Shen, C.; Qin, G.; Ashraf, M.; Weintraub, N.; Ma, G.; Tang, Y. Cardiac Progenitor-Derived Exosomes Protect Ischemic Myocardium from Acute Ischemia/Reperfusion Injury. *Biochemical and Biophysical Research Communications* **2013**, *431* (3), 566–571. https://doi.org/10.1016/j.bbrc.2013.01.015.

(248) Mineo, M.; Garfield, S. H.; Taverna, S.; Flugy, A.; De Leo, G.; Alessandro, R.; Kohn, E. C. Exosomes Released by K562 Chronic Myeloid Leukemia Cells Promote Angiogenesis in a Src-Dependent Fashion. *Angiogenesis* **2012**, *15* (1), 33–45. https://doi.org/10.1007/s10456-011-9241-1.

(249) Banizs, A. B.; Huang, T.; Dryden, K.; Berr, S. S.; Stone, J. R.; Nakamoto, R. K.; Shi, W.; He, J. In Vitro Evaluation of Endothelial Exosomes as Carriers for Small Interfering Ribonucleic Acid Delivery. *Int J Nanomedicine* **2014**, *9*, 4223–4230. https://doi.org/10.2147/IJN.S64267.

(250) Tian, Y.; Li, S.; Song, J.; Ji, T.; Zhu, M.; Anderson, G. J.; Wei, J.; Nie, G. A Doxorubicin Delivery Platform Using Engineered Natural Membrane Vesicle Exosomes for Targeted Tumor Therapy. *Biomaterials* **2014**, *35* (7), 2383–2390. https://doi.org/10.1016/j.biomaterials.2013.11.083.

(251) Beit-Yannai, E.; Tabak, S.; Stamer, W. D. Physical Exosome:Exosome Interactions. *Journal of Cellular and Molecular Medicine* **2018**, *22* (3), 2001–2006. https://doi.org/10.1111/jcmm.13479.

(252) Horibe, S.; Tanahashi, T.; Kawauchi, S.; Murakami, Y.; Rikitake, Y. Mechanism of Recipient Cell-Dependent Differences in Exosome Uptake. *BMC Cancer* **2018**, *18* (1), 47. https://doi.org/10.1186/s12885-017-3958-1.

(253) Fei, X.; Gu, Y. Progress in Modifications and Applications of Fluorescent Dye Probe. *Progress in Natural Science* **2009**, *19* (1), 1–7. https://doi.org/10.1016/j.pnsc.2008.06.004.

(254) Goftar, M. K.; Moradi, K.; Kor, N. M. Spectroscopic Studies on Aggregation Phenomena of Dyes. **2014**, 10.

(255) McKay, I. C.; Forman, D.; White, R. G. A Comparison of Fluorescein Isothiocyanate and Lissamine Rhodamine (RB 200) as Labels for Antibody in the Fluorescent Antibody Technique. *Immunology* **1981**, *43* (3), 591–602.

(256) Kawasaki, E. S.; Player, A. Nanotechnology, Nanomedicine, and the Development of New, Effective Therapies for Cancer. *Nanomedicine* **2005**, *1* (2), 101–109. https://doi.org/10.1016/j.nano.2005.03.002.

(257) Gao, X.; Yang, L.; Petros, J. A.; Marshall, F. F.; Simons, J. W.; Nie, S. In Vivo Molecular and Cellular Imaging with Quantum Dots. *Curr Opin Biotechnol* **2005**, *16* (1), 63–72. https://doi.org/10.1016/j.copbio.2004.11.003.

(258) Jia, H.-R.; Zhu, Y.-X.; Xu, K.-F.; Pan, G.-Y.; Liu, X.; Qiao, Y.; Wu, F.-G. Efficient Cell Surface Labelling of Live Zebrafish Embryos: Wash-Free Fluorescence Imaging for Cellular Dynamics Tracking and Nanotoxicity Evaluation. *Chemical Science* **2019**, *10* (14), 4062–4068. https://doi.org/10.1039/C8SC04884C.

(259) He, F.; Liu, H.; Guo, X.; Yin, B.-C.; Ye, B.-C. Direct Exosome Quantification via Bivalent-Cholesterol-Labeled DNA Anchor for Signal Amplification. *Anal. Chem.* **2017**, *89* (23), 12968–12975. https://doi.org/10.1021/acs.analchem.7b03919.

(260) Park, J. J.; Lee, T. S.; Son, J. J.; Kang, J. H.; Kim, K. I.; Choi, C. W.; Lim, S. M. Comparison between Direct and Indirect Labeling Methods for Monitoring Cell Trafficking. *Journal of Nuclear Medicine* **2009**, *50* (supplement 2), 1018–1018.

CCC Marketplace™

This is a License Agreement between Vojtech Vinduska ("You") and Nancy International Ltd Subsidiary AME Publishing Company ("Publisher") provided by Copyright Clearance Center ("CCC"). The license consists of your order details, the terms and conditions provided by Nancy International Ltd Subsidiary AME Publishing Company, and the CCC terms and conditions.

All payments must be made in full to CCC.

Order Date	01-Jun-2021	**Type of Use**	Republish in a thesis/dissertation
Order License ID	1122896-1		
ISSN	2218-676X	**Publisher**	Pioneer Bioscience Publishing Company
		Portion	Image/photo/illustration

LICENSED CONTENT

Publication Title	Translational cancer research	**Country**	China
		Rightsholder	Nancy International Ltd Subsidiary AME Publishing Company
Date	12/31/2011		
Language	English		
		Publication Type	Journal

REQUEST DETAILS

Portion Type	Image/photo/illustration	**Distribution**	United States
Number of images / photos / illustrations	1	**Translation**	Original language of publication
Format (select all that apply)	Electronic	**Copies for the disabled?**	No
		Minor editing privileges?	No
Who will republish the content?	Academic institution	**Incidental promotional use?**	No
Duration of Use	Life of current edition	**Currency**	USD
Lifetime Unit Quantity	Up to 499		
Rights Requested	Main product		

NEW WORK DETAILS

Title	DEVELOPMENT OF EXOSOMAL PROTEIN DETECTION ASSAYS FOR CANCER DIAGNOSTICS USING NANOMATERIALS IN CONJUCTION WITH OPTICAL SPECTROSCOPY AND IMAGING	**Institution name**	University of Memphis
		Expected presentation date	2021-06-01
Instructor name	Vojtech Vinduska		

ADDITIONAL DETAILS

Order reference number	N/A

The requesting person / organization to appear on the license	Vojtech Vinduska

REUSE CONTENT DETAILS

Title, description or numeric reference of the portion(s)	DEVELOPMENT OF EXOSOMAL PROTEIN DETECTION ASSAYS FOR CANCER DIAGNOSTICS USING NANOMATERIALS IN CONJUCTION WITH OPTICAL SPECTROSCOPY AND IMAGING	**Title of the article/chapter the portion is from**	1.1. Morphology and Composition of Exosomes
		Author of portion(s)	Vojtech Vinduska
		Issue, if republishing an article from a serial	N/A
		Publication date of portion	2021-06-01
Editor of portion(s)	Vojtech Vinduska		
Volume of serial or monograph	N/A		
Page or page range of portion	14		

RIGHTSHOLDER TERMS AND CONDITIONS

CCC Marketplace™

This is a License Agreement between Vojtech Vinduska ("You") and Rockefeller University Press ("Publisher") provided by Copyright Clearance Center ("CCC"). The license consists of your order details, the terms and conditions provided by Rockefeller University Press, and the CCC terms and conditions.

All payments must be made in full to CCC.

Order Date	01-Jun-2021	**Type of Use**	Republish in a thesis/dissertation
Order License ID	1122899-1		
ISSN	1540-8140	**Publisher**	ROCKEFELLER UNIVERSITY PRESS
		Portion	Image/photo/illustration

LICENSED CONTENT

Publication Title	The journal of cell biology	**Publication Type**	e-Journal
Article Title	Extracellular vesicles: exosomes, microvesicles, and friends.	**Start Page**	373
		End Page	383
Date	12/31/1961	**Issue**	4
Language	English	**Volume**	200
Country	United States of America	**URL**	http://www.jcb.org/
Rightsholder	Rockefeller University Press		

REQUEST DETAILS

Portion Type	Image/photo/illustration	**Distribution**	United States
Number of images / photos / illustrations	1	**Translation**	Original language of publication
Format (select all that apply)	Electronic	**Copies for the disabled?**	No
		Minor editing privileges?	No
Who will republish the content?	Academic institution	**Incidental promotional use?**	No
Duration of Use	Life of current edition	**Currency**	USD
Lifetime Unit Quantity	Up to 499		
Rights Requested	Main product and any product related to main product		

NEW WORK DETAILS

Title	DEVELOPMENT OF EXOSOMAL PROTEIN DETECTION ASSAYS FOR CANCER DIAGNOSTICS USING NANOMATERIALS IN CONJUCTION WITH OPTICAL SPECTROSCOPY AND IMAGING	**Institution name**	University of Memphis
		Expected presentation date	2021-06-02

Instructor name	Xiaohua Huang

ADDITIONAL DETAILS

Order reference number	N/A	**The requesting person / organization to appear on the license**	Vojtech Vinduska

REUSE CONTENT DETAILS

Title, description or numeric reference of the portion(s)	Figure 2. Release of MVs and exosomes.	**Title of the article/chapter the portion is from**	Extracellular vesicles: exosomes, microvesicles, and friends.
Editor of portion(s)	Raposo, Graça; Stoorvogel, Willem	**Author of portion(s)**	Raposo, Graça; Stoorvogel, Willem
Volume of serial or monograph	200	**Issue, if republishing an article from a serial**	4
Page or page range of portion	373-383	**Publication date of portion**	2013-02-17

CCC Marketplace™

This is a License Agreement between Vojtech Vinduska ("User") and Copyright Clearance Center, Inc. ("CCC") on behalf of the Rightsholder identified in the order details below. The license consists of the order details, the CCC Terms and Conditions below, and any Rightsholder Terms and Conditions which are included below.

All payments must be made in full to CCC in accordance with the CCC Terms and Conditions below.

Order Date	23-Jun-2021	**Type of Use**	Republish in a thesis/dissertation
Order License ID	1128150-1		
ISSN	0009-9147	**Publisher**	P.B. HOEBER,
		Portion	Image/photo/illustration

LICENSED CONTENT

Publication Title	Clinical chemistry	**Rightsholder**	Oxford University Press - Journals
Article Title	The Role of Exosomes in Breast Cancer.	**Publication Type**	Journal
Author/Editor	AMERICAN ASSOCIATION FOR CLINICAL CHEMISTRY., AMERICAN ASSOCIATION OF CLINICAL CHEMISTS.	**Start Page**	1457
		End Page	1465
		Issue	12
		Volume	61
Date	12/31/1954		
Language	English		
Country	United States of America		

REQUEST DETAILS

Portion Type	Image/photo/illustration	**Distribution**	United States
Number of images / photos / illustrations	1	**Translation**	Original language of publication
Format (select all that apply)	Print, Electronic	**Copies for the disabled?**	No
		Minor editing privileges?	No
Who will republish the content?	Academic institution	**Incidental promotional use?**	No
Duration of Use	Life of current edition	**Currency**	USD
Lifetime Unit Quantity	Up to 499		
Rights Requested	Main product		

NEW WORK DETAILS

Title	DEVELOPMENT OF EXOSOMAL PROTEIN DETECTION ASSAYS FOR CANCER DIAGNOSTICS USING NANOMATERIALS IN CONJUCTION WITH OPTICAL SPECTROSCOPY AND IMAGING	**Institution name**	University of Memphis
		Expected presentation date	2021-06-30
Instructor name	Xiaohua Huang		

ADDITIONAL DETAILS

Order reference number	N/A	**The requesting person / organization to appear on the license**	Vojtech Vinduska

REUSE CONTENT DETAILS

Title, description or numeric reference of the portion(s)	The role of exosomes in breast cancer. Exosomes are released from breast cancer and stromal/cancer associated fibroblast cells into the extracellular milieu and tumor microenvironment.	**Title of the article/chapter the portion is from**	The Role of Exosomes in Breast Cancer.
		Author of portion(s)	Lowry, Michelle C; Gallagher, William M; O'Driscoll, Lorraine
		Issue, if republishing an article from a serial	12
Editor of portion(s)	Lowry, Michelle C; Gallagher, William M; O'Driscoll, Lorraine	**Publication date of portion**	2015-11-30
Volume of serial or monograph	61		
Page or page range of portion	1457-1465		